

Confinement and Anisotropy of Ultrahigh-Energy
Cosmic Rays in Isotropic Plasma Wave Turbulence

DISSERTATION

zur Erlangung des Grades eines Doktors der
Naturwissenschaften

der Fakultät für Physik und Astronomie der Ruhr-Universität Bochum

vorgelegt von

Miroslava Vukčević

Bochum 2007

Names of examiners:

Prof. Dr. Reinhard Schlickeiser

Dr. Horst Fichtner

Date: 25. 10. 2007

To Ana and Vladimir

Abstract

Context: The mean free path and anisotropy of galactic cosmic rays is calculated in weak plasma wave turbulence that is isotropically distributed with respect to the ordered uniform magnetic field.

Aims: The modifications on the value of the Hillas energy, above which cosmic rays are not confined to the Galaxy, are calculated. The original determination of the Hillas limit has been based on the case of slab turbulence where only parallel propagating plasma waves are allowed.

Methods: We use quasilinear cosmic ray Fokker-Planck coefficients to calculate the mean free path and the anisotropy in isotropic plasma wave turbulence.

Results: In isotropic plasma wave turbulence the Hillas limit is enhanced by about four orders of magnitude to $E_c = 2.03 \cdot 10^4 A n_e^{1/2} (L_{\max}/1 \text{ pc})$ resulting from the dominating influence of transit-time damping interactions that obliquely propagating magnetosonic waves undergo with cosmic rays.

Conclusions: Below the energy E_c the cosmic ray mean free path and the anisotropy exhibit the well known $E^{1/3}$ energy dependence for relevant undamped waves. In case of damped waves, the cosmic ray mean free path and the anisotropy do not depend on energy. At energies higher than E_c both transport parameters steepen to a E^3 -dependence for undamped and damped waves. This implies that cosmic rays even with ultrahigh energies of several tens of EeV can be rapidly pitch-angle scattered by interstellar plasma turbulence, and are thus confined to the Galaxy.

Kurzfassung

Kontext: In der vorliegenden Arbeit werden die mittlere freie Weglänge sowie die Anisotropie der kosmischen Strahlung in schwachen Plasmawellenturbulenzen bestimmt, die eine isotrope Verteilung in Bezug auf das gleichmäßige Magnetfeld aufweisen.

Ziele: Die Hillas Energie, jenseits derer die kosmische Strahlung die Galaxie verlassen kann, wird in einem verbesserten Modell berechnet. Die ursprüngliche Bestimmung dieses Limits basiert auf 'slab' turbulenzen, die nur parallel propagierende Plasmawellen berücksichtigt.

Methoden: Quasilineare Fokker-Planck Koeffizienten der kosmischen Strahlung werden zur Berechnung der mittleren freien Weglänge und Anisotropie in isotropen Plasmawellenturbulenzen verwendet.

Ergebnisse: In isotropen Plasmawellenturbulenzen erhöht sich die Hillas Energie um vier Größenordnungen auf einen Wert von $E_c = 2.03 \cdot 10^4 A n_e^{1/2} (L_{\max}/1 \text{ pc})$. Dies wird durch den dominierenden Einfluß der 'transit-time damping' Wechselwirkungen sich schräg ausbreitender magnetosonic Wellen mit der kosmischen Strahlung hervorgerufen.

Schlußfolgerungen: Unterhalb der Energie E_c zeigen mittlere freie Weglänge und Anisotropie die typische $E^{1/3}$ Energieabhängigkeit ungedämpfter Wellen. Im Falle gedämpfter Wellen sind beide Transportparameter energieunabhängig. Oberhalb von E_c verstärkt sich die Energieabhängigkeit zu einem E^3 -Verhalten. Dies bedeutet, daß kosmische Strahlen selbst bei ultrahohen Energien von einigen zehn EeV schnell 'pitch-angle' gestreut werden können und daher in der Galaxie gebunden sind.

Contents

| | | |
|----------|-------------------------------------------------------------------------|-----------|
| 1 | Introduction | 1 |
| 2 | Observations and Theoretical Background of Cosmic Rays | 2 |
| 2.1 | The Cosmic Ray Landscape | 2 |
| 2.2 | Anisotropy | 4 |
| 2.2.1 | Harmonic Analysis | 5 |
| 2.3 | Ultrahigh Energy Cosmic Rays | 7 |
| 2.3.1 | Interaction between Cosmic Ray Nuclei and Photons | 8 |
| 2.3.2 | Detectors and Observations of UHECR | 9 |
| 2.4 | Cosmic Ray Scattering, Confinement and Isotropy | 11 |
| 3 | Transport Coefficients for Cosmic Rays | 14 |
| 3.1 | Transport Equations | 14 |
| 3.2 | The Diffusion Approximation | 19 |
| 3.2.1 | Cosmic Ray Anisotropy | 22 |
| 3.2.2 | The Diffusion-Convection Transport Equation | 23 |
| 4 | Derivation of the Fokker-Planck Coefficients | 25 |
| 4.1 | The Fokker-Planck coefficient $D_{\mu\mu}$ | 25 |
| 4.1.1 | Equations of Motion | 25 |
| 4.1.2 | Step 1: Quasilinear Approximation | 26 |
| 4.1.3 | Step 2: The Kubo Formalism | 27 |
| 4.1.4 | Step 3: Homogenous Turbulence | 29 |
| 4.1.5 | Step 4: Plasma Wave Turbulence | 30 |
| 4.2 | The Other Fokker-Planck Coefficients $D_{\mu p}$ and D_{pp} | 32 |
| 4.3 | Derivation of $D_{\mu\mu}$ for Fast Mode Waves | 33 |
| 4.3.1 | Dispersion Relation | 33 |
| 4.3.2 | Reduction of the Fokker-Planck Coefficient $D_{\mu\mu}$ | 34 |
| 4.4 | Derivation of $D_{\mu\mu}$ for Slow Mode Waves | 36 |
| 4.4.1 | Dispersion Relation | 36 |
| 4.4.2 | Reduction of F-P Coefficient $D_{\mu\mu}$ | 37 |

| | | |
|----------|-----------------------------------------------------------------------------------------------------|-----------|
| 4.4.3 | The Other Fokker-Planck Coefficients $D_{\mu p}$ and D_{pp} for Slow Magnetosonic Waves | 37 |
| 5 | Undamped Waves | 38 |
| 5.1 | Relevant Magnetohydrodynamic Plasma Modes | 41 |
| 5.1.1 | Resonant Interactions of Shear Alfvén Waves | 42 |
| 5.1.2 | Resonant Interactions of Fast Magnetosonic Waves | 42 |
| 5.1.3 | Implications for Cosmic Ray Transport | 43 |
| 5.2 | Quasilinear Cosmic ray Mean Free Path and Anisotropy for Isotropic Plasma Wave Turbulence | 45 |
| 5.2.1 | Fast Mode Waves | 45 |
| 5.2.2 | Shear Alfvén Waves | 46 |
| 5.2.3 | Gyroresonant Fokker-Planck Coefficients at $\mu = 0$ | 47 |
| 5.2.4 | Cosmic Ray Mean Free Path | 49 |
| 5.2.5 | Anisotropy | 50 |
| 6 | Implication of Damped Waves | 51 |
| 6.1 | Damping Rate of Fast Mode Waves | 52 |
| 6.1.1 | Dominance of Transit-time Damping | 53 |
| 6.1.2 | Rate of Adiabatic Deceleration | 56 |
| 6.1.3 | Pitch-angle Fokker-Planck Coefficient | 56 |
| 6.1.4 | Cosmic Ray Mean Free Path for FMS Waves | 57 |
| 6.1.5 | Cosmic Ray Momentum Diffusion from FMS Waves | 58 |
| 6.2 | Slow Magnetosonic Waves | 59 |
| 6.2.1 | Cosmic Ray Mean Free Path for SMS Waves | 62 |
| 6.2.2 | Cosmic Ray Momentum Diffusion from SMS Waves | 63 |
| 7 | Summary | 65 |
| 8 | Appendix A: Asymptotic calculation of the integral (164) | 67 |
| 8.1 | Case $k_{min}R_L\epsilon \leq 1$ | 67 |
| 8.2 | Case $k_{min}R_L\epsilon > 1$ | 68 |

| | | |
|-----------|-------------------------------------------------|-----------|
| 9 | Appendix B: Evaluation of the function G | 71 |
| 9.1 | Case $G(k_{min}R_L \gg 1)$ | 71 |
| 9.2 | Case $G(k_{min}R_L \ll 1)$ | 72 |
| 9.2.1 | Flat turbulence spectrum $1 < q < 2$ | 73 |
| 9.2.2 | Steep turbulence spectrum $2 < q < 6$ | 74 |
| 10 | Appendix C: Evaluation of the function G | 75 |
| 10.1 | Case $G(k_{min}R_L \gg 1)$ | 75 |
| 10.2 | Case $G(k_{min}R_L \ll 1)$ | 77 |

1 Introduction

Cosmic rays are defined as extraterrestrial charged particle radiation. Although we use word 'rays', we should not forget that we deal with particles, or more precise, it consists of a flux of electrons, positrons and nucleons with kinetic energies greater than 1KeV that bombards the Earth from outside. To understand the origin and dynamics of these particles one should combine theory and observations.

As far as the theory is concerned, of particular interests are particles interaction processes with electromagnetic fields, their collective phenomena, their spontaneous and coherent radiation processes and the role of nuclear interactions with ordinary matter. It means that theoretical development relies to a large extent on our understanding of plasma physics.

Concerning observations, astronomy spans frequencies from 10^4 cm radio-waves to 10^{-14} cm, particles of GeV energies. The new astronomy probes the Universe with new wavelengths, smaller than 10^{-14} cm, or particle energies larger than 10 GeV. Origin of low energy cosmic rays is Sun, while for ultrahigh-energy cosmic rays (UHECR) it is still questionable.

The main purpose of this work is analytical study of the ultrahigh-energy cosmic rays. We calculate transport parameters using quasilinear theory. In chapter II, we give short overview of experimental and theoretical achievements on UHECR. Quasilinear theory and derivation of relevant cosmic transport parameters are explained in chapter III. In chapter IV we have calculated the Fokker-Planck coefficients (FPC) step by step. Discussion and results related with different type of undamped plasma waves are given in chapter V. Influence of damping and relevant results calculated for magnetosonic waves are discussed in chapter VI. In chapter VII we present summary and conclusion for possible galactic origin of UHECR and give some topics for further research. Some parts of chapters II and III are taken from the book Cosmic Ray Astrophysics (Schlickeiser, 2006).

2 Observations and Theoretical Background of Cosmic Rays

There are two ways to detect cosmic rays. There are ground based detectors and the second are out of the Earth atmosphere launching satellites into extraterrestrial space. The ground based observations have the advantage of long exposure time and no limit on the size of detectors but their results have to be corrected for the influence of the Earth's atmosphere. In the atmosphere the in-falling primary cosmic rays undergo inelastic collisions with the atoms and molecules in the atmosphere, producing secondary particles which, again, are subject to further interactions (Fig.1). It is said that a whole 'shower' of particles reaches the ground and in order to investigate properties of the in-falling cosmic rays, one has to reconstruct the 'shower' with the help of numerical model calculations. It means that the quality of the cosmic ray measurements using these methods depends on understanding and modeling of the interaction processes in the atmosphere. In the case when cosmic ray detection is flown outside the atmosphere these disturbing atmospheric effects disappear, but here, because of the limited size and weight of detectors and limited observing time of experiment (which is less of several weeks in the case of space shuttle experiments), weak cosmic ray intensities cannot be measured. These instrumental limitations may improve with time as more sophisticated platforms (space stations) become available in the future. Today's information on the flux of cosmic rays below energies of $\sim 10^{14}$ eV/nucleon stems mainly from satellite and balloon experiments, whereas at higher energies $> 10^{14}$ eV/nucleon, because of the rather weak intensities, information on cosmic rays is provided solely by ground-based detectors.

2.1 The Cosmic Ray Landscape

Taking a view of the cosmic ray landscape (Lund 1986), most of it is still hidden from our point of view by clouds, but there are some general physical arguments limit the ultimate extent of the region (Fig. 2). Up- and downwards in nuclear charge, nuclear stability sets two boundaries. Towards the high energy side the boundary is set by the universal background radiation which destroys heavy cosmic ray nuclei with energies in excess of $\sim 10^{19}$ eV/nucleon by photonuclear collisions $A + \gamma \rightarrow (A - 1) + n$ (Greisen1966, Zatsepin

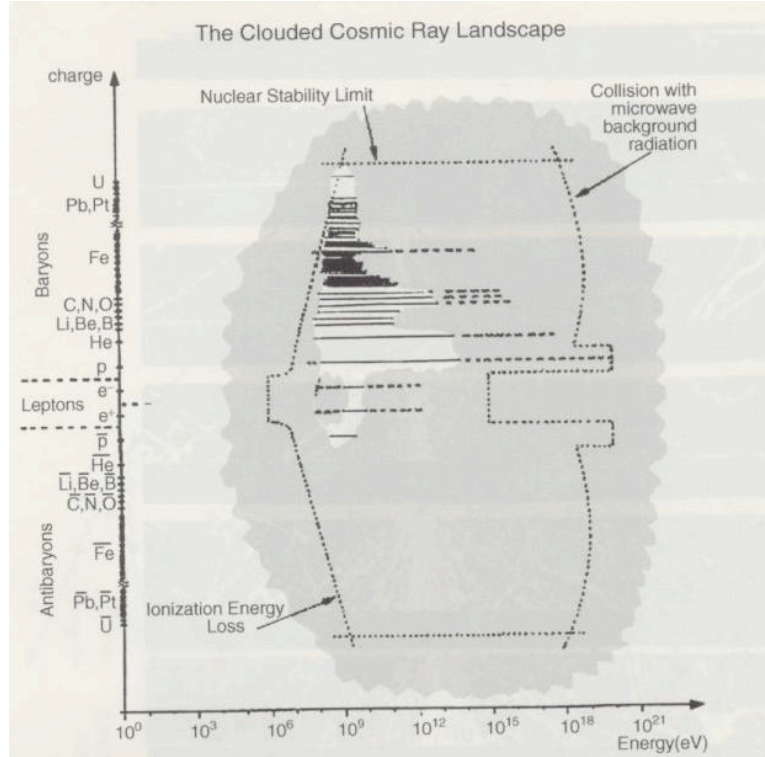


Figure 2: An outline of the cosmic ray landscape

a) The outstreaming solar wind disturbs the determination of particle fluxes below kinetic energies of ~ 500 MeV/nucleon for nuclei and below 5 GeV for electrons. This phenomena is referred as solar modulation.

b) The Sun itself and some planets produce cosmic radiation which has to be distinguished from the galactic and extragalactic component.

The study of these solar cosmic rays is itself an interesting area of investigation since in situ observations of these particles provide much more detailed information than the limited studies of extrasolar cosmic rays. However, we concentrate our analysis on the later one.

2.2 Anisotropy

The study of anisotropy in the arrival directions of cosmic rays is clearly of great interest to locate their possible sources. With specific position of our solar system with respect to the galactic disk, one would expect an anisotropy towards the direction $l = 0, b = 0$ (heliocentric galactic coordinates, sun is the center, toward galactic center) if the cosmic

ray sources are galactic objects. Experimental data on anisotropy predominantly come from ground-based shower detectors. There are numbers of problems in interpreting the data on anisotropy. At the highest energies, the data are statistically limited and subject to fluctuations. Another experimental problem is the bias of each detector due to the non-uniform acceptance of cosmic ray arrival directions. For instance, detector located in the northern hemisphere do not see a region around the south magnetic pole. This hole in acceptance, if not properly accounted for, can produce biases in event distributions (Sokolsky 1979,503). At the end, since we usually search for anisotropy as a function of energy, biases in determining energy will cause problems and uncertainties.

2.2.1 Harmonic Analysis

For a detector operating approximately uniformly with respect to sidereal time the zenith angle dependent shower detector and direction reconstruction efficiency is a strong function of declination but not of the right ascension (RA). Therefore one usually searches for anisotropy in RA only within a given declination band. This is done by measuring the counting rate as a function of sidereal time (RA) and performing a harmonic analysis, e.g. fitting the data by

$$R(t) = A_0 + A_1 \sin\left(\frac{2\pi t}{24} + \phi_1\right) + A_2 \sin\left(\frac{2\pi t}{12} + \phi_2\right), \quad (1)$$

where A_0, A_1 , and A_2 are the amplitudes of the zeroth, first and second harmonics, respectively, and ϕ_1 and ϕ_2 are the phases of the first and second harmonics. In Fig. 3 we show the amplitude A_1/A_0 and the phase ϕ_1 of the first harmonic. One notes that

- a) at energies less than 10^{14} eV the anisotropy is small (~ 0.07) and has constant phase ($\sim 3^h RA$),
- b) the anisotropy starts to increase as the energy rises above $\sim 10^{15}$ eV,
- c) the phases of the relatively large amplitude anisotropies (several percent) above 10^{17} eV vary rapidly with energy but are consistent between the various experiments.

These data do not convincingly establish a significant anisotropy beyond 10^{17} eV. The data show no evidence of anisotropy at any energy, regardless of the energy calibration model chosen.

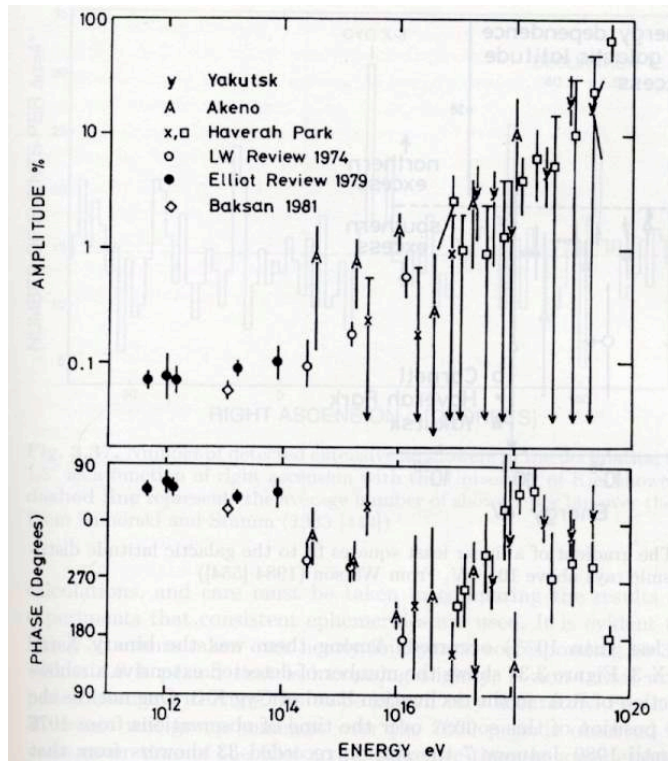


Figure 3: A summary of data on the phase and the amplitude of the first harmonic of cosmic ray anisotropy in right ascension, Watson, 1984

2.3 Ultrahigh Energy Cosmic Rays

In the context of cosmic ray anisotropy we have described some results of ground-based observations of cosmic rays with energies above 10^{14} eV. Here, we concentrate on the measurements of the energy spectrum and the composition of these ultrahigh energy particles. Studies of the composition are indirect by measuring the muon content of the airshowers, since their muon multiplicity depends on the atomic number of the primary particle, and by analyzing the lateral shower distribution on the ground. A common problem of the method is that such high primary energies are not available in terrestrial accelerators, so that the interpretation relies on the theoretical extrapolation of nuclear interactions to these energies. It is clear that the same observations made in this way can be interpreted quite differently and that many controversial results exist on the composition ranging from a dominantly protonic composition to a dominantly Fe composition of UHECR. We restrict discussion to the energy spectrum as a function of the total energy of the primary particle. It should be mentioned that it is much harder to measure the all-particle spectrum at 10^{15} eV than it is at 10^{18} eV for example, since showers produced by 10^{15} eV primaries are rather small, even at the highest altitude laboratory, so that fluctuations are a severe problem (Watson 1984). Of particular interest are cosmic ray particles with total energy larger than 10^{19} eV. Soon after the discovery in 1965 of the universal microwave background radiation, Greisen, Zatsepin and Kuzmin (GZK 1966) pointed out that protons of these energy would interact with this microwave background through photo-pion reactions and lose energy on a length scale of about $\simeq 10$ Mpc which is a relatively short distance in cosmological terms (radius of a flat disk of our Galaxy is $\simeq 15$ kpc, $1 \text{ kpc} \sim 3 \times 10^{21}$ cm). It was therefore anticipated that the UHECR spectrum would show a cutoff at these energies. However, airshower arrays in the US and Japan have detected seven particles at energies clearly above 10^{20} eV with no indication of GZK cutoff. Within conventional explanations of cosmic ray acceleration this means that the potential sources have to be relatively nearby within 50 Mpc. But the detection of these UHECR has also stimulated a great deal of speculation about possible new physics. However, more data are required, although the fluxes at these energies are only of order one per square kilometer per century.

2.3.1 Interaction between Cosmic Ray Nuclei and Photons

The photo-hadron production process is dominated by photo-pion production, e.g. for protons at threshold the channels $p+\gamma \rightarrow \pi^0+p$ and $p+\gamma \rightarrow \pi^++n$ dominate and at higher energies by multi-pion production. Baryon production and K-meson production can be neglected in most astrophysical applications. Photo-pion production by nuclei of mass number A obeys the simple Glauber rule $\sigma_A \simeq A^{2/3}\sigma_p$. However, in any astrophysical environment nuclei cannot be accelerated to energies above pion threshold, since they are destroyed before by photo-disintegration that has much lower threshold of about 10 MeV in the nucleus rest frame compared to pion production which requires at least 145 MeV. For a cosmic ray proton of Lorentz factor γ_p , traversing an isotropic photon field of number density $n(\epsilon, \mathbf{r})$, one obtains the energy loss rate

$$-\frac{d\gamma}{dt} = \frac{c}{2\gamma_p} \int_{\epsilon'_{th}/(2\gamma_p)}^{\infty} d\epsilon n(\epsilon \mathbf{r}) \epsilon^{-2} \int_{\epsilon'_{th}}^{2\gamma_p \epsilon} d\epsilon' \epsilon' \sigma(\epsilon') K_p(\epsilon'), \quad (2)$$

where $\sigma(\epsilon')$ and $K_p(\epsilon')$ are the total photo-hadron production cross-section and inelasticity, respectively, as a function of the photon energy in the proton rest frame, while the proton rest frame threshold energy $\epsilon'_{th,K\pi}$ is given by $\epsilon'_{th,K\pi} = Km_\pi c^2 (1 + \frac{Km_\pi}{2m_p})$ for the respective reaction. Crucial for further evaluation is the knowledge of both the photo-hadron production cross-section and inelasticity as a function of energy ϵ' . Here, we just list literature for more detailed discussion on it, since there exist a vast number of phenomenological particle physics models for the photo-hadron production cross-section and inelasticity as a function of energy whose free parameters are adjusted by available accelerator studies of individual reactions (Stecker 1968, Sikora et al. 1987, Mannheim, Biermann 1989, Begelmann et al. 1990, Mannheim, Schlickeiser 1994).

It is clear from all experiments that the particle nature of the cosmic rays is either protons or, possible, nuclei. Since the Universe is opaque to the photons with energies of tens TeV because they annihilate into electron pairs in interaction with mentioned background light, it is necessary to investigate interactions between protons and background light above a threshold energy E_p of about 50 EeV. The major source of proton energy loss is photoproduction of pions on a target of cosmic microwave photons. Therefore, the Universe is also opaque to the highest energy cosmic rays, with an absorption length $\lambda_{\gamma p} = (n_{CMB}\sigma_{p\gamma})^{-1} \simeq 10$ Mpc. This is mentioned GZK cutoff which depend only on two

known numbers: $n_{CMB} = 400cm^{-3}$ and $\sigma_{\gamma p} = 10^{-28}cm^2$. Protons with energies in excess of 100 EeV, emitted in distant quasars and gamma ray bursts, would have lost their energy to pions before reaching detectors on the Earth. There are three possible resolutions:

- 1.) the protons are accelerated in nearby sources,
- 2.) they do reach us from distant sources which accelerate them to much higher energies than we observe, thus exacerbating the acceleration problem, or
- 3.) the highest energy cosmic rays are not protons.

The first possibility motivates to find an appropriate accelerating mechanism by confining these source even to our own galaxy or nearby our galaxy. It will be analyzed and discussed in details through this work.

2.3.2 Detectors and Observations of UHECR

There are two detected events of energies above GZK cutoff done by two detectors. In 1991, The Fly's Eye cosmic ray detector recorded an event of energy $\sim 10^{20}$ eV. The second one, detected for the first time in 1993 by AGASA air shower array in Japan. AGASA has by now accumulated an impressive 10 events with energy in excess of 10^{20} eV (Fig.4).

In order to improve the detection and collect as much as possible data, in 1995 started building The Pierre Auger Cosmic Ray Observatory, the biggest detector of UHECR. It consists of two parts, one on northern hemisphere (Millard Country, Utah, USA), and the other, on the southern (Malarge, Province of Mendoza, Argentina). This observatory will allow continual exposition of the whole sky, which is important in order to find out are the distribution of directions of cosmic rays isotropic, or there is some structure on larger scale. Two mentioned independent detectors are correlated in one, which allow higher resolution and better control of systematic errors. The shower can be observed by

- a) sampling the electromagnetic and hadronic components when they reach the ground with an array of particle detectors such as scintillators,
- b) detecting the fluorescent light emitted by atmospheric nitrogen excited by the passage of the shower particles,
- c) detecting the Cerenkov light emitted by the large number of particles at shower maximum, and

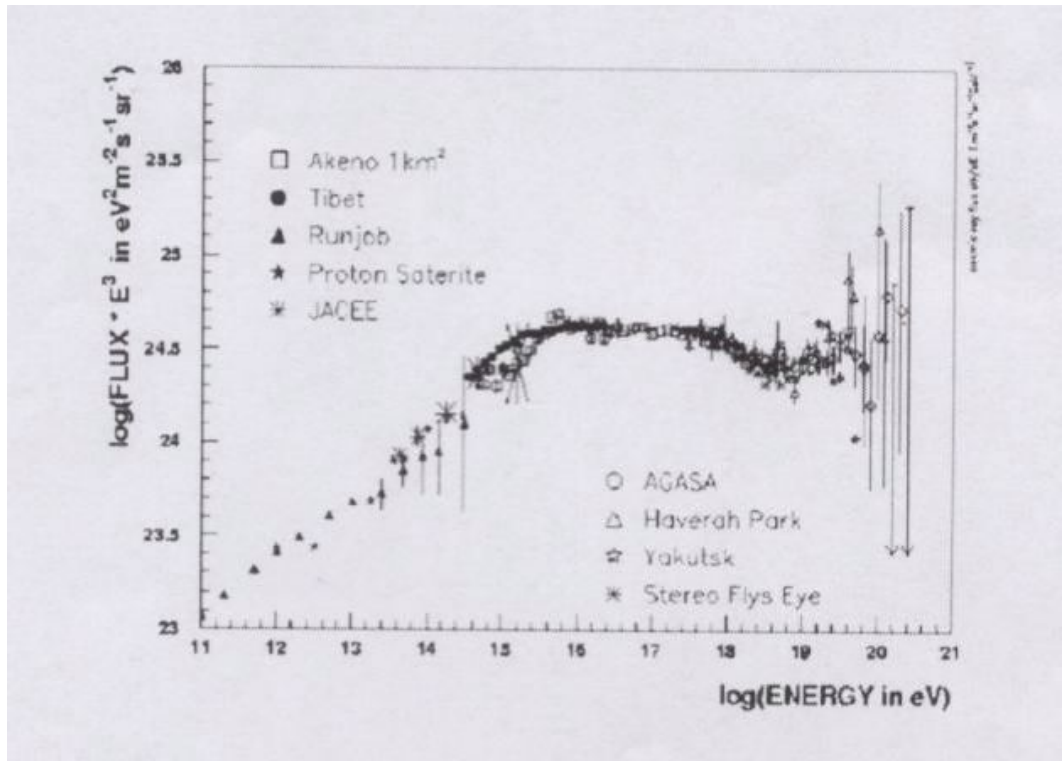


Figure 4: The cosmic ray spectrum. There are three important parts: knee, ankle and fingers. The highest energy cosmic rays belong to the part named fingers, measured by the AGASA and HiRes.

d) detecting muons and neutrinos underground. Cerenkov and fluorescent light is collected by large mirrors and recorded by arrays of photomultipliers in their focus.

Cosmic rays travel through the vacuum with velocity close to the velocity of light. When these particles enter the medium which is not vacuum, but is denser than vacuum, they travel with velocity bigger than real velocity of light in that medium. As a result it is possible to detect so called Cerenkov light of the blue color. Great number of the cosmic rays are able to excite the nitrogen molecules in the atmosphere. The consequence of these excitations is spontaneous cascade de-excitations through the emission of fluorescent photons in optical part of spectrum. Detector for this type of light is Fly's Eye. Detectors of cosmic rays on the Earth are mostly scintillators. Cosmic ray showers passing by the atmosphere spread out, so that on the earth surface it is scattered from few hundred square meters up to few hundred square kilometers. That is the reason why scintillation detectors are connected in the net of large area. According to the statistics, flux for particles of energies $E > 10^{19}$ eV is 1 particle/ km^2 in one year, while flux for the particles with $E > 10^{20}$ eV is 1 particle/ km^2 in 100 years. Since these events are very rare, as large the area is, bigger chances are to catch the event. The Pierre Auger observatory will use 1600 Cerenkov detectors on the area of 3000 km^2 , and 24 fluorescent detectors, each in every 15 km. Informations from each detector are transfered via radiowaves to the main station where the shower is reconstructed and analyzed (<http://www.cosmic-ray.org>, <http://www-zeuthen.desy.de>).

2.4 Cosmic Ray Scattering, Confinement and Isotropy

Summarizing the observational material on galactic cosmic rays we note that the solar system is bombarded by cosmic rays from all sides isotropically. However, a successful model for the origin of of galactic cosmic ray has to explain the following key issues:

- a) an over 10^9 yr constant ray power of $\sim 10^{40}$ erg/s,
- b) a nearly uniform and isotropic distribution of cosmic ray nucleons and electrons with energies below 10^{15} eV over the Galaxy,
- c) elemental and isotopic composition similar to solar flare particles,
- d) electron/nucleon ratio in relativistic cosmic rays at the same Lorentz factor of about 0.01,

e) the formation of power law energy spectra for all species of cosmic rays over large energy ranges accounting for the systematic differences in the spectral index values of primary and secondary cosmic ray nucleons and cosmic ray electrons.

The general problem of the origin of cosmic rays can be divided into two parts. The first part concerns the actual origin or injection of the cosmic rays into the Galaxy by sources which keep up the power over a long time, while the second part concerns the subsequent behavior of the cosmic rays, their motion, transport and confinement in the Galaxy. We will concentrate in the second one. It is generally recognized that due to their small Larmor radii, for cosmic ray nucleons of momentum p

$$R_L = \frac{pc/eV}{300B/Gauss} cm, \quad (3)$$

as compared to galactic dimensions, the majority of cosmic rays with energies below $\sim 10^{15}$ eV propagate along the galactic magnetic field. Because of the observed isotropy and age of cosmic rays, it seems clear that the cosmic rays cannot propagate freely along the lines of force but must be continually scattered. If they were to propagate freely with the speed of light, they would leave the galaxy within 10^4 to $4 \cdot 10^5$ years, as the dimension of our Galaxy suggest. But from the measured abundance of the cosmogenic cosmic ray clocks we know that their average lifetime in the Galaxy is $\sim 10^7$ years. Moreover, if there is no scattering, we would expect a strong anisotropy towards the direction of the galactic center due to specific location of the solar system, since there should be more sources of the type discussed in previous section towards the inner galaxy. Yet we do not see this anisotropy for cosmic rays with energies less than 10^{15} eV which apparently is lost due to multiple scattering of the cosmic rays on their path from the sources to us. The scattering cannot be by particles (Coulomb scattering) since the energies of cosmic rays are much higher than nuclear binding energies and such collisions would destroy all nuclear species heavier than protons in the interstellar medium, which is not the case (Kulsrud, Pearce 1969). Moreover, the mean free path for Coulomb collision of relativistic nucleons in the dilute interstellar medium of order $\sim 10^{23} \gamma / n_H (cm^{-3})$ is far too long. Thus, the most likely scattering mechanism is of plasma waves, i.e. fluctuating electromagnetic fields in the interstellar medium. How these plasma waves are produced and how they influence the dynamics of cosmic ray particles are the main topics of this work and will be discussed

in detail in the following chapters.

3 Transport Coefficients for Cosmic Rays

In this chapter we discuss the basic equations and necessary approximations we have to made in order to model interaction between charged particles moving in certain plasma.

3.1 Transport Equations

In order to describe interaction between particle and waves we start from the relativistic Vlasov equations

$$\frac{\partial f_a}{\partial t} + \mathbf{v} \cdot \frac{\partial f_a}{\partial \mathbf{x}} + \dot{\mathbf{p}} \cdot \frac{\partial f_a}{\partial \mathbf{p}} = S_a(\mathbf{x}, \mathbf{p}, t), \quad (4)$$

with the equations of motion

$$\dot{\mathbf{p}} = q_a[\mathbf{E}_T(\mathbf{x}, t) + \frac{\mathbf{v} \times \mathbf{B}_T(\mathbf{x}, t)}{c}], \quad (5)$$

$$\dot{\mathbf{x}} = \mathbf{v} = \frac{\mathbf{p}}{\gamma m_a}. \quad (6)$$

S_a in (4) denotes sources and sinks of particles. We can neglect any large scale electric field because of the high conductivity of plasmas, so that the total electromagnetic field is a superposition of the uniform magnetic field $\mathbf{B}_0 = B_0 \mathbf{e}_z$ and the plasma turbulence $(\delta \mathbf{E}, \delta \mathbf{B})$ is

$$\mathbf{B}_T = \mathbf{B}_0 + \delta \mathbf{B}(\mathbf{x}, t), \mathbf{E}_T = \delta \mathbf{E}_T(\mathbf{x}, t). \quad (7)$$

We can follow, instead of the actual position of the particles, the coordinates of the guiding center, because of the gyrorotation of the particles

$$\mathbf{R} = (X, Y, Z) = \mathbf{x} + \frac{\mathbf{v} \times \mathbf{e}_z}{o\Omega}, \quad (8)$$

where Ω denotes the absolute value of the particle's gyrofrequency in the uniform field and $o = q_a/|q_a|$ the charge sign. It is also convenient to use spherical coordinates (p, μ, ϕ) in momentum space defined by

$$p_x = p \cos \phi \sqrt{1 - \mu^2}, p_y = p \sin \phi \sqrt{1 - \mu^2}, p_z = p\mu. \quad (9)$$

Consequently

$$X = x + \frac{v\sqrt{1-\mu^2}}{o\Omega} \sin \phi, Y = y - \frac{v\sqrt{1-\mu^2}}{o\Omega} \cos \phi, Z = z. \quad (10)$$

Transforming (4) to the coordinate set

$$x_\sigma = (p, \mu, \phi, X, Y, Z) \quad (11)$$

by using (5)-(10) and the Einstein summation convention, one obtains the appropriate form of the Vlasov equation (Hall, Sturrock 1968, and Urch 1977)

$$\frac{\partial f_a}{\partial t} + v\mu \frac{\partial f_a}{\partial Z} - o\Omega \frac{\partial f_a}{\partial \phi} + \frac{1}{p^2} \frac{\partial (p^2 g_{x\sigma} f_a)}{\partial x_\sigma} = S_a(\mathbf{x}, \mathbf{p}, t) \quad (12)$$

where the generalized force term g_σ includes the effect of the randomly fluctuating electromagnetic fields. Solutions of (12) with $g_\sigma = 0$ will be called "unperturbed orbits". The components of the fluctuating force term are

$$g_p = \dot{p} = \frac{m_a c \gamma \Omega}{p B_0} \mathbf{p} \cdot \delta \mathbf{E} = \frac{\Omega p c}{v B_0} \left[\mu \delta E_{\parallel} + \sqrt{\frac{1-\mu^2}{2}} (\delta E_l e^{-i\phi} + \delta E_r e^{i\phi}) \right], \quad (13)$$

$$g_\mu = \dot{\mu} = \frac{\Omega \sqrt{1-\mu^2}}{B_0} \left[\frac{c}{v} \sqrt{1-\mu^2} \delta E_{\parallel} + \frac{i}{\sqrt{2}} \left[e^{i\phi} (\delta B_r + i\mu \frac{c}{v} \delta E_r) - e^{-i\phi} (\delta B_l - i\mu \frac{c}{v} \delta E_l) \right] \right], \quad (14)$$

$$g_\phi = -o\Omega \frac{\delta B_{\parallel}}{B_0} + \frac{o\Omega}{\sqrt{2(1-\mu^2)}} B_0 \left[e^{i\phi} (\mu \delta B_r + i \frac{c}{v} \delta E_r) + e^{-i\phi} (\mu \delta B_l - i \frac{c}{v} \delta E_l) \right], \quad (15)$$

$$g_X = -v \sqrt{1-\mu^2} \cos \phi \frac{\delta B_{\parallel}}{B_0} + \frac{ic}{\sqrt{2} B_0} \left[\delta E_r - \delta E_l - \frac{i\mu v}{c} (\delta B_l + \delta B_r) \right], \quad (16)$$

$$g_Y = -v \sqrt{1-\mu^2} \sin \phi \frac{\delta B_{\parallel}}{B_0} - \frac{c}{\sqrt{2} B_0} \left[\delta E_r + \delta E_l + \frac{i\mu v}{c} (\delta B_l - \delta B_r) \right], \quad (17)$$

$$g_Z = 0. \quad (18)$$

In the derivation we have introduced

$$\delta B_{l,r} = \frac{1}{\sqrt{2}}(\delta B_x \pm i\delta B_y), \delta B_{||} = \delta B_z, \quad (19)$$

and

$$\delta E_{l,r} = \frac{1}{\sqrt{2}}(\delta E_x \pm i\delta E_y), \delta E_{||} = \delta E_z, \quad (20)$$

which are related to the left-handed and right-handed polarized field components. The function f_a develops in an irregular way under the influence of g_σ , but the detailed fluctuations are not of interest. An expectation value of f_a must be found in terms of the statistical properties of g_σ , so we consider an ensemble of distribution functions all beginning with identical values at some time $t = t_0$. Let each of these function be subject to a different member of an ensemble of realizations of g_σ , i.e. fluctuating field histories which are independent of one another in detail, but identical as to statistical averages. At any time $t > t_0$, the various functions differ from each other, and we require an equation for

$$\langle f_a(\mathbf{x}, \mathbf{p}, t) \rangle = F_a(\mathbf{x}, \mathbf{p}, t), \quad (21)$$

the average of f_a over all members of the ensemble. This is obtained by taking the average of (12) using

$$\langle \delta \mathbf{B}(\mathbf{x}, t) \rangle = \langle \delta \mathbf{E}(\mathbf{x}, t) \rangle = 0, \quad (22)$$

implying

$$\langle \mathbf{B}(\mathbf{x}, t) \rangle = \mathbf{B}_0, \langle \mathbf{E}(\mathbf{x}, t) \rangle = 0. \quad (23)$$

We find

$$\frac{\partial F_a}{\partial t} + v\mu \frac{\partial F_a}{\partial Z} - o\Omega \frac{\partial F_a}{\partial \phi} = S_a(\mathbf{x}, \mathbf{p}, t) - \frac{1}{p^2} \frac{\partial (\langle p^2 g_{x\sigma} \delta f_a \rangle)}{\partial x_\sigma}, \quad (24)$$

where

$$\delta f_a(\mathbf{x}, \mathbf{p}, t) = f_a(\mathbf{x}, \mathbf{p}, t) - F_a(\mathbf{x}, \mathbf{p}, t). \quad (25)$$

Subtracting (24) from (12) gives an equation for the fluctuation

$$\frac{\partial \delta f_a}{\partial t} + v\mu \frac{\partial \delta f_a}{\partial Z} - o\Omega \frac{\partial \delta f_a}{\partial \phi} = -g_{x\sigma} \frac{\partial F_a}{\partial x_\sigma} - g_{x\sigma} \frac{\partial \delta f_a}{\partial x_\sigma} + \langle g_{x\sigma} \frac{\partial \delta f_a}{\partial x_\sigma} \rangle, \quad (26)$$

where we used

$$\frac{1}{p^2} \frac{\partial (p^2 g_{x\sigma})}{\partial x_\sigma} = 0. \quad (27)$$

We use perturbation method (referred to as the quasilinear approximation) to solve these equations, which is based on the assumption that the fluctuations are of small amplitude - g_σ must be significantly small, so that, there exists a time scale T satisfying

$$t_c \ll T \ll t_F, \quad (28)$$

where t_F represents the time scale on which g_σ effects the evolution of the distribution function and t_c is correlation time. From the equation of motion t_F can be estimated as

$$t_F = \frac{F_a}{g_{x\sigma} \frac{\partial F_a}{\partial x_\sigma}}. \quad (29)$$

Then according to (26) the variation δf_a generated by g_σ within a time T must remain much smaller than F_a , and the right-hand side of (26) may be approximated by its first term, leading to

$$\frac{\partial \delta f_a}{\partial t} + v\mu \frac{\partial \delta f_a}{\partial Z} - o\Omega \frac{\partial \delta f_a}{\partial \phi} \simeq -g_{x\sigma} \frac{\partial F_a}{\partial x_\sigma}. \quad (30)$$

Equation (30) can readily be solved by the method of characteristics and we obtain

$$\delta f_a(t) = \delta f_a(t_0) - \int_{t_0}^t ds [g_{x\sigma}(x_\nu^*, s) \frac{\partial F_a(x_\nu, s)}{\partial x_\sigma}]', \quad (31)$$

where the prime indicates that the bracketed quantities are to be evaluated along the characteristics, i.e. an unperturbed particle orbit in the uniform magnetic field, given by

$$\begin{aligned} \bar{X} &= x_0, \bar{Y} = y_0, \bar{Z} = z_0 + v\mu(s - t), \\ \bar{x} &= x_0 - \frac{v\sqrt{1-\mu^2}}{o\Omega} \sin(\bar{\phi}), \\ \bar{y} &= y_0 + \frac{v\sqrt{1-\mu^2}}{o\Omega} \cos(\bar{\phi}), \\ \bar{z} &= z_0 + v\mu(s - t) \end{aligned}$$

$$\bar{p} = p, \bar{\mu} = \mu, \bar{\phi} = \phi_0 - o\Omega(s - t), \quad (32)$$

where all $(x_0, y_0, z_0, \phi_0, p, \mu)$ denote the initial phase space coordinate values at time t_0 . Moreover, we demand that at the initial time t_0 the particle's phase space density is completely uncorrelated to the turbulent field, so that the ensemble average

$$\langle \delta f_a g_{x_\sigma} \rangle = 0 \quad (33)$$

vanishes. Then, inserting (31) into the averaged (24) leads to

$$\frac{\partial F_a}{\partial t} + v\mu \frac{\partial F_a}{\partial Z} - o\Omega \frac{\partial F_a}{\partial \phi} = S_a(\mathbf{x}, \mathbf{p}, t) + \frac{1}{p^2} \frac{\partial}{\partial x_\sigma} \left(\langle p^2 g_{x_\sigma} \int_{t_0}^t ds [g_{x_\nu}(x_\nu, s) \frac{\partial F_a(x_\nu, s)}{\partial x_\sigma}]' \rangle \right). \quad (34)$$

Note that the third term on the right-side of (26) if kept, would vanish in (34) because $\langle g_{x_\sigma} \rangle = 0$. Here $(t - t_0) \sim T$, where T satisfies the restriction (28). Under certain physical conditions the integrodifferential equation (34) reduces to a differential equation for F_a . The second term on the right-hand side of (34) can be rearranged as

$$\begin{aligned} M_1 &= \frac{1}{p^2} \frac{\partial}{\partial x_\sigma} \left(\langle p^2 g_{x_\sigma} \int_{t_0}^t ds [g_{x_\nu}(x_\nu, s) \frac{\partial F_a(x_\nu, s)}{\partial x_\sigma}]' \rangle \right) \\ &= \frac{1}{p^2} \frac{\partial}{\partial x_\sigma} \left(p^2 \int_{t_0}^t ds \langle g_{x_\sigma} g'_{x_\nu}(x_\nu, s) \rangle \left[\frac{\partial F_a(x_\nu, s)}{\partial x_\sigma} \right]' \right). \end{aligned} \quad (35)$$

Suppose that there exists a correlation time t_c so that the correlation function of magnetic and electric irregularities that determine the correlation function $\langle g_{x_\sigma} g'_{x_\nu} \rangle$, falls to a negligible magnitude for times $t - s > t_c$. This means that the important contribution to the right-hand side of (35) comes from the integral from $t - t_c$ to t which can be assumed to be finite. Moreover, suppose that the variation of $[\partial F_a / \partial x_\nu]'$ during this time interval is small enough to consider that the value is nearly equal to that as $s = t$. Then the term (35) reduces to

$$\begin{aligned} M_1 &\simeq \frac{1}{p^2} \frac{\partial}{\partial x_\sigma} \left(p^2 \left[\int_{t-t_c}^t ds \langle g_{x_\sigma} g_{x_\nu}(x_\nu, s) \rangle \right]' \frac{\partial F_a(x_\nu, s)}{\partial x_\sigma} \right) \\ &= \frac{1}{p^2} \frac{\partial}{\partial x_\sigma} \left(p^2 \left[\int_0^t ds \langle g_{x_\sigma} g_{x_\nu}(x_\nu, s) \rangle \right]' \frac{\partial F_a(x_\nu, s)}{\partial x_\sigma} \right). \end{aligned} \quad (36)$$

The requirement (28), i.e. $t - t_0 \gg t_c$, makes the term (36) a function of t alone, eliminating any dependence upon conditions at t_0 which justifies the replacement 0 for

$t - t_c$ in the lower boundary of the integration. With these rearrangements (34) reduces to a diffusion equation, involving only second order correlation functions of the fluctuating field g_{x_σ} integrated along the unperturbed orbit. This equation, named Fokker-Planck equation is

$$\frac{\partial F_a}{\partial t} + v\mu \frac{\partial F_a}{\partial Z} - o\Omega \frac{\partial F_a}{\partial \phi} = S_a(\mathbf{x}, \mathbf{p}, t) + \frac{1}{p^2} \frac{\partial}{\partial x_\sigma} (p^2 D_{x_\sigma x_\nu} \frac{\partial F_a}{\partial x_\nu}), \quad (37)$$

with the Fokker-Planck coefficients

$$D_{\sigma\nu}(x_\nu, t) = \int_0^t ds \langle \bar{g}_{x_\sigma}(t) \bar{g}_{x_\nu}(s) \rangle, \quad (38)$$

being homogenous integrals along unperturbed particle orbits of the fluctuating force field's correlations functions. The bar notation indicates that the force fields have to be calculated along unperturbed orbit of the particles.

3.2 The Diffusion Approximation

The Fokker-Planck equation (37) with its 25 Fokker-Planck coefficients is very complicated and cannot be solved in most cases. However, that in comparison to

$$\frac{\partial}{\partial \mu} D_{\mu\mu} \frac{\partial F_a}{\partial \mu} + \frac{\partial}{\partial \mu} D_{\mu\phi} \frac{\partial F_a}{\partial \phi} + \frac{\partial}{\partial \phi} D_{\phi\mu} \frac{\partial F_a}{\partial \mu} + \frac{\partial}{\partial \phi} D_{\phi\phi} \frac{\partial F_a}{\partial \phi} \quad (39)$$

apart from the injection function S_a all other terms on the right-hand of (37) are of the order (v_{ph}/v) , $(v_{ph}/v)^2$, $(v_{ph}/v)(R_L/R)$ or $(R_L/R)^2$, where $v_{ph} = \omega_R/k$ is the plasma waves phase speed, $R_L = v/\Omega$ is the gyroradius of a particle and R is a typical length scale for the variation of F_a in X and Y . Therefore, if we consider only particle distributions which are weakly variable in X and Y , i.e. $R_L \ll R$, we can argue that the fastest particle-wave interaction processes are diffusion in gyrophase ϕ and pitch angle μ , since for low frequency magnetohydrodynamical waves the phase speed v_{ph} is much less than the individual cosmic ray particle speeds, i.e. $v_{ph}/v \ll 1$. Then, we can follow the analysis splitting the particle distribution function into its average in pitch angle and an isotropic part (Jokipii 1966, Hasselmann and Wibberenz 1968, and Skilling, 1975)

$$F_a(\mathbf{x}, p, \mu, \phi, t) = M_a(\mathbf{x}, p, t) + G_a(\mathbf{x}, p, \mu, \phi, t), \quad (40)$$

where

$$M_a(\mathbf{x}, p, t) = \frac{1}{4\pi} \int_0^{2\pi} d\phi \int_{-1}^1 d\mu F_a(\mathbf{x}, p, \mu, \phi, t),$$

$$\frac{1}{4\pi} \int_0^{2\pi} d\phi \int_{-1}^1 d\mu G_a(\mathbf{x}, p, \mu, \phi, t) = 0. \quad (41)$$

Substituting (40) in the Fokker-Planck equation (37) and averaging over μ and ϕ using (41) we obtain

$$\begin{aligned} & \frac{\partial M_a}{\partial t} + \frac{v}{4\pi} \frac{\partial}{\partial Z} \int_0^{2\pi} d\phi \int_{-1}^1 d\mu \mu G_a - S_a(\mathbf{x}, \mathbf{p}, t) = \\ & \frac{1}{p^2} \frac{\partial}{\partial p} \left[\frac{1}{4\pi} \int_0^{2\pi} d\phi \int_{-1}^1 d\mu p^2 (D_{pp} \frac{\partial M_a}{\partial p} + D_{pX} \frac{\partial M_a}{\partial X} + D_{pY} \frac{\partial M_a}{\partial Y}) \right] + \\ & \frac{\partial}{\partial X} \left[\frac{1}{4\pi} \int_0^{2\pi} d\phi \int_{-1}^1 d\mu (D_{Xp} \frac{\partial M_a}{\partial p} + D_{XX} \frac{\partial M_a}{\partial X} + D_{XY} \frac{\partial M_a}{\partial Y}) \right] + \\ & \frac{\partial}{\partial Y} \left[\frac{1}{4\pi} \int_0^{2\pi} d\phi \int_{-1}^1 d\mu (D_{Yp} \frac{\partial M_a}{\partial p} + D_{YX} \frac{\partial M_a}{\partial X} + D_{YY} \frac{\partial M_a}{\partial Y}) \right] + \\ & \frac{1}{p^2} \frac{\partial}{\partial x_{ii=(p,X,Y)}} \left[\frac{1}{4\pi} \int_0^{2\pi} d\phi \int_{-1}^1 d\mu p^2 (d_{ij} \frac{\partial G_a}{\partial x_{jj=(p,\mu,\phi,X,Y)}}) \right], \end{aligned} \quad (42)$$

where we have used $D_{\mu x_i} = 0$ for $|\mu| = 1$ and the periodicity $G_a(\phi) = G_a(\phi + 2\pi)$. The diffusion approximation applies if the particle densities are slowly varying in the time and space, i.e.

$$\begin{aligned} \frac{\partial M_a}{\partial t} &= o\left(\frac{M_a}{T}\right), \quad \frac{\partial M_a}{\partial Z} = o\left(\frac{M_a}{L}\right), \\ \frac{\partial G_a}{\partial t} &= o\left(\frac{G_a}{T}\right), \quad \frac{\partial G_a}{\partial Z} = o\left(\frac{G_a}{L}\right), \end{aligned} \quad (43)$$

where $T \gg \tau \simeq o(1/D_{\mu\mu})$ and $L \gg v\tau$, where τ denotes the pitch angle relaxation time. In this case, the cosmic ray particles have time to adjust locally to a near isotropic equilibrium, so that $G_a \ll M_a$. Subtracting the averaged Fokker-Planck equation (42) from the full Fokker-Planck equation (37) and keeping only terms which are at most of first order in the small quantities (τ/T) , $(v\tau/L)$, (v_{ph}/v) and (R_L/R) , we obtain to lowest order an approximation for anisotropy G_a in terms of the isotropic distribution function M_a :

$$\begin{aligned} & [o\Omega + \frac{\partial}{\partial \mu} D_{\mu\phi}] \frac{\partial G_a}{\partial \phi} + \frac{\partial}{\partial \phi} (D_{\phi\phi} \frac{\partial G_a}{\partial \phi}) + \frac{\partial}{\partial \mu} (D_{\mu\mu} \frac{\partial G_a}{\partial \mu}) \simeq \\ & v\mu \frac{\partial M_a}{\partial Z} - \frac{\partial}{\partial \mu} (D_{\mu p} \frac{\partial M_a}{\partial p}) - \frac{\partial}{\partial \mu} (D_{\mu X} \frac{\partial M_a}{\partial X}) - \end{aligned}$$

$$\frac{\partial}{\partial \mu}(D_{\mu Y} \frac{\partial M_a}{\partial Y}) - \frac{\partial}{\partial \phi}(D_{\phi X} \frac{\partial M_a}{\partial X}) - \frac{\partial}{\partial \phi}(D_{\phi Y} \frac{\partial M_a}{\partial Y}). \quad (44)$$

Since G_a is periodic in the gyrophase we can express it as a Fourier series

$$G_a(\mathbf{x}, p, \mu, \phi) = \sum_{s=-\infty}^{\infty} G_s(\mathbf{x}, p, \mu) e^{is\phi}. \quad (45)$$

For our purpose only G_{-1} , G_0 and G_1 are of interest since all other terms do not contribute to the averaged Fokker-Planck equation (42) because all Fokker-Planck coefficients have a periodicity in gyrophase with a maximal period of 2π . Inserting (45) into (44) and comparing coefficients we derive the two equations

$$\frac{\partial}{\partial \mu} [D_{\mu\mu} \frac{\partial G_0}{\partial \mu} + D_{\mu p} \frac{\partial M_a}{\partial p}] = v\mu \frac{\partial M_a}{\partial Z}, \quad (46)$$

and

$$[io\Omega - D_{\phi\phi}]G_1 + \frac{\partial}{\partial \mu} D_{\mu\mu} \frac{\partial G_1}{\partial \mu} = \Lambda, \quad (47)$$

where

$$\Lambda = -[\frac{\partial D_{\mu X}}{\partial \phi} + \frac{\partial}{\partial \phi}(D_{\phi X}) \frac{\partial M_a}{\partial X}] - [\frac{\partial}{\partial \mu}(D_{\mu Y} + \frac{\partial D_{\phi Y}}{\partial \phi}) \frac{\partial M_a}{\partial Y}], \quad (48)$$

and where we neglected $D_{\mu\phi}$ in comparison to Ω . The equation for G_{-1} is not necessary since the anisotropy G_a is real and therefore the complex conjugate $G_1^* = G_{-1}$. Since $\Omega/D_{\mu\mu} \simeq o(B_0^2/\delta B^2)$ we may neglect the pitch angle diffusion term in (47) to obtain

$$G_1 \simeq \frac{\Lambda}{io\Omega - D_{\phi\phi}} \simeq \frac{\Lambda}{io\Omega}, \quad (49)$$

since gyrorotation is faster than gyrophase diffusion. Combining (48) and (49) we note that

$$G_1 \simeq o(\frac{(\delta B)^2}{B_0^2} M_a) \quad (50)$$

would be of second order in the small parameter $(\delta B/B_0)^2 \ll 1$. Reinserting G_1 and G_{-1} into the averaged Fokker-Planck equation (42) would then yield terms of the order $(\delta B/B_0)^4$. However, the Fokker-Planck equation was derived by truncation of the order $(\delta B/B_0)^2$. For consistency, G_1 has to be neglected and we approximate (45) by

$$G_a \simeq G_0, \quad (51)$$

where G_0 obeys (46).

3.2.1 Cosmic Ray Anisotropy

Integrating (46) over μ we obtain

$$D_{\mu\mu} \frac{\partial G_a}{\partial \mu} + D_{\mu p} \frac{\partial M_a}{\partial p} = c_1 + \frac{v\mu^2}{2} \frac{\partial M_a}{\partial Z}, \quad (52)$$

where the integration constant c_1 is determined from the requirement that the left-hand side of (52) vanishes for $\mu = \pm 1$, yielding

$$c_1 = -\frac{v}{2} \frac{\partial M_a}{\partial Z}. \quad (53)$$

Using (53) in (52) we derive

$$\frac{\partial G_a}{\partial \mu} = -\frac{1-\mu^2}{2D_{\mu\mu}} v \frac{\partial M_a}{\partial Z} - \frac{D_{\mu p}}{D_{\mu\mu}} \frac{\partial M_a}{\partial p}. \quad (54)$$

Integrating this equation gives for anisotropy

$$G_a(\mu) = c_2 - \frac{v}{2} \frac{\partial M_a}{\partial Z} \int_{-1}^{\mu} d\nu \frac{1-\nu^2}{D_{\mu\mu}(\nu)} - \frac{\partial M_a}{\partial p} \int_{-1}^{\mu} d\nu \frac{D_{\mu p}(\nu)}{D_{\mu\mu}(\nu)}, \quad (55)$$

where the integration constant c_2 is determined by condition (41). We then obtain for the anisotropy

$$\begin{aligned} G_a(\mu) = & \frac{v}{4} \frac{\partial M_a}{\partial Z} \left[\int_{-1}^1 d\mu \frac{(1-\mu^2)(1-\mu)}{D_{\mu\mu}(\mu)} - 2 \int_{-1}^{\mu} d\nu \frac{1-\nu^2}{D_{\mu\mu}(\nu)} \right] + \\ & \frac{1}{2} \frac{\partial M_a}{\partial p} \left[\int_{-1}^1 d\mu (1-\mu) \frac{D_{\mu p}(\mu)}{D_{\mu\mu}(\mu)} - 2 \int_{-1}^{\mu} d\nu \frac{D_{\mu p}(\nu)}{D_{\mu\mu}(\nu)} \right]. \end{aligned} \quad (56)$$

Apparently the anisotropy (56) is made up of two components. The first is related to pitch angle scattering and the spatial gradient of the isotropic distribution M . This term will provide the spatial diffusion of particles. Pitch angle diffusion produces spatial effects in a plasma if a density gradient along the ordered magnetic field, $\partial M_a/\partial Z$, is present. The second contribution to the anisotropy (55) stems from the moment gradient of M_a and is related to the Compton-Getting effect (Compton, Getting 1935). Expanding the anisotropy (56) into orthonormal Legendre polynomials $P_l(\mu)$, i.e.

$$G_a(\mu, Z, p) = \sum_{l=0}^{\infty} A_l(Z, p) P_l(\mu), \quad (57)$$

defines the harmonics $A_l(Z, p)$ of the anisotropy.

3.2.2 The Diffusion-Convection Transport Equation

We insert (54) and (55) into the averaged Fokker-Planck equation (42). For the two μ -integrals we obtain

$$\begin{aligned} \int_{-1}^1 d\mu \mu G_a(\mu) &= \frac{v}{2} \frac{\partial M_a}{\partial Z} \int_{-1}^1 d\mu \int_{-1}^{\mu} d\nu \frac{1 - \nu^2}{D_{\mu\mu}(\nu)} - \\ &\frac{\partial M_a}{\partial p} \int_{-1}^1 d\mu \mu \int_{-1}^{\mu} d\nu \frac{D_{\mu p}(\nu)}{D_{\mu\mu}(\nu)} = \\ &-\frac{v}{4} \frac{\partial M_a}{\partial Z} \int_{-1}^1 d\mu \frac{(1 - \mu^2)^2}{D_{\mu\mu}(\mu)} - \\ &\frac{1}{2} \frac{\partial M_a}{\partial p} \int_{-1}^1 d\mu \frac{1 - \mu^2 D_{\mu p}(\mu)}{D_{\mu\mu}(\mu)}, \end{aligned} \quad (58)$$

where we partially integrated the right-hand side, and

$$\int_{-1}^1 d\mu D_{\mu p} \frac{\partial G_a}{\partial \mu} = -\frac{v}{2} \frac{\partial M_a}{\partial Z} \int_{-1}^1 d\mu \frac{(1 - \mu^2) D_{\mu p}(\mu)}{D_{\mu\mu}(\mu)} - \frac{\partial M_a}{\partial p} \int_{-1}^1 d\mu \frac{D_{\mu p}^2(\mu)}{D_{\mu\mu}(\mu)}. \quad (59)$$

Collecting terms in (42) we obtain

$$\begin{aligned} \frac{\partial M_a}{\partial t} - S_a(\mathbf{x}, \mathbf{p}, t) &= \frac{\partial}{\partial z} \kappa_{zz} \frac{\partial M_a}{\partial z} - \frac{1}{4p^2} \frac{\partial(p^2 v A_1)}{\partial p} \frac{\partial M_a}{\partial z} + \\ &\frac{\partial}{\partial X} [\kappa_{XX} \frac{\partial M_a}{\partial X} + \kappa_{XY} \frac{\partial M_a}{\partial Y}] + \\ &\frac{\partial}{\partial Y} [\kappa_{YY} \frac{\partial M_a}{\partial Y} + \kappa_{YX} \frac{\partial M_a}{\partial X}] + \\ &\frac{1}{p^2} \frac{\partial}{\partial p} (p^2 A_2 \frac{\partial M_a}{\partial p}) + \frac{v}{4} \frac{\partial A_1}{\partial z} \frac{\partial M_a}{\partial p}, \end{aligned} \quad (60)$$

where the components of the spatial diffusion tensor κ_{ij} , the rate of adiabatic deceleration A_1 and the momentum diffusion coefficient A_2 are determined by the pitch angle averages of Fokker-Planck coefficients as

$$\kappa_{zz} = v\lambda/3 = \frac{v^2}{8} \int_{-1}^1 d\mu \frac{(1 - \mu^2)^2}{D_{\mu\mu}(\mu)}, \quad (61)$$

$$\kappa_{XX} = \frac{1}{2} \int_{-1}^1 d\mu D_{XX}(\mu), \quad (62)$$

$$\kappa_{XY} = \frac{1}{2} \int_{-1}^1 d\mu D_{XY}(\mu), \quad (63)$$

$$\kappa_{YY} = \frac{1}{2} \int_{-1}^1 d\mu D_{YY}(\mu), \quad (64)$$

$$\kappa_{YX} = \frac{1}{2} \int_{-1}^1 d\mu D_{YX}(\mu), \quad (65)$$

$$A_1 = \int_{-1}^1 d\mu (1 - \mu^2) \frac{D_{\mu p}(\mu)}{D_{\mu\mu}(\mu)}, \quad (66)$$

and

$$A_2 = \frac{1}{2} \int_{-1}^1 d\mu \left[D_{pp}(\mu) - \frac{D_{\mu p}^2(\mu)}{D_{\mu\mu}(\mu)} \right]. \quad (67)$$

Equation (60) is commonly referred to as the diffusion-convection equation for the isotropic pitch-angle averaged particle distribution function $M_a(\mathbf{x}, p, t)$. In its the most general form it contains spatial diffusion and convection terms, describing the propagation of cosmic rays in space, as well as momentum diffusion and convection terms, describing the acceleration of cosmic rays, i.e. the transport in momentum space. Whether in a specific physical situation all seven cosmic ray transport parameters (61)-(67) arise and are different from zero, depends solely on the nature and the statistical properties of the plasma turbulence and the background medium. In (61) we also defined the spatial diffusion coefficient along the ordered magnetic field κ_{zz} in terms of the mean free path for scattering λ . Note that the diffusion-convection equation (60) has been derived in the comoving reference frame, i.e. the rest system of the moving plasma. If the situation is that the background plasma, supporting the plasma waves, moves with respect to the observer with non-relativistic bulk speed $U \ll c$ along the ordered magnetic field, we can apply a simple Galilean transformation to (60).

4 Derivation of the Fokker-Planck Coefficients

We are particularly interested in the UHECR component of the cosmic rays. We start from the generally-accepted hypothesis that galactic point sources like supernova remnants would inject cosmic ray particles only at energies below 10^{14} eV. Our purpose is to find out if there is some other mechanism able to accelerate particles up to ultrahigh energies.

Observationally it is well established that the interstellar medium is turbulent up to the largest scales, due to the motion of giant clouds, supernova explosions, stellar winds and formation of superbubbles, loops and so on. Measurements of the density fluctuations indicate the presence of Kolmogorov-type fluctuations spectrum up to scales of 100 pc. Together with an interstellar magnetic field strength of $\simeq 5\mu$ G this would allow acceleration up to particle energies $\sim 10^{17}$ eV. In this chapter, in order to model plasma turbulence, we give basic equations and step by step calculation of Fokker-Planck coefficients.

4.1 The Fokker-Planck coefficient $D_{\mu\mu}$

4.1.1 Equations of Motion

In order to derive relevant transport coefficients, spatial diffusion coefficient κ , the cosmic ray bulk speed V and momentum diffusion coefficient A_2 , we start from the random parts of the Lorentz force for the coordinates μ and p of the guiding center (S2002, 12.1)

$$g_\mu = \dot{\mu} = \frac{\Omega\sqrt{1-\mu^2}}{B_0} \left[\frac{c}{v}\sqrt{1-\mu^2}\delta E_{\parallel} + \frac{i}{\sqrt{2}} \left[e^{i\phi}(\delta B_r + i\mu\frac{c}{v}\delta E_r) - e^{-i\phi}(\delta B_l - i\mu\frac{c}{v}\delta E_l) \right] \right], \quad (68)$$

$$g_p = \dot{p} = \frac{m_a c \gamma \Omega}{p B_0} \mathbf{p} \cdot \delta \mathbf{E} = \frac{\Omega p c}{v B_0} \left[\mu \delta E_{\parallel} + \sqrt{\frac{1-\mu^2}{2}} (\delta E_l e^{-i\phi} + \delta E_r e^{i\phi}) \right], \quad (69)$$

In these equations we use pitch-angle cosine μ , the particle speed v , the gyrophase ϕ , the cosmic ray particle gyrofrequency $\Omega = ZeB_0/(mc\gamma)$ in the background field B_0 and the turbulent fields $\delta B_{l,r}$ and $\delta E_{l,r}$ which are related to the left-handed and right-handed polarized field components. These random force terms determine the corresponding Fokker-Planck coefficients (Hall & Sturrock 1968)

$$\begin{aligned}
D_{\mu\mu} &= \lim_{t \rightarrow \infty} \frac{\langle (\Delta\mu)^2 \rangle}{2t} \\
D_{\mu p} &= \lim_{t \rightarrow \infty} \frac{\langle \Delta\mu(\Delta p)^* \rangle}{2t} \\
D_{p\mu} &= \lim_{t \rightarrow \infty} \frac{\langle \Delta p(\Delta\mu)^* \rangle}{2t} \\
D_{pp} &= \lim_{t \rightarrow \infty} \frac{\langle (\Delta p)^2 \rangle}{2t}
\end{aligned} \tag{70}$$

which are calculated from the respective displacements $(\Delta\mu)$ and (Δp) caused by the stochastic field components. In this section we calculate step by step the Fokker-Planck coefficient $D_{\mu\mu}$; the other coefficients are calculated similarly.

4.1.2 Step 1: Quasilinear Approximation

The quasilinear approximation is achieved by replacing in the Fourier transform of the fluctuating electric and magnetic field

$$\delta\mathbf{E}(\mathbf{x}(t), t) = \int_{-\infty}^{+\infty} d^3k \delta\mathbf{E}(\mathbf{k}, t) e^{i\mathbf{k}\cdot\mathbf{x}(t)} \simeq \int_{-\infty}^{+\infty} d^3k \delta\mathbf{E}(\mathbf{k}, t) e^{i\mathbf{k}\cdot\mathbf{x}^0(t)} \tag{71}$$

$$\delta\mathbf{B}(\mathbf{x}(t), t) = \int_{-\infty}^{+\infty} d^3k \delta\mathbf{B}(\mathbf{k}, t) e^{i\mathbf{k}\cdot\mathbf{x}(t)} \simeq \int_{-\infty}^{+\infty} d^3k \delta\mathbf{B}(\mathbf{k}, t) e^{i\mathbf{k}\cdot\mathbf{x}^0(t)} \tag{72}$$

the true particle orbit $\mathbf{x}(t)$ by the unperturbed orbit $\mathbf{x}^0(t)$, resulting in

$$\phi(t) = \phi_0 - \Omega t \tag{73}$$

and (Schlickeiser 2002, (12.2.3a))

$$\delta B_{l,r,\parallel} \approx \sum_{n=-\infty}^{+\infty} d^3k \delta B_{l,r,\parallel}(\mathbf{k}, t) J_n(W) e^{in(\psi-\phi_0)+i(k_{\parallel}v_{\parallel}+n\Omega)t+i\mathbf{k}\cdot\mathbf{x}_0}, \tag{74}$$

respectively, where $\mathbf{x}_0 = (x_0, y_0, z_0)$ denotes the initial ($t = 0$) position of the cosmic ray particle and $W = \frac{v}{|\Omega|} \cdot k_{\perp} \sqrt{1 - \mu^2} = R_L \cdot k_{\perp} \sqrt{1 - \mu^2}$ involving the cosmic ray Larmor radius $R_L = v/|\Omega|$. For the wave vector \mathbf{k} we have used cylindrical coordinates:

$$\begin{aligned}
k_{\parallel} &= k_z, \\
k_{\perp} &= \sqrt{k_x^2 + k_y^2}, \\
\psi &= \operatorname{arccot}\left(\frac{k_x}{k_y}\right).
\end{aligned} \tag{75}$$

With these approximations the equations of motion become

$$\begin{aligned} \frac{d\mu}{dt} \simeq h_\mu(t) &= \frac{\Omega\sqrt{1-\mu^2}}{B_0} \sum_{n=-\infty}^{\infty} \int d^3k e^{in(\psi-\phi_0)+i(k_{\parallel}v_{\parallel}+n\Omega)t+i\mathbf{k}\cdot\mathbf{x}_0} \left(\frac{c}{v} \sqrt{1-\mu^2} J_n(W) \delta E_{\parallel}(\mathbf{k}, t) \right. \\ &+ \left. \frac{i}{\sqrt{2}} J_{n+1}(W) e^{i\psi} [\delta B_r(\mathbf{k}, t) + i\mu \frac{c}{v} \delta E_r(\mathbf{k}, t)] - \frac{i}{\sqrt{2}} J_{n-1}(W) e^{-i\psi} [\delta B_l(\mathbf{k}, t) - i\mu \frac{c}{v} \delta E_l(\mathbf{k}, t)] \right) \end{aligned} \quad (76)$$

and

$$\begin{aligned} \frac{dp}{dt} \simeq h_p(t) &= \frac{\Omega pc}{vB_0} \sum_{n=-\infty}^{\infty} \int d^3k e^{in(\psi-\phi_0)+i(k_{\parallel}v_{\parallel}+n\Omega)t+i\mathbf{k}\cdot\mathbf{x}_0} \\ &\left(\mu J_n(W) \delta E_{\parallel}(\mathbf{k}, t) + \frac{\sqrt{1-\mu^2}}{2} [J_{n+1}(W) e^{i\psi} \delta E_r(\mathbf{k}, t) + J_{n-1}(W) e^{-i\psi} \delta E_l(\mathbf{k}, t)] \right) \end{aligned} \quad (77)$$

4.1.3 Step 2: The Kubo Formalism

Integration of (76) yields

$$\Delta\mu(t) = \int_0^t dt_1 h_\mu(t_1) \quad (78)$$

for the displacement in pitch angle cosine. We then find for the ensemble average

$$\langle (\Delta\mu)^2 \rangle = \langle \int_0^t dt_1 h_\mu(t_1) \int_0^t dt_2 h_\mu^*(t_2) \rangle \quad (79)$$

which we evaluate using the Taylor-Green-Kubo formalism (Green 1951, Kubo 1957). As illustrated in Fig. 5, instead of integrating over the full box we may integrate over the hatched triangle and multiply by the factor 2 (Peskin & Schroeder 1995) implying

$$\begin{aligned} \langle (\Delta\mu)^2 \rangle &= 2 \langle \int_0^t dt_1 h_\mu(t_1) \int_0^{t_1} dt_2 h_\mu^*(t_2) \rangle = 2 \langle \int_0^t dt_1 h_\mu(t_1) \int_{-t_1}^0 d\tau h_\mu^*(\tau + t_1) \rangle \\ &= 2 \int_0^t dt_1 \int_{-t_1}^0 d\tau \langle h_\mu(t_1) h_\mu^*(\tau + t_1) \rangle \end{aligned} \quad (80)$$

where we substituted $\tau = t_2 - t_1$.

As second assumption (after the quasilinear approximation) we use the *quasi-stationary turbulence condition* that the correlation function $\langle h_\mu(t_1) h_\mu^*(\tau + t_1) \rangle$ depends only on the absolute value of the time difference $[t_2 - t_1] = |\tau|$ so that

$$\langle h_\mu(t_1) h_\mu^*(\tau + t_1) \rangle = \langle h_\mu(0) h_\mu^*(0 + \tau) \rangle \quad (81)$$

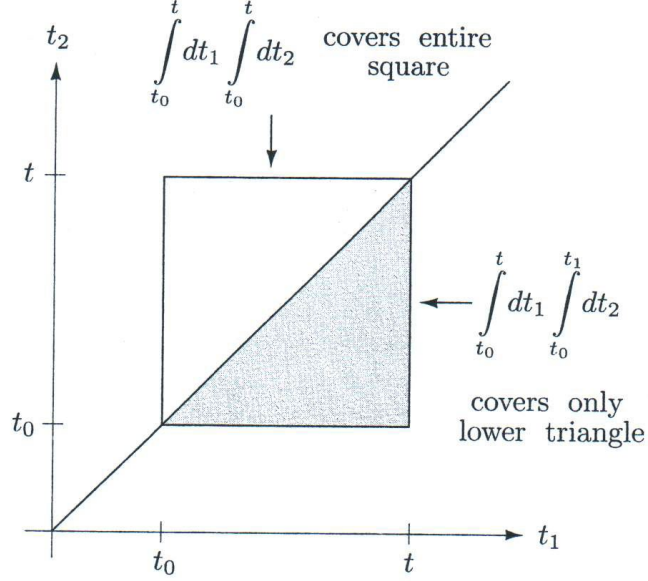


Figure 5: Geometric interpretation of (79)

implying with the substitution $s = -\tau$

$$\langle (\Delta\mu)^2 \rangle = 2 \int_0^t dt_1 \int_{-t_1}^0 d\tau \langle h_\mu(0)h_\mu^*(0 + \tau) \rangle = 2 \int_0^t dt_1 \int_0^{t_1} ds \langle h_\mu(0)h_\mu^*(s) \rangle \quad (82)$$

Thirdly, we assume that there exists a finite correlation time t_c such that the correlation function $\langle h_\mu(0)h_\mu^*(s) \rangle \rightarrow 0$ falls to a negligible magnitude for $s \rightarrow \infty$. This allows us to replace the upper integration boundary in the second integral by infinity so that

$$\langle (\Delta\mu)^2 \rangle \simeq 2 \int_0^t dt_1 \int_0^\infty ds \langle h_\mu(0)h_\mu^*(s) \rangle = 2t \int_0^\infty ds \langle h_\mu(0)h_\mu^*(s) \rangle \quad (83)$$

As can be seen, the two assumptions of quasi-stationary turbulence and the existence of a finite correlation time t_c guarantee diffusive behaviour of quasilinear transport in agreement with the conclusion of Shalchi & Schlickeiser (2004). For the quasilinear Fokker-Planck coefficients (70) we then obtain

$$D_{\mu\mu} = \int_0^\infty ds \langle h_\mu(0)h_\mu^*(s) \rangle \quad (84)$$

and similarly

$$D_{\mu p} = D_{p\mu} = \int_0^\infty ds \langle h_\mu(0)h_p^*(s) \rangle \quad (85)$$

and

$$D_{pp} = \int_0^\infty ds < h_p(0)h_p^*(s) > \quad (86)$$

4.1.4 Step 3: Homogenous Turbulence

From the quasilinear equation of motion (76) we infer

$$\begin{aligned} h_\mu(0)h_\mu^*(s) &= \frac{\Omega^2}{B_0^2}(1 - \mu^2) \sum_{n=-\infty}^{\infty} \sum_{m=-\infty}^{\infty} \int d^3k \int d^3k' e^{i(n-m)(\psi-\phi_0) - i(k'_\parallel v_\parallel + m\Omega)s + i(\mathbf{k}-\mathbf{k}') \cdot \mathbf{x}_0} \\ &\quad \left[\frac{c}{v} \sqrt{1 - \mu^2} J_n(W) \delta E_\parallel(\mathbf{k}, 0) + \frac{i}{\sqrt{2}} J_{n+1}(W) e^{i\psi} [\delta B_r(\mathbf{k}, 0) + i\mu \frac{c}{v} \delta E_r(\mathbf{k}, 0)] \right. \\ &\quad \left. - \frac{i}{\sqrt{2}} J_{n-1}(W) e^{-i\psi} [B_l(\mathbf{k}, 0) - i\mu \frac{c}{v} \delta E_l(\mathbf{k}, 0)] \right] \\ &\quad \left[\frac{c}{v} \sqrt{1 - \mu^2} J_m(W') \delta E_\parallel^*(\mathbf{k}', s) - \frac{i}{\sqrt{2}} J_{m+1}(W') e^{-i\psi} [\delta B_r^*(\mathbf{k}', s) - i\mu \frac{c}{v} \delta E_r^*(\mathbf{k}', s)] \right. \\ &\quad \left. + \frac{i}{\sqrt{2}} J_{m-1}(W') e^{i\psi} [B_l^*(\mathbf{k}', s) + i\mu \frac{c}{v} \delta E_l^*(\mathbf{k}', s)] \right] \end{aligned} \quad (87)$$

Next, as fourth assumption we use that the turbulence field which is homogeneously distributed, and average (87) over the initial spatial position of the cosmic ray particles using

$$\frac{1}{(2\pi)^3} \int_{-\infty}^{+\infty} d^3\mathbf{x}_0 e^{i(\mathbf{k}-\mathbf{k}') \cdot \mathbf{x}_0} = \delta(\mathbf{k} - \mathbf{k}') \quad (88)$$

implying that turbulence fields at different wavevectors are uncorrelated. The respective ensemble average of (87) then involve the correlation tensors

$$< \delta B_\alpha(\mathbf{k}, 0) \delta B_\beta^*(\mathbf{k}', s) > = \delta(\mathbf{k} - \mathbf{k}') P_{\alpha\beta}(\mathbf{k}, s) \quad (89)$$

$$< \delta E_\alpha(\mathbf{k}, 0) \delta E_\beta^*(\mathbf{k}', s) > = \delta(\mathbf{k} - \mathbf{k}') R_{\alpha\beta}(\mathbf{k}, s) \quad (90)$$

$$< \delta B_\alpha(\mathbf{k}, 0) \delta E_\beta^*(\mathbf{k}', s) > = \delta(\mathbf{k} - \mathbf{k}') T_{\alpha\beta}(\mathbf{k}, s) \quad (91)$$

$$< \delta E_\alpha(\mathbf{k}, 0) \delta B_\beta^*(\mathbf{k}', s) > = \delta(\mathbf{k} - \mathbf{k}') Q_{\alpha\beta}(\mathbf{k}, s). \quad (92)$$

After performing the \mathbf{k}' -integration and employing the random phase approximation, that the initial phase ϕ_0 of the cosmic particle is a random variable that can take on any value between 0 and 2π , the averaging over ϕ_0 results in

$$\begin{aligned}
D_{\mu\mu} &= \frac{1}{(2\pi)^4} \int_{-\infty}^{+\infty} d^3\mathbf{x}_0 e^{i(\mathbf{k}-\mathbf{k}')\cdot\mathbf{x}_0} \int_0^{2\pi} d\phi_0 \int_0^\infty ds \langle h_\mu(0)h_\mu^*(s) \rangle = \\
&\quad \frac{\Omega^2}{B_0^2} (1-\mu^2) \sum_{n=-\infty}^{\infty} \int_{-\infty}^{\infty} d^3k \int_0^\infty ds e^{-i(k_{\parallel}v_{\parallel}+n\Omega)s} \\
&\cdot \left(\frac{c^2}{v^2} (1-\mu^2) J_n^2(W) R_{\parallel}(\mathbf{k}, s) + \frac{1}{2} J_{n+1}^2(W) [P_{RR}(\mathbf{k}, s)] + \mu^2 \frac{c^2}{v^2} R_{RR}(\mathbf{k}, s) + i\mu \frac{c}{v} (Q_{RR}(\mathbf{k}, s) - T_{RR}(\mathbf{k}, s)) \right) \\
&\quad + \frac{1}{2} J_{n-1}^2(W) [P_{LL}(\mathbf{k}, s) + \mu^2 \frac{c^2}{v^2} R_{LL}(\mathbf{k}, s) + i\mu \frac{c}{v} (T_{LL}(\mathbf{k}, s) - Q_{LL}(\mathbf{k}, s))] \\
&\quad - \frac{1}{2} J_{n-1}(W) J_{n+1}(W) [e^{2i\psi} (P_{RL}(\mathbf{k}, s) - \mu^2 \frac{c^2}{v^2} R_{RL}(\mathbf{k}, s) + i\mu \frac{c}{v} (T_{RL}(\mathbf{k}, s) + Q_{RL}(\mathbf{k}, s))) \\
&\quad + e^{-2i\psi} (P_{LR}(\mathbf{k}, s) - \mu^2 \frac{c^2}{v^2} R_{LR}(\mathbf{k}, s)) - i\mu \frac{c}{v} (T_{LR}(\mathbf{k}, s) + Q_{LR}(\mathbf{k}, s))] \\
&+ \frac{ic\sqrt{1-\mu^2}}{\sqrt{2}v} J_n(W) [J_{n+1}(W) (e^{i\psi} T_{R\parallel}(\mathbf{k}, s) - e^{-i\psi} Q_{\parallel R}(\mathbf{k}, s) + i\mu \frac{c}{v} (R_{R\parallel}(\mathbf{k}, s) e^{i\psi} + R_{\parallel R}(\mathbf{k}, s) e^{-i\psi})) \\
&\quad + J_{n-1}(W) (e^{i\psi} Q_{\parallel L}(\mathbf{k}, s) - e^{-i\psi} T_{\parallel L}(\mathbf{k}, s) + i\mu \frac{c}{v} (R_{\parallel L}(\mathbf{k}, s) e^{i\psi} + R_{L\parallel}(\mathbf{k}, s) e^{-i\psi}))] \quad (93)
\end{aligned}$$

4.1.5 Step 4: Plasma Wave Turbulence

In order to further reduce (93) we have to make additional assumptions about the geometry of the turbulence, and specially, the time dependance of the correlation functions, in order to perform the time(s)-integration. The geometry will be discussed in the Sec. 5.2. Here, we first define the properties of the plasma turbulence that will be considered. We follow the approach for the electromagnetic turbulence that represents the Fourier transforms of the magnetic and electric field fluctuations as superposition of N individual weakly damped plasma modes of frequencies

$$\omega = \omega_j(\mathbf{k}) = \omega_{R,j}(\mathbf{k}) - i\gamma_j(\mathbf{k}), \quad (94)$$

$j = 1, \dots, N$, which can have both the real and imaginary parts with $|\gamma_j| \ll |\omega_{R,j}|$, so that

$$[\mathbf{B}(\mathbf{k}, t), \mathbf{E}(\mathbf{k}, t)] = \sum_{j=1}^N [\mathbf{B}^j(\mathbf{k}), \mathbf{E}^j(\mathbf{k})] e^{-i\omega_j t} \quad (95)$$

Damping of the waves is counted with the a positive $\gamma^j > 0$. We need to add Maxwell's induction law

$$\mathbf{B}^j(\mathbf{k}) = \frac{c}{\omega_{R,j}} \mathbf{k} \times \mathbf{E}^j(\mathbf{k}). \quad (96)$$

As a consequence of (95), the magnetic correlation tensor (89) becomes

$$P_{\alpha\beta}(\mathbf{k}, s) = \sum_{j=1}^N P_{\alpha\beta}^j(\mathbf{k}) e^{-i\omega_{R,j}(\mathbf{k})s - \gamma_j(\mathbf{k})s}, \quad (97)$$

where

$$P_{\alpha\beta}^j(\mathbf{k}) = \langle B_{\alpha}^j(\mathbf{k}) B_{\beta}^{j*}(\mathbf{k}_1) \rangle \delta(\mathbf{k} - \mathbf{k}_1). \quad (98)$$

Corresponding relations hold for the other three correlation tensors.

With (97) we derive for the Fokker-Planck coefficient (93)

$$\begin{aligned} D_{\mu\mu} = & \frac{\Omega^2}{B_0^2} (1 - \mu^2) \sum_{j=1}^N \sum_{n=-\infty}^{\infty} \int_{-\infty}^{\infty} d^3k \int_0^{\infty} ds e^{-i(k_{\parallel}v_{\parallel} + \omega_{R,j} + n\Omega)s - \gamma_j s} \\ & \cdot \left(\frac{c^2}{v^2} (1 - \mu^2) J_n^2(W) R_{\parallel}^j(\mathbf{k}, s) + \frac{1}{2} J_{n+1}^2(W) [P_{RR}^j(\mathbf{k}, s)] + \mu^2 \frac{c^2}{v^2} R_{RR}^j(\mathbf{k}, s) + i\mu \frac{c}{v} (Q_{RR}^j(\mathbf{k}, s) - T_{RR}^j(\mathbf{k}, s)) \right) \\ & + \frac{1}{2} J_{n-1}^2(W) [P_{LL}^j(\mathbf{k}, s) + \mu^2 \frac{c^2}{v^2} R_{LL}^j(\mathbf{k}, s) + i\mu \frac{c}{v} (T_{LL}^j(\mathbf{k}, s) - Q_{LL}^j(\mathbf{k}, s))] \\ & - \frac{1}{2} J_{n-1}(W) J_{n+1}(W) [e^{2i\psi} (P_{RL}^j(\mathbf{k}, s) - \mu^2 \frac{c^2}{v^2} R_{RL}^j(\mathbf{k}, s) + i\mu \frac{c}{v} (T_{RL}^j(\mathbf{k}, s) + Q_{RL}^j(\mathbf{k}, s))) \\ & + e^{-2i\psi} (P_{LR}^j(\mathbf{k}, s) - \mu^2 \frac{c^2}{v^2} R_{LR}^j(\mathbf{k}, s)) - i\mu \frac{c}{v} (T_{LR}^j(\mathbf{k}, s) + Q_{LR}^j(\mathbf{k}, s))] \\ & + \frac{ic\sqrt{1-\mu^2}}{\sqrt{2}v} J_n(W) [J_{n+1}(W) (e^{i\psi} T_{R|}^j(\mathbf{k}, s) - e^{-i\psi} Q_{|R}^j(\mathbf{k}, s) + i\mu \frac{c}{v} (R_{R|}^j(\mathbf{k}, s) e^{i\psi} + R_{|R}^j(\mathbf{k}, s) e^{-i\psi})) \\ & + J_{n-1}(W) (e^{i\psi} Q_{|L}^j(\mathbf{k}, s) - e^{-i\psi} T_{L|}^j(\mathbf{k}, s) + i\mu \frac{c}{v} (R_{|L}^j(\mathbf{k}, s) e^{i\psi} + R_{L|}^j(\mathbf{k}, s) e^{-i\psi})))] \quad (99) \end{aligned}$$

The s -integration is readily perform and yields the Lorentzian resonance function

$$\mathcal{R}_j(\gamma_j) = \int_0^{\infty} ds e^{-i(k_{\parallel}v_{\parallel} + \omega_{R,j} + n\Omega)s - \gamma_j s} = \frac{\gamma_j(\mathbf{k})}{\gamma_j^2(\mathbf{k}) + [k_{\parallel}v_{\parallel} + \omega_{R,j}(\mathbf{k}) + n\Omega]^2} \quad (100)$$

In the case of negligible damping $\gamma \rightarrow 0$, use of the δ -function representation

$$\lim_{\gamma \rightarrow 0} \frac{\gamma}{\gamma^2 + \xi^2} = \pi \delta(\xi) \quad (101)$$

reduces the resonance function (100) to sharp δ -functions

$$\mathbf{R}^j(\gamma = 0) = \pi\delta(k_{\parallel}v_{\parallel} + \omega_{R,j} + n\Omega). \quad (102)$$

The Fokker-Planck coefficient (99) finally reads

$$\begin{aligned} D_{\mu\mu} &= \frac{\Omega^2}{B_0^2}(1 - \mu^2) \sum_{j=1}^N \sum_{n=-\infty}^{\infty} \int_{-\infty}^{\infty} d^3k \frac{\gamma_j(\mathbf{k})}{\gamma_j^2(\mathbf{k}) + [k_{\parallel}v_{\parallel} + \omega_{R,j}(\mathbf{k}) + n\Omega]^2} \\ &\cdot \left[\frac{c^2}{v^2}(1 - \mu^2) J_n^2(W) R_{\parallel}^j(\mathbf{k}, s) + \frac{1}{2} J_{n+1}^2(W) [P_{RR}^j(\mathbf{k}, s) + \mu^2 \frac{c^2}{v^2} R_{RR}^j(\mathbf{k}, s) + i\mu \frac{c}{v} (Q_{RR}^j(\mathbf{k}, s) - T_{RR}^j(\mathbf{k}, s))] \right. \\ &\quad + \frac{1}{2} J_{n-1}^2(W) [P_{LL}^j(\mathbf{k}, s) + \mu^2 \frac{c^2}{v^2} R_{LL}^j(\mathbf{k}, s) + i\mu \frac{c}{v} (T_{LL}^j(\mathbf{k}, s) - Q_{LL}^j(\mathbf{k}, s))] \\ &\quad - \frac{1}{2} J_{n-1}(W) J_{n+1}(W) [e^{2i\psi} (P_{RL}^j(\mathbf{k}, s) - \mu^2 \frac{c^2}{v^2} R_{RL}^j(\mathbf{k}, s) + i\mu \frac{c}{v} (T_{RL}^j(\mathbf{k}, s) + Q_{RL}^j(\mathbf{k}, s))) \\ &\quad \left. + e^{-2i\psi} (P_{LR}^j(\mathbf{k}, s) - \mu^2 \frac{c^2}{v^2} R_{LR}^j(\mathbf{k}, s)) - i\mu \frac{c}{v} (T_{LR}^j(\mathbf{k}, s) + Q_{LR}^j(\mathbf{k}, s))] \right. \\ &\quad + \frac{ic\sqrt{1 - \mu^2}}{\sqrt{2}v} J_n(W) [J_{n+1}(W) (e^{i\psi} T_{R|}^j(\mathbf{k}, s) - e^{-i\psi} Q_{|R}^j(\mathbf{k}, s) + i\mu \frac{c}{v} (R_{R|}^j(\mathbf{k}, s) e^{i\psi} + R_{|R}^j(\mathbf{k}, s) e^{-i\psi})) \\ &\quad \left. + J_{n-1}(W) (e^{i\psi} Q_{|L}^j(\mathbf{k}, s) - e^{-i\psi} T_{L|}^j(\mathbf{k}, s) + i\mu \frac{c}{v} (R_{|L}^j(\mathbf{k}, s) e^{i\psi} + R_{L|}^j(\mathbf{k}, s) e^{-i\psi})) \right] \quad (103) \end{aligned}$$

It remains to specify the geometry of the plasma wave turbulence through the correlation tensors which, according to Mattheaus & Smith (1981), have the form

$$P_{\alpha\beta}^j(\mathbf{k}) = \frac{g_i^j(\mathbf{k})}{k^2} \left[\delta_{\alpha\beta} - \frac{k_{\alpha}k_{\beta}}{k^2} + i\sigma(\mathbf{k})\epsilon_{\alpha\beta\lambda} \frac{k_{\lambda}}{k} \right], \quad (104)$$

where $\sigma(\mathbf{k})$ is the magnetic helicity and the function $g(\mathbf{k})$ determines different turbulence geometries. This will be discussed in Sec. 5.2.

4.2 The Other Fokker-Planck Coefficients $D_{\mu p}$ and D_{pp}

Applying the same approximations as in the last section to the other Fokker-Planck coefficients in (70) results in

$$\begin{aligned} D_{\mu p} &= D_{p\mu} = \frac{\Omega^2}{B_0^2} \sqrt{(1 - \mu^2)} \frac{pc}{v} \sum_{j=1}^N \sum_{n=-\infty}^{\infty} \int_{-\infty}^{\infty} d^3k \frac{\gamma_j(\mathbf{k})}{\gamma_j^2(\mathbf{k}) + [k_{\parallel}v_{\parallel} + \omega_{R,j}(\mathbf{k}) + n\Omega]^2} \\ &\cdot \left[\frac{c}{v} \mu \sqrt{(1 - \mu^2)} J_n^2(W) R_{\parallel}^j(\mathbf{k}, s) + \frac{c(1 - \mu^2)}{2} (J_n(W) J_{n+1}(W) e^{-i\psi} R_{|R}^j(\mathbf{k}, s) + \right. \\ &\quad \left. J_n(W) J_{n-1}(W) e^{i\psi} R_{|L}^j(\mathbf{k}, s)) + \frac{i\mu}{\sqrt{2}} J_n(W) J_{n+1}(W) e^{i\psi} T_{R|}^j(\mathbf{k}, s) - \frac{c}{v} \frac{\mu^2}{\sqrt{2}} J_n(W) J_{n+1}(W) e^{i\psi} R_{R|}^j(\mathbf{k}, s) \right] \end{aligned}$$

$$\begin{aligned}
& + \frac{i\sqrt{(1-\mu^2)}}{2\sqrt{2}} (J_{n+1}^2(W)T_{RR}^j(\mathbf{k}, s) + J_{n-1}(W)J_{n+1}(W)e^{2i\psi}T_{RL}^j(\mathbf{k}, s)) \\
& - \frac{c\mu\sqrt{1-\mu^2}}{v} \frac{1}{2\sqrt{2}} (J_{n+1}^2(W)R_{RR}^j(\mathbf{k}, s) + J_{n-1}(W)J_{n+1}(W)e^{2i\psi}R_{RL}^j(\mathbf{k}, s)) - \\
& \frac{i\mu}{\sqrt{2}} J_{n-1}(W)J_n(W)e^{-i\psi}T_{L|}^j(\mathbf{k}, s) - \frac{c}{v} \frac{\mu^2}{\sqrt{2}} J_n(W)J_{n-1}(W)e^{-i\psi}R_{L|}^j(\mathbf{k}, s) \\
& - \frac{i\sqrt{(1-\mu^2)}}{2\sqrt{2}} (J_{n-1}(W)J_{n+1}(W)e^{-2i\psi}T_{LR}^j(\mathbf{k}, s) + J_{n-1}^2(W)T_{LL}^j(\mathbf{k}, s)) \\
& - \frac{c\mu\sqrt{1-\mu^2}}{v} \frac{1}{2\sqrt{2}} e^{-2i\psi} J_{n-1}(W)J_{n+1}(W)R_{LR}^j(\mathbf{k}, s) - \frac{c\mu\sqrt{1-\mu^2}}{v} \frac{1}{2\sqrt{2}} J_{n-1}^2(W)R_{LL}^j(\mathbf{k}, s) \Big] \quad (105)
\end{aligned}$$

and

$$\begin{aligned}
D_{pp} &= \frac{\Omega^2 p^2 c^2}{v^2 B_0^2} \sum_{j=1}^N \sum_{n=-\infty}^{\infty} \int_{-\infty}^{\infty} d^3k \frac{\gamma_j(\mathbf{k})}{\gamma_j^2(\mathbf{k}) + [k_{\parallel} v_{\parallel} + \omega_{R,j}(\mathbf{k}) + n\Omega]^2} \\
& \cdot \left[\mu^2 J_n^2(W)R_{\parallel}^j(\mathbf{k}, s) + \frac{1-\mu^2}{4} (J_{n+1}^2(W)R_{RR}^j(\mathbf{k}, s) + J_{n-1}^2(W)R_{LL}^j(\mathbf{k}, s)) \right. \\
& + J_{n-1}(W)J_{n+1}(W)e^{2i\psi}R_{RL}^j(\mathbf{k}, s) + J_{n-1}(W)J_{n+1}(W)e^{-2i\psi}R_{LR}^j(\mathbf{k}, s) \\
& + \mu J_n(W) \frac{\sqrt{1-\mu^2}}{2} (J_{n+1}(W)e^{-i\psi}R_{|R}^j(\mathbf{k}, s) + J_{n-1}(W)e^{i\psi}R_{|L}^j(\mathbf{k}, s) + J_{n+1}(W)e^{i\psi}R_{R|}^j(\mathbf{k}, s) \\
& \left. + J_{n-1}(W)e^{-i\psi}R_{L|}^j(\mathbf{k}, s)) \right] \quad (106)
\end{aligned}$$

4.3 Derivation of $D_{\mu\mu}$ for Fast Mode Waves

4.3.1 Dispersion Relation

Using the high phase velocity approximation $\omega_R/k > V_A(\beta/2)^{1/4}$ for low beta plasmas Ragot & Schlickeiser (1998) have calculated the dispersion relation of fast magnetosonic waves in a magnetized electron-proton fluid plasma (Braginskii 1957, Stringer 1963, Swansson 1989) as

$$\omega_R^2 \simeq \frac{1}{2} R \Omega_{0,p}^2 \left[1 + (R+1)\eta^2 + \sqrt{[1 + (R+1)\eta^2]^2 - 4\eta^2} \right] \quad (107)$$

with $\eta = \cos \theta$ and

$$R(k) = \frac{\xi^2 k^2}{k^2 + (\xi k_c)^2} \quad (108)$$

where $\xi = \sqrt{m_p/m_e} = 43$ and $k_c = \omega_{p,p}/c$ is the inverse proton skin length. For wavenumbers well below the inverse electron skin length $k \ll \xi k_c$, (108) approaches $R(k) \simeq (k/k_c)^2$ which is much smaller than unity in the MHD-wave range $k \ll k_c$ and much larger than unity at wavenumbers $k_c \ll k \ll \xi k_c$.

In the MHD wave range that is of our interest, the dispersion relation (107) then simplifies to

$$\omega_R \simeq jkV_A \quad (109)$$

describing forward ($j = 1$) and backward ($j = -1$) moving fast mode waves. The associated electric field and magnetic field polarizations are (e.g. Dogan et al. 2006)

$$\delta E_L = -\delta E_R, \quad \delta E_{\parallel} = 0, \quad \delta B_L = \delta B_R, \quad \delta B_{\parallel} \neq 0 \quad (110)$$

4.3.2 Reduction of the Fokker-Planck Coefficient $D_{\mu\mu}$

From the polarization properties (110) we deduce (Schlickeiser & Miller 1998) for the correlation functions

$$\begin{aligned} P_{LL} &= P_{RR} = P_{LR} = P_{RL} \\ Q_{LR} &= -Q_{RL} = Q_{LL} = -Q_{RR} \\ T_{LR} &= -T_{RL} = -T_{LL} = -T_{RR} \\ R_{LR} &= R_{RL} = -R_{LL} = -R_{RR} \\ R_{\parallel\parallel} &= R_{\parallel L} = R_{\parallel R} = R_{L\parallel} = R_{R\parallel} = T_{L\parallel} = T_{R\parallel} = Q_{\parallel L} = Q_{\parallel R} = 0 \\ T_{\parallel L} &= -T_{\parallel R} \\ Q_{L\parallel} &= -Q_{R\parallel} \\ P_{L\parallel} &= P_{R\parallel}, \quad P_{\parallel L} = P_{\parallel R} \end{aligned} \quad (111)$$

yielding for the coefficient (103) for fast mode waves

$$D_{\mu\mu} = \frac{\Omega^2}{2B_0^2} (1-\mu^2) \sum_{j=\pm 1} \sum_{n=-\infty}^{\infty} \int_{-\infty}^{\infty} d^3k \mathcal{R}_F^j(n) [J_{n+1}^2(W) + J_{n-1}^2(W) - J_{n+1}(W)J_{n-1}(W) \cos 2\psi] \\ [P_{RR}^j(\mathbf{k}) + \mu^2 \frac{c^2}{v^2} R_{RR}^j(\mathbf{k}) + i\mu \frac{c}{v} (Q_{RR}^j(\mathbf{k}) - T_{RR}^j(\mathbf{k}))] \quad (112)$$

Faraday's induction law

$$\delta \mathbf{E} = -\frac{\omega_{R,j}}{ck^2} \mathbf{k} \times \delta \mathbf{B} \quad (113)$$

implies

$$\delta E_L = -\frac{i\omega_{R,j}}{ck^2} \left[k_{\parallel} \delta B_L - \frac{k_{\perp}}{2^{1/2}} \delta B_{\parallel} \right], \quad \delta E_R = -\frac{i\omega_{R,j}}{ck^2} \left[-k_{\parallel} \delta B_R + \frac{k_{\perp}}{2^{1/2}} \delta B_{\parallel} \right], \quad (114)$$

allowing us to all tensors in terms of magnetic field fluctuation tensor, i. e.

$$R_{RR} = \frac{\omega_{Rj}^2}{c^2 k^4} \left[k_{\parallel}^2 P_{RR} + \frac{k_{\perp}^2}{2} P_{\parallel\parallel} - \frac{k_{\parallel} k_{\perp}}{2} (P_{R\parallel} + P_{\parallel R}) \right] \\ = \frac{V_A^2}{c^2} \left[\cos^2 \theta P_{RR} + \frac{\sin^2 \theta}{2} P_{\parallel\parallel} - \frac{\sin \theta \cos \theta}{2^{1/2}} (P_{R\parallel} + P_{\parallel R}) \right], \quad (115)$$

$$Q_{RR} = \frac{i\omega_{Rj}}{ck} \left[k_{\parallel} P_{RR} - \frac{k_{\perp}}{2^{1/2}} P_{\parallel R} \right] = \frac{ijV_A}{c} \left[\cos \theta P_{RR} - \frac{\sin \theta}{2^{1/2}} P_{\parallel R} \right], \quad (116)$$

$$T_{RR} = \frac{i\omega_{Rj}}{ck} \left[-k_{\parallel} P_{RR} + \frac{k_{\perp}}{2^{1/2}} P_{\parallel R} \right] = \frac{ijV_A}{c} \left[-\cos \theta P_{RR} + \frac{\sin \theta}{2^{1/2}} P_{\parallel R} \right], \quad (117)$$

so that

$$P_{RR}^j + \mu^2 \frac{c^2}{v^2} R_{RR}^j + i\mu \frac{c}{v} (Q_{RR}^j - T_{RR}^j) = (1 - \frac{j\mu V_A}{v} \cos \theta)^2 P_{RR}^j + \frac{\mu^2 V_A^2}{2v^2} \sin^2 \theta P_{\parallel\parallel}^j \\ - \frac{V_A \mu}{\sqrt{2}v} \sin \theta (j + \frac{\mu V_A}{v} \cos \theta) [P_{R\parallel}^j + P_{\parallel R}^j] \quad (118)$$

which can be inserted into (112) yielding

$$D_{\mu\mu}^F = \frac{\Omega^2}{2B_0^2} (1-\mu^2) \sum_{j=\pm 1} \sum_{n=-\infty}^{\infty} \int_{-\infty}^{\infty} d^3k \mathcal{R}_F^j(n) [J_{n+1}^2(W) + J_{n-1}^2(W) - 2J_{n+1}(W)J_{n-1}(W) \cos 2\psi] \\ \left[(1 - \frac{j\mu V_A}{v} \cos \theta)^2 P_{RR}^j(\mathbf{k}) + \frac{\mu^2 V_A^2}{2v^2} \sin^2 \theta P_{\parallel\parallel}^j - \frac{V_A \mu}{\sqrt{2}v} \sin \theta (j + \frac{\mu V_A}{v} \cos \theta) [P_{R\parallel}^j + P_{\parallel R}^j] \right] \quad (119)$$

4.4 Derivation of $D_{\mu\mu}$ for Slow Mode Waves

4.4.1 Dispersion Relation

Dispersion relation for slow magnetosonic waves in low- β plasma reads (Dogan et al. 2006)

$$\omega_R^2 \simeq k^2 V_A^2 \left(\frac{\eta\beta}{1+\beta} + \frac{\eta^2\beta^2}{(1+\beta)^3} \right) \quad (120)$$

with $\eta = \cos\theta$ and β is the ratio of thermal and magnetic pressure. In the last equation, in the first approximation, we neglect the second term in brackets since it is one order smaller than the first term. The associated electric field and magnetic field polarizations are

$$\delta E_L = -\delta E_R, \quad \delta E_{\parallel} = 0, \quad \delta B_L = \delta B_R, \quad \delta B_{\parallel} \neq 0. \quad (121)$$

which implies

$$\begin{aligned} P_{LL} &= P_{RR} = P_{LR} = P_{RL} \\ Q_{LR} &= -Q_{RL} = Q_{LL} = -Q_{RR} \\ T_{LR} &= -T_{RL} = -T_{LL} = -T_{RR} \\ R_{LR} &= R_{RL} = -R_{LL} = -R_{RR} \\ R_{\parallel\parallel} &= R_{\parallel L} = R_{\parallel R} = R_{L\parallel} = R_{R\parallel} = T_{L\parallel} = T_{R\parallel} = Q_{\parallel L} = Q_{\parallel R} = 0 \\ T_{\parallel L} &= -T_{\parallel R} \\ Q_{L\parallel} &= -Q_{R\parallel} \\ P_{L\parallel} &= P_{R\parallel}, \quad P_{\parallel L} = P_{\parallel R}. \end{aligned} \quad (122)$$

So that, all tensors in terms of magnetic field fluctuation tensor for slow mode waves are

$$\begin{aligned} R_{RR} &= \frac{\omega_{Rj}^2}{c^2 k^2} \left[k_{\parallel}^2 P_{RR} + \frac{k_{\perp}^2}{2} P_{\parallel\parallel} - \frac{k_{\parallel} k_{\perp}}{2} (P_{R\parallel} + P_{\parallel R}) \right] \\ &= \frac{V_A^2}{c^2} \frac{\eta\beta}{1+\beta} \left[\cos^2\theta P_{RR} + \frac{\sin^2\theta}{2} P_{\parallel\parallel} - \frac{\sin\theta \cos\theta}{2^{1/2}} (P_{R\parallel} + P_{\parallel R}) \right], \end{aligned} \quad (123)$$

$$Q_{RR} = \frac{i\omega_{Rj}}{ck} \left[k_{\parallel} P_{RR} - \frac{k_{\perp}}{2^{1/2}} P_{\parallel R} \right] = \frac{ijV_A}{c} \sqrt{\frac{\eta\beta}{1+\beta}} \left[\cos\theta P_{RR} - \frac{\sin\theta}{2^{1/2}} P_{\parallel R} \right], \quad (124)$$

$$T_{RR} = \frac{i\omega_{Rj}}{ck} \left[-k_{\parallel} P_{RR} + \frac{k_{\perp}}{2^{1/2}} P_{\parallel R} \right] = \frac{ijV_A}{c} \sqrt{\frac{\eta\beta}{1+\beta}} \left[-\cos\theta P_{RR} + \frac{\sin\theta}{2^{1/2}} P_{\parallel R} \right]. \quad (125)$$

4.4.2 Reduction of F-P Coefficient $D_{\mu\mu}$

Using (122)-(125), we derive

$$D_{\mu\mu}^S = \frac{\Omega^2}{2B_0^2} (1-\mu^2) \sum_{j=\pm 1} \sum_{n=-\infty}^{\infty} \int_{-\infty}^{\infty} d^3k \mathcal{R}_F^j(n) [J_{n+1}^2(W) + J_{n-1}^2(W) - 2J_{n+1}(W)J_{n-1}(W) \cos 2\psi] \\ \left[\left(1 - \frac{j\mu V_A}{v} \sqrt{\frac{\beta}{1+\beta}} \cos\theta\right)^2 P_{RR}^j(\mathbf{k}) + \frac{\mu^2 V_A^2}{2v^2} \frac{\beta}{1+\beta} \sin^2\theta P_{\parallel\parallel} \right. \\ \left. - \frac{V_A \mu}{\sqrt{2}v} \sqrt{\frac{\beta}{1+\beta}} \sin\theta \left(j + \frac{\mu V_A}{v} \sqrt{\frac{\beta}{1+\beta}} \cos\theta \right) [P_{R\parallel}^j + P_{\parallel R}^j] \right]. \quad (126)$$

4.4.3 The Other Fokker-Planck Coefficients $D_{\mu p}$ and D_{pp} for Slow Magnetosonic Waves

The other two Fokker-Planck coefficients $D_{\mu p}$ and D_{pp} for slow magnetosonic waves are the same as for fast mode waves (105) and (106). The differences will appear when we insert resonance function and dispersion relation for slow mode waves. We will do it in Sec. 6.

5 Undamped Waves

To unravel the nature of cosmic sources that accelerate cosmic rays to ultrahigh energies has been identified as one of the eleven fundamental science questions for the new century (Turner et al. 2002). Cosmic rays with energies up to at least 10^{14} eV are likely accelerated at the shock fronts associated with supernova remnants (for review see Blandford & Eichler 1987), and radio emissions and X-rays give conclusive evidence that electrons are accelerated there to near-light speed (Koyama et al 1995, Koyama et al. 1997, Tanimori et al. 2001, Allen et al. 1997, Slane et al. 1999, Borkowski et al. 2001). The evidence for a supernova origin of hadrons below 10^{14} eV is less conclusive (Enomoto et al. 2002, Reimer & Pohl 2002) although consistent with the observed GeV excess of diffuse galactic gamma radiation from the inner Galaxy (Büsching et al. 2001). Most puzzling are the much higher energy cosmic rays with energies as large as $10^{20.5}$ eV for which an extragalactic origin is favored by many researchers. Extragalactic ultrahigh-energy cosmic rays (UHECRs) coming from cosmological distances ≥ 50 Mpc should interact with the universal cosmic microwave background radiation (CMBR) and produce pions. For an extragalactic origin of UHECRs the detection or non-detection of the Greisen-Kuzmin-Zatsepin cutoff resulting from the photopion attenuation in the CMBR will have far-reaching consequences not only for astrophysics but also for fundamental particle physics as e.g. the breakup of Lorentz symmetry (Coleman & Glashow 1997) or the non-commutative quantum picture of spacetime (Amelio-Camella et al. 1998).

It is well known (e.g. Schlickeiser 2002, Ch. 17) that after injection further distributed acceleration over the whole interstellar medium results from the resonant wave-particle interactions of cosmic ray particles with low-frequency magnetohydrodynamic plasma turbulence that reveals itself by density fluctuations in observations of interstellar scintillations, dispersion measures and Faraday rotation measures (Rickett 1990, Spangler 1991, Armstrong et al. 1995) over 11 decades in wavenumber below the ion skin length. Within a plasma wave viewpoint this interstellar turbulence is a mixture of fast and slow magnetosonic waves and shear Alfvén waves because the plasma beta $\beta = 0.22$ of the diffuse interstellar intercloud phase is much smaller unity. The rate of distributed acceleration of cosmic rays, particularly its dependence on cosmic ray energy, is determined by the statistical properties of the interstellar plasma turbulence, i.e. the power spectra of the

magnetic field fluctuations.

For many years the theoretical development of the resonant wave-particle interactions has mainly concentrated on the special case that the plasma waves propagate only parallel or antiparallel to the ordered magnetic field – the so-called slab turbulence. In this case only cosmic ray particles with gyroradii R_L smaller than the longest parallel wavelength $L_{\parallel,max}$ of the plasma waves can resonantly interact.

This condition is equivalent to a limit on the maximum particle rigidity R :

$$R = \frac{p}{Z} \leq eB_0 L_{\parallel,max}. \quad (127)$$

An alternative way to express the condition (127) is

$$E_{15}/Z \leq 4 \cdot \left(\frac{B_0}{4\mu \text{ G}} \right) \left(\frac{L_{\parallel,max}}{\text{parsec}} \right), \quad (128)$$

where E_{15} denotes the cosmic ray particle energy in units of 10^{15} eV. The limit set by the right hand side of (128) is referred to as Hillas limit (Hillas 1984). According to this limit, cosmic ray protons of energies larger than 4 PeV = $4 \cdot 10^{15}$ eV cannot be confined or accelerated in the Milky Way, and an extragalactic origin for this cosmic ray component has to be invoked. In Fig. 6 are plotted some cosmic sites where particle acceleration may occur, with sizes from kilometers to megaparsecs. Sites lying below the diagonal line fail to satisfy conditions (128) and (129) for 10^{20} eV protons. For these high cosmic ray energies only very few sites remain as possibilities: either highly condensed objects with huge magnetic field strength such as neutron stars, or enormously extended objects such as clusters of galaxies or radio galaxy lobes. As we have already mentioned, supernova remnant shock waves can only accelerate particles up to rigidities of $\simeq 10^{15}$ eV.

Moreover, as the cosmic ray mean free path in case of spatial gradients is closely related to the cosmic ray anisotropy (Schlickeiser 1989, (94)), the Hillas limit (128) implies strong anisotropies at energies above 4 PeV which have not been observed by the KASCADE experiment (Antoni et al. 2004; Hörandel, Kalmykov and Timokhin 2006).

In this chapter we investigate how the Hillas limit (129) is affected if we discard the assumption of purely slab plasma waves, i.e. if we allow for oblique propagation angles θ of the plasma waves with respect to the ordered magnetic field component. There is observational evidence that obliquely propagating magnetohydrodynamic plasma wave exists

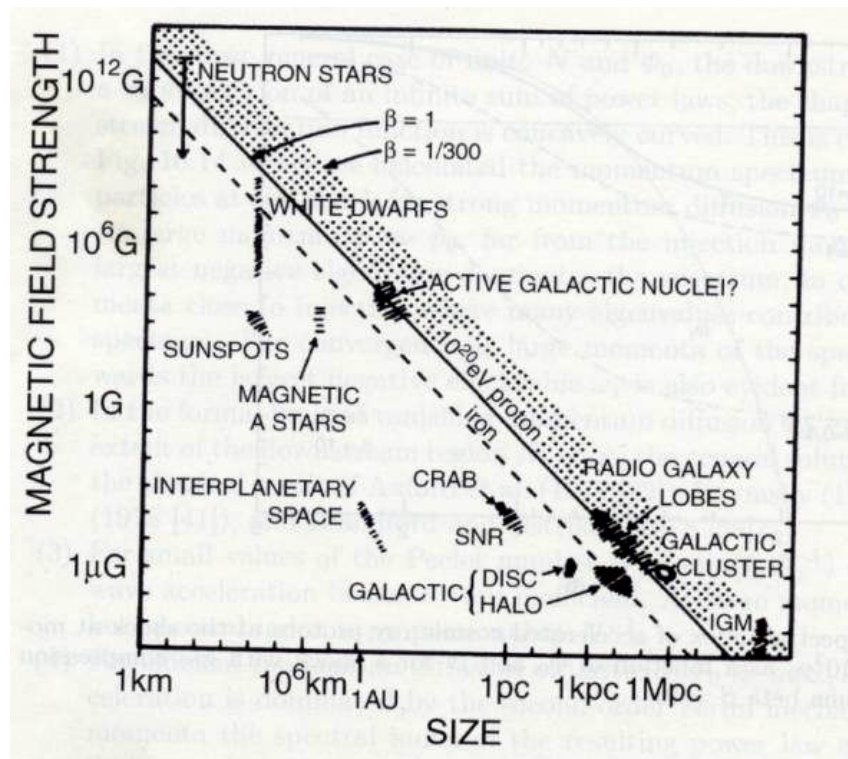


Figure 6: Size and magnetic field strength of possible sites of particle acceleration (Hillas 1984)

in the interstellar medium (Armstrong et al. 1995, Lithwick and Goldreich 2001, Cho et al. 2002). In particular, we will consider the alternative extreme limit that the plasma waves propagation angles are isotropically distributed around the magnetic field direction. It has been emphasised before by Schlickeiser and Miller (1998) that oblique propagation angles of fast magnetosonic waves leads to an order of magnitude quicker stochastic acceleration rate as compared to the slab case, since the compressional component of the obliquely propagating fast mode waves allows the effect of transit-time damping acceleration of cosmic ray particles. Here we will demonstrate that the obliqueness of fast mode and shear Alfvén wave propagation also modifies the resulting parallel spatial diffusion coefficient and the limit. Moreover we will show that the maximum wavelength L_{\max} of isotropic waves does not have such a strong effect on the maximum particle rigidity as in the slab case.

5.1 Relevant Magnetohydrodynamic Plasma Modes

Most cosmic plasmas have a small value of the plasma beta $\beta = c_S^2/V_A^2$, which is defined by the ratio of the ion sound to Alfvén speed, and thus indicates the ratio of thermal to magnetic pressure. For low-beta plasmas the two relevant magnetohydrodynamic wave modes are the

(1) incompressional *shear Alfvén waves* with dispersion relation

$$\omega_R^2 = V_A^2 k_{\parallel}^2 \quad (129)$$

at parallel wavenumbers $|k_{\parallel}| \ll \Omega_{p,0}/V_A$, which have no magnetic field component along the ordered background magnetic field $\delta B_z (\parallel \vec{B}_0) = 0$,

(2) the *fast magnetosonic waves* with dispersion relation

$$\omega_R^2 = V_A^2 k^2, \quad k^2 = k_{\parallel}^2 + k_{\perp}^2 \quad (130)$$

for wavenumbers $|k| \ll \Omega_{p,0}/V_A$, which have a compressive magnetic field component $\delta B_z \neq 0$ for oblique propagation angles $\theta = \arccos^{-1}(k_{\parallel}/k) \neq 0$.

In the limiting case (commonly referred to as slab model) of parallel (to \vec{B}_0) propagation ($\theta = k_{\perp} = 0$) the shear Alfvén waves become the left-handed circularly polarised

Alfven-ion-cyclotron waves, whereas the fast magnetosonic waves become the right-handed circularly polarised Alfven-Whistler-electron-cyclotron waves.

Schlickeiser and Miller (1998) investigated the quasilinear interactions of charged particles with these two plasma waves. In case of negligible wave damping the interactions are of resonant nature: a cosmic ray particle of given velocity v , pitch angle cosine μ and gyrofrequency $\Omega_c = \Omega_{c,0}/\gamma$ interacts with waves whose wavenumber and real frequencies obey the condition

$$\omega_R(k) = v\mu k_{\parallel} + n\Omega_c, \quad (131)$$

for entire $n = 0, \pm 1, \pm 2, \dots$.

5.1.1 Resonant Interactions of Shear Alfven Waves

For shear Alfven waves only interactions with $n \neq 0$ are possible. These are referred to as *gyroresonances* because inserting the dispersion relation (129) in the resonance condition (131) yields for the resonance parallel wavenumber

$$k_{\parallel,A} = \frac{n\Omega_c}{\pm V_A - v\mu}, \quad (132)$$

which apart from very small values of $|\mu| \leq V_A/v$ typically equals the inverse of the cosmic ray particle's gyroradius, $k_{\parallel,A} \simeq n/R_L$ and higher harmonics.

5.1.2 Resonant Interactions of Fast Magnetosonic Waves

In contrast, for fast magnetosonic waves the $n = 0$ resonance is possible for oblique propagation due its compressive magnetic field component. The $n = 0$ interactions are referred to as *transit-time damping*, hereafter TTD. Inserting the dispersion relation (130) into the resonance condition (131) in the case $n = 0$ yields

$$v\mu = \pm V_A / \cos \theta \quad (133)$$

as necessary condition which is independent from the wavenumber value k . Apparently all super-Alfvenic ($v \geq V_A$) cosmic ray particles are subject to TTD provided their parallel velocity $v\mu$ equals at least the wave speeds $\pm V_A$. Hence, equation (133) is equivalent to the two conditions

$$|\mu| \geq V_A/v, \quad v \geq V_A. \quad (134)$$

Additionally, fast mode waves also allow gyroresonances ($n \neq 0$) at wavenumbers

$$k_F = \frac{n\Omega_c}{\pm V_A - v\mu \cos \theta}, \quad (135)$$

which is very similar to (132).

5.1.3 Implications for Cosmic Ray Transport

The simple considerations of the last two subsections allow us the following immediate conclusions:

(1) With TTD-interactions alone, it would not be possible to scatter particles with $|\mu| \leq V_A/v$, i.e., particles with pitch angles near 90° . Obviously, these particles have basically no parallel velocity and cannot catch up with fast mode waves that propagate with the small but finite speeds $\pm V_A$. In particular this implies that with TTD alone it is not possible to establish an isotropic cosmic ray distribution function. We always need gyroresonances to provide the crucial finite scattering at small values of μ .

(2) Conditions (133) and (134) reveal that TTD is no gyroradius effect. It involves fast mode waves at all wavenumbers provided the cosmic ray particles are super-Alfvenic and have large enough values of μ as required by (134). Because gyroresonances occur at single resonant wavenumbers only, see (132) and (135), their contribution to the value of the Fokker–Planck coefficients in the interval $|\mu| \geq V_A/v$ is much smaller than the contribution from TTD. Therefore for comparable intensities of fast mode and shear Alfven waves, TTD will provide the overwhelming contribution to all Fokker–Planck coefficients $D_{\mu\mu}$, $D_{\mu p}$ and D_{pp} in the interval $|\mu| \geq V_A/v$. At small values of $|\mu| < V_A/v$ only gyroresonances contribute to the values of the Fokker–Planck coefficients involving according to (132) and (135) wavenumbers at $k_{\parallel,A} = k_R \simeq \pm n\Omega_c/V_A$.

(3) The momentum diffusion coefficient

$$A_2 = \frac{1}{2} \int_{-1}^1 d\mu \left[D_{pp}(\mu) - \frac{D_{\mu p}^2(\mu)}{D_{\mu\mu}(\mu)} \right] = A_T + A_F \quad (136)$$

has contributions both from transit-time damping of fast mode waves,

$$A_T \simeq \int_{V_A/v}^1 d\mu D_{pp}^{\text{TTD}}(\mu), \quad (137)$$

and from second-order Fermi gyroresonant acceleration by shear Alfvén waves (Schlickeiser 1989)

$$A_F = \frac{1}{2} \int_{-1}^1 d\mu \left[D_{pp}^A(\mu) - \frac{[D_{\mu p}^A(\mu)]^2}{D_{\mu\mu}^A(\mu)} \right]. \quad (138)$$

(4) On the other hand, the spatial diffusion coefficient

$$\kappa = \frac{v^2}{8} \int_{-1}^1 d\mu (1 - \mu^2)^2 D_{\mu\mu}^{-1}(\mu) \quad (139)$$

is given by the integral over the *inverse* of the Fokker–Planck coefficient $D_{\mu\mu}$, so that here the smallest values of $D_{\mu\mu}$ due to gyroresonant interactions in the interval $|\mu| < V_A/v$ determine the spatial diffusion coefficient and the corresponding parallel mean free path

$$\kappa = v\lambda/3 \simeq \frac{v^2}{8} \int_{-V_A/v}^{V_A/v} \frac{d\mu}{D_{\mu\mu}^G(\mu)}. \quad (140)$$

The gyroresonances can be due to shear Alfvén waves or fast magnetosonic waves. For relativistic cosmic rays the relevant range of pitch angle cosines $|\mu| \leq v_A/v$ is very small allowing us the approximation $D_{\mu\mu}^G(\mu) \simeq D_{\mu\mu}^G(0)$ so that

$$\kappa = v\lambda/3 \simeq \frac{v^2}{4} \frac{\epsilon}{D_{\mu\mu}^G(0)} = \frac{vV_A}{4D_{\mu\mu}^G(0)}. \quad (141)$$

(5) According to (90) of Schlickeiser (1989) the streaming cosmic ray anisotropy due to spatial gradients in the cosmic ray density is given by

$$\delta = \frac{F_{\max} - F_{\min}}{F_{\max} + F_{\min}} = \frac{1}{2F} \frac{v}{4} \frac{\partial F}{\partial z} \int_{-1}^1 d\mu (1 - \mu^2)^2 D_{\mu\mu}^{-1}(\mu) \quad (142)$$

which also is determined by the smallest value of $D_{\mu\mu}$ around $\mu = 0$. Approximating again $D_{\mu\mu}(\mu) \simeq D_{\mu\mu}^G(0)$ for $|\mu| \leq \epsilon = V_A/v$ we derive with (141) the direct proportionality of the cosmic ray anisotropy with the parallel mean free path, i.e.

$$\delta \simeq \frac{v}{8} \frac{\partial F}{\partial \ln z} \frac{2V_A}{vD_{\mu\mu}^G(0)} = \frac{v_A}{4} \frac{1}{D_{\mu\mu}^G(0)} \frac{\partial F}{\partial \ln z} = \frac{1}{3} \lambda \frac{\partial F}{\partial \ln z} \quad (143)$$

Introducing the characteristic spatial gradient of the cosmic ray density $\langle z \rangle^{-1} \equiv (1/F)|\partial F/\partial z|$ (143) reads

$$\delta = \frac{\lambda}{3 \langle z \rangle} \quad (144)$$

5.2 Quasilinear Cosmic ray Mean Free Path and Anisotropy for Isotropic Plasma Wave Turbulence

Throughout this work we consider isotropic linearly polarised magnetohydrodynamic turbulence so that the components of the magnetic turbulence tensor for plasma mode j is

$$P_{\alpha\beta}^j(\vec{k}) = \frac{g^j(\vec{k})}{8\pi k^2} (\delta_{\alpha\beta} - \frac{k_\alpha k_\beta}{k^2}). \quad (145)$$

The magnetic energy density in wave component j then is

$$(\delta B)_j^2 = \int d^3k \sum_{i=1}^3 P_{ii}(\vec{k}) = \int_0^\infty dk g^j(k) \quad (146)$$

We also adopt a Kolmogorov-like power law dependence (index $q > 1$) of $g^j(k)$ above the minimum wavenumber k_{min}

$$g^j(k) = g_0^j k^{-q} \quad \text{for } k > k_{min}. \quad (147)$$

The normalisation (147) then implies

$$g_0^j = (q - 1)(\delta B)_j^2 k_{min}^{q-1}. \quad (148)$$

Moreover we adopt a vanishing cross helicity of each plasma mode, i.e. equal intensity of forward and backward moving waves, so that g_0^j refers to the total energy density of each mode.

5.2.1 Fast Mode Waves

According to (30) of Schlickeiser and Miller (1998) the Fokker-Planck coefficients $D_{\mu\mu}^F$ and $D_{pp}^F = \epsilon^2 p^2 D_{\mu\mu}$ with $\epsilon = V_A/v$ for fast mode waves are the sum of contributions from transit-time damping (T) and gyroresonant interactions (G):

$$D_{\mu\mu}^F(\mu) = \frac{\pi\Omega^2(1-\mu^2)}{4B_0^2} [D_T(\mu) + D_G(\mu)] \quad (149)$$

with

$$D_T(\mu) = (q - 1)(\delta B)_F^2 |\Omega|^{-1} (R_L k_{min})^{q-1} H[|\mu| - \epsilon] \frac{1 + (\epsilon/\mu)^2}{|\mu|} [(1 - \mu^2)(1 - (\epsilon/\mu)^2)]^{q/2}$$

$$\times \int_U^\infty ds s^{-(1+q)} J_1^2(s), \quad (150)$$

where the lower integration boundary is

$$U = k_{min} R_L \sqrt{(1 - \mu^2)(1 - (\epsilon/\mu)^2)}. \quad (151)$$

$\eta = \cos\theta$, $R_L = v/|\Omega|$ denotes the gyrofrequency of the cosmic ray particle, H is the Heaviside' step function and $J_1(s)$ is the Bessel function of the first kind.

The gyroresonant contribution from fast mode waves is

$$D_G(\mu) = \frac{q-1}{2} (\delta B)_F^2 k_{min}^{q-1} \sum_{n=1}^\infty \sum_{j=\pm 1} \int_{-1}^1 d\eta (1 + \eta^2) \int_{k_{min}}^\infty dk k^{-q} \\ \times [J'_n(k R_L \sqrt{(1 - \eta^2)(1 - \mu^2)})^2 [\delta(k[v\mu\eta - jV_A] + n\Omega) + \delta(k[v\mu\eta - jV_A] - n\Omega)] \quad (152)$$

Equations (150) and (152) are obtained using (119), (102) and (130).

5.2.2 Shear Alfvén Waves

On the other hand shear Alfvén waves provide only gyroresonant ($n \neq 1$) interactions yielding

$$(D_{\mu\mu}^A, D_{\mu p}^A, D_{pp}^A) = \pi(q-1)\Omega^2(1 - \mu^2)k_{min}^{q-1} \frac{(\delta B)_A^2}{32B_0^2} \sum_{n=1}^\infty \sum_{j=\pm 1} ([1 - j\mu\epsilon]^2, j\epsilon p[1 - j\mu\epsilon], (\epsilon p)^2) \\ \int_{-1}^1 d\eta (1 + \eta^2) \int_{k_{min}}^\infty dk k^{-q} [\delta([v\mu - jV_A]\eta k + n\Omega) + \delta([v\mu - jV_A]\eta k - n\Omega)] \\ (J_{n-1}(k R_L \sqrt{(1 - \mu^2)(1 - \eta^2)}) + J_{n+1}(k R_L \sqrt{(1 - \mu^2)(1 - \eta^2)}))^2. \quad (153)$$

According to Schlickeiser and Miller (1998) at particle pitch-angles outside the interval $|\mu| \geq \epsilon$ transit-time damping provides the dominant and overwhelming contribution to these Fokker-Planck coefficients. This justifies the approximations to derive (141) and (143) for the cosmic ray mean free path and anisotropy, respectively. Both transport parameters are primarily fixed by the small but finite scattering due to gyroresonant interactions in the interval $|\mu| < \epsilon$. We then derive

$$\lambda \simeq \frac{3v}{8} \int_{-\epsilon}^\epsilon d\mu (1 - \mu^2)^2 [D_{\mu\mu}^F(\mu) + D_{\mu\mu}^A(\mu)]^{-1} \simeq \frac{3v\epsilon}{4[D_{\mu\mu}^F(\mu=0) + D_{\mu\mu}^A(\mu=0)]}, \quad (154)$$

and

$$\delta = \frac{1}{3}\lambda \frac{\partial F}{\partial \ln z} \simeq \frac{v\epsilon}{4[D_{\mu\mu}^F(\mu=0) + D_{\mu\mu}^A(\mu=0)]} \frac{\partial F}{\partial \ln z} \quad (155)$$

In the following, we consider both transport coefficients for positively charged cosmic ray particles with $\Omega > 0$ especially in the limit $k_{min}R_L \gg 1$.

5.2.3 Gyroresonant Fokker-Planck Coefficients at $\mu = 0$

At $\mu = 0$ the contribution from shear Alfvén waves to the pitch-angle Fokker-Planck coefficient is according to (153)

$$D_{\mu\mu}^A(\mu=0) \simeq \frac{\pi(q-1)\Omega^2 k_{min}^{q-1} (\delta B)_A^2}{16B_0^2} \sum_{n=1}^{\infty} \int_{k_{min}}^{\infty} dk \times k^{-q-1} \left(1 + \frac{n^2\Omega^2}{V_A^2 k^2}\right) H\left[k - \frac{n\Omega}{V_A}\right] \left(J_{n-1}\left(R_L \sqrt{k^2 - \frac{n^2\Omega^2}{V_A^2}}\right) + J_{n+1}\left(R_L \sqrt{k^2 - \frac{n^2\Omega^2}{V_A^2}}\right)\right)^2, \quad (156)$$

where we readily performed the η -integration. Substituting $t = R_L[k^2 - (n^2\Omega^2/V_A^2)]^{1/2}$, and using $V_A/\Omega = \epsilon R_L$, (156) reduces to

$$D_{\mu\mu}^A(\mu=0) \simeq \frac{\pi(q-1)\Omega(\delta B)_A^2}{16\epsilon B_0^2} [k_{min}R_L]^{q-1} \sum_{n=1}^{\infty} \int_{U_A}^{\infty} dt t \left(t^2 + \frac{2n^2}{\epsilon^2}\right) \left[t^2 + \frac{n^2}{\epsilon^2}\right]^{-(q+4)/2} \left(J_{n-1}(t) + J_{n+1}(t)\right)^2 \quad (157)$$

where

$$U_A = \max(0, [R_L^2 k_{min}^2 - \frac{n^2}{\epsilon^2}]^{1/2}). \quad (158)$$

Likewise the contribution from gyroresonant interactions with fast mode waves is according to (149) and (152)

$$D_{\mu\mu}^F(\mu=0) \simeq \frac{\pi(q-1)\Omega^2 k_{min}^{q-1} (\delta B)_F^2}{4V_A B_0^2} \left[\frac{V_A}{\Omega}\right]^q \times \sum_{n=1}^{\infty} n^{-q} H\left[n - \frac{k_{min}V_A}{\Omega}\right] \int_{-1}^1 d\eta (1 + \eta^2) \left(J'_n\left(\frac{n}{\epsilon} \sqrt{1 - \eta^2}\right)\right)^2 \quad (159)$$

where we performed the k -integration. With $V_A/\Omega = \epsilon R_L$, (159) becomes

$$D_{\mu\mu}^F(\mu=0) \simeq \frac{\pi(q-1)\Omega(\delta B)_F^2}{4B_0^2} [k_{min}R_L\epsilon]^{q-1} \sum_{n=1}^{\infty} n^{-q} H[n - \epsilon R_L k_{min}] \times \int_{-1}^1 d\eta (1 + \eta^2) \left(J'_n\left(\frac{n}{\epsilon} \sqrt{1 - \eta^2}\right)\right)^2 \quad (160)$$

The Bessel function integral in (160)

$$I_1 = \int_{-1}^1 d\eta (1 + \eta^2) l(J'_n(\frac{n}{\epsilon} \sqrt{1 - \eta^2}))^2 \quad (161)$$

has been calculated asymptotically by Schlickeiser and Miller (1998) to lowest order in the small quantity $\epsilon = V_A/v \ll 1$ as

$$I_1 \simeq \frac{3}{2} \frac{\epsilon}{n} \quad (162)$$

yielding

$$D_{\mu\mu}^F(\mu = 0) \simeq \frac{3\pi(q-1)\Omega\epsilon(\delta B)_F^2}{4B_0^2} [k_{min}R_L\epsilon]^{q-1} \sum_{n=1}^{\infty} n^{-(q+1)} H[n - \epsilon R_L k_{min}]. \quad (163)$$

In Appendix A we evaluate the Bessel function integral in (157)

$$I_2 = \int_{U_A}^{\infty} dt t (t^2 + \frac{2n^2}{\epsilon^2}) [t^2 + \frac{n^2}{\epsilon^2}]^{-(q+4)/2} (J_{n-1}(t) + J_{n+1}(t))^2 \quad (164)$$

for small and large values of $k_{min}R_L\epsilon$.

For values $k_{min}R_L\epsilon \leq 1$ we obtain approximately

$$I_2(k_{min}R_L\epsilon \leq 1) \simeq \frac{8}{\pi} \epsilon^{q+2} n^{-q} [1 + (-1)^n 1.00813] \quad (165)$$

yielding

$$D_{\mu\mu}^A(\mu = 0, k_{min}R_L\epsilon \leq 1) \simeq \frac{(q-1)\Omega\epsilon^2(\delta B)_A^2}{2^{1+q}B_0^2} [k_{min}R_L\epsilon]^{q-1} \times [2.00813\zeta(q) + 0.00813\zeta(q, 0.5)]. \quad (166)$$

in terms of the zeta and the generalised zeta functions of Riemann (Whittaker and Watson 1978).

For values of $k_{min}R_L\epsilon > 1$ we obtain (165) for values of $n \geq N + 1$, where $N = \text{inf}[k_{min}R_L\epsilon]$ is the largest integer smaller than $\epsilon R_L k_{min}$, while for smaller n

$$I_2(k_{min}R_L\epsilon > 1, n = N) \simeq 4\epsilon^{q+2} N^{-(q+1)} \quad (167)$$

and

$$I_2(k_{\min}R_L\epsilon > 1, n \leq N-1) \simeq \frac{4n^2}{\pi(q+3)}U_A^{-(q+3)}. \quad (168)$$

According to (158) this yields

$$D_{\mu\mu}^A(\mu = 0, k_{\min}R_L\epsilon > 1) \simeq \frac{(q-1)\Omega\epsilon^2(\delta B)_A^2}{2B_0^2}[k_{\min}R_L\epsilon]^{q-1}\left[\frac{\pi}{2N^{q+1}} + \frac{\epsilon}{2(q+3)}\sum_{n=1}^{N-1}n^{-(q+1)}\left[\left(\frac{R_Lk_{\min}\epsilon}{n}\right)^2 - 1\right]^{-(q+3)/2} + \sum_{n=N+1}^{\infty}n^{-q}[1 + (-1)^n 1.00813]\right]. \quad (169)$$

Comparing the Fokker-Planck coefficients from fast mode waves (163) and Alfvén waves (166) and (169) we note that the latter one is always smaller by the small ratio $\epsilon = V_A/v$ than the first one:

$$D_{\mu\mu}^A(\mu = 0) \simeq \epsilon D_{\mu\mu}^F(\mu = 0) \quad (170)$$

so that the gyroresonant contribution from Alfvén waves can be neglected in comparison to the gyroresonant contribution from fast mode waves.

5.2.4 Cosmic Ray Mean Free Path

Neglecting $D_{\mu\mu}^A(\mu = 0)$ we obtain for the cosmic ray mean free path (154)

$$\lambda(\gamma) \simeq \frac{3v\epsilon}{4D_{\mu\mu}^F(\mu = 0)} = \frac{1}{\pi(q-1)}\frac{B_0^2}{(\delta B)_F^2}\frac{R_L(k_{\min}R_L\epsilon)^{1-q}}{\sum_{n=1}^{\infty}n^{-(q+1)}H[n - \epsilon R_Lk_{\min}]}, \quad (171)$$

which exhibits the familiar Lorentzfactor dependence $\propto \beta\gamma^{2-q} \simeq \gamma^{2-q}$ at Lorentz factors $\gamma \leq \gamma_c$ below a critical Lorentz factor defined by

$$\gamma_c = k_c/k_{\min} \quad (172)$$

with $k_c = \Omega_{0,p}/V_A = \omega_{p,i}/c$ being the inverse ion skin length. The Lorentzfactor dependence $\lambda \propto \gamma^{2-q}$ especially holds at rigidities $1 \leq k_{\min}R_L \leq 1/\epsilon = c/V_A$, in a rigidity range where the slab turbulence model would predict an infinitely large mean free path.

Expressing $k_{\min} = L_{\max}/2\pi$ in terms of the longest wavelength of isotropic fast mode waves $L_{\max} = 1$ pc yields

$$\gamma_c = \frac{\omega_{p,i}L_{\max}}{2\pi c} = 2.16 \cdot 10^{10}n_e^{1/2}\left(\frac{L_{\max}}{1 \text{ pc}}\right) \quad (173)$$

The corresponding cosmic ray hadron energy is

$$E_c = A\gamma_c m_p c^2 = 2.03 \cdot 10^4 A n_e^{1/2} \left(\frac{L_{\max}}{1 \text{ pc}} \right) \text{ PeV} \quad (174)$$

which is four orders of magnitude larger than the Hillas limit (128) for equal values of the maximum wavelength. This difference demonstrates the dramatic influence of the plasma turbulence geometry (slab versus isotropically distributed waves) on the confinement of cosmic rays in the Galaxy. With isotropically distributed fast mode waves, even ultrahigh energy cosmic rays obey the scaling $\lambda\gamma^{q-2} = \text{const.}$.

Only, at ultrahigh Lorentz factors $\gamma > \gamma_c$ or energies $E > E_c$ the mean free path (171) approaches the much steeper dependence

$$\lambda(\gamma > \gamma_c) \simeq \frac{1}{\pi(q-1)} \frac{B_0^2}{(\delta B)_F^2} R_L (k_{\min} R_L \epsilon)^2 \propto \beta \gamma^3 \simeq \gamma^3. \quad (175)$$

independent from the turbulence spectral index q . Here the mean free path quickly attains very large values greater than the typical scales of the Galaxy.

5.2.5 Anisotropy

Because of the direct proportionality between mean free path and anisotropy, the cosmic ray anisotropy (155) shows the same behaviour as a function of energy:

$$\delta(E) \simeq \frac{1}{3\pi(q-1)} \frac{B_0^2}{(\delta B)_F^2} \frac{\partial F}{\partial \ln z} \frac{R_L (k_{\min} R_L \epsilon)^{1-q}}{\sum_{n=1}^{\infty} n^{-(q+1)} H[n - \epsilon R_L k_{\min}]} \quad (176)$$

which is proportional $\delta(E \leq E_c) \propto E^{2-q}$ at energies below E_c and $\delta(E > E_c) \propto E^3$ at energies above E_c . In particular we obtain no drastic change in the energy dependence of the anisotropy at PeV energies.

6 Implication of Damped Waves

The steepening of the magnetic power spectra at high wavenumbers most probably results from the collisionless cyclotron damping of the transverse Alfvén waves at wavenumbers near $\simeq \Omega_{0,p}/v_A$. It has been emphasized that this damping enters twice into the calculation of cosmic ray transport parameters:

1) the plasma wave intensity at long wavelength is drastically reduced, which is reflected by the cutoff ,

2) wave damping modifies the resonance function in the Fokker-Planck coefficients from sharp delta-function resonances to broadened Breit-Wigner resonance function (Schlick-eiser, Achatz, 1993a).

Considering only the first effect leads to quasilinear mean free paths of cosmic rays drastically larger than those measured, in obvious contradiction to the observational evidence. For the second effect, in the case of cosmic ray protons, the scattering of particles in pitch angle is markedly different at small and large particle momenta. At large relativistic momenta at all pitch angles the resonant interaction with undamped waves controls the scattering $D_{\mu\mu}$. At nonrelativistic energies there exists a small pitch angle interval $|\mu| < v_A/c$ where the undamped left and right handed polarized Alfvén waves do not contribute. In this interval the scattering relies entirely on the small but finite resonance broadened contribution from damped right-handed polarized waves. Because the mean free path is sensitively determined by the minimum value of $D_{\mu\mu}$ one finds a quite different behavior of the mean free path at small and large particle momenta. In this chapter, we investigate influence of damping on the relevant cosmic ray transport coefficients, for fast and slow magnetosonic waves, in small pitch angle interval $|\mu| < \epsilon = v_A/v$, where v is the speed of cosmic ray (for the relativistic case $v = c$). We consider dominant viscous damping of fast mode waves.

We have already discussed in previous chapter for undamped waves how the rigidity limit (128) is affected if we discard the assumption of purely slab plasma waves, i.e. if we allow for oblique propagation angles θ of the plasma waves with respect to the ordered magnetic field component. In particular, we have considered the alternative extreme limit that the plasma waves propagation angles are isotropically distributed around the magnetic field direction. As we have already mentioned, it has been emphasised by

Schlickeiser and Miller (1998) that oblique propagation angles of fast magnetosonic waves leads to an order of magnitude quicker stochastic acceleration rate as compared to the slab case, since the compressional component of the obliquely propagating fast mode waves allows the effect of transit-time damping acceleration of cosmic ray particles. In the case of damped waves, the wavenumber at which the resonance condition occurs is, for fast mode waves the same as in the case of undamped waves (136) , and for slow mode waves is somewhat changed by the factor $\sqrt{\frac{1+\beta}{\cos\theta\beta}}$ and reads (see dispersion relation for slow mode waves (120))

$$k_S = \frac{n\Omega_c}{\pm V_A \sqrt{\frac{\cos\theta\beta}{1+\beta}} - v\mu \cos\theta}. \quad (177)$$

However, the corresponding cosmic ray hadron energy, in the case of damped fast mode waves will be the same as (174). For damped slow mode waves, it will be modified by the factor $\sqrt{\frac{1+\beta}{\cos\theta\beta}}$. Here we will use the same approach to demonstrate how fast and slow mode wave propagation also modifies the resulting parallel spatial diffusion coefficient and the limit.

When discussing the nature of interstellar turbulence, it is necessary to consider the fact that the interstellar medium contains a number of plasmas of very diverse characteristics, not only cold plasma. In this work, we include the temperature effects to the first order (Dogan et al. 2006), in deriving the relevant Fokker-Planck coefficients.

6.1 Damping Rate of Fast Mode Waves

The damping of fast mode waves is caused both by collisionless Landau damping and collisional viscous damping, Joule damping and ion-neutral friction. According to Spanier & Schlickeiser (2005) and Lerche, Spanier & Schlickeiser (2006) the dominating contribution is provided viscous damping with the rate calculated for plasma parameters of the diffuse intercloud medium

$$\gamma_F = \frac{1}{12}\beta V_A^2 \tau_i k^2 [\sin^2\theta + 5 \cdot 10^{-9} \cos^2\theta] = 2.9 \cdot 10^5 \beta V_A^2 k^2 [\sin^2\theta + 5 \cdot 10^{-9} \cos^2\theta] \quad (178)$$

in terms of the ion-ion collisional time $\tau_i = 3.5 \cdot 10^6$ s. Except at very small propagation angles the second term in (178) is negligible small and we infer

$$\gamma_F \simeq 2.9 \cdot 10^5 \beta V_A^2 k^2 \sin^2 \theta. \quad (179)$$

For the ratio of damping rate to real frequency we obtain

$$\frac{\gamma_F}{|\omega_R|} \simeq 2.9 \cdot 10^5 \beta V_A k \sin^2 \theta = 2.9 \cdot 10^5 \beta \omega_R \sin^2 \theta. \quad (180)$$

Because in the interstellar medium $\Omega_{0,p} = 3.6 \cdot 10^{-2} B(4\mu G)$ Hz, we see that in the far MHD-wave region $\omega_R \leq 10^{-4} \Omega_{0,p} / \beta$, the weak damping limit is fulfilled.

6.1.1 Dominance of Transit-time Damping

With (109) and (179) the resonance function (100) for forward and backward moving fast mode waves becomes

$$\mathcal{R}_F^j(n) = \frac{2.9 \cdot 10^5 \beta V_A^2 k^2 \sin^2 \theta}{(2.9 \cdot 10^5 \beta V_A^2 k^2 \sin^2 \theta)^2 + [kv\mu \cos \theta + jV_A k + n\Omega]^2} \quad (181)$$

describing both gyroresonant ($n \neq 0$) and transit-time damping ($n = 0$) wave-particle interactions.

The non-vanishing parallel magnetic field component $B_{\parallel} \neq 0$ (see (110)) of fast mode waves allows transit-time damping interactions with $n = 0$. It has been pointed out by Schlickeiser & Miller (1998) that this transit-time damping (TTD) contribution provides the overwhelming contribution to particle scattering because in this interaction the cosmic ray particle interacts with the whole wave spectrum, in contrast to gyroresonances that singles out individual resonant wave numbers (see also the discussion in Schlickeiser (2003)). The inclusion of resonance broadening due to wave damping in the resonance function (100) guarantees that this dominance also holds for cosmic ray particles at small pitch angle cosines $\mu \leq |V_a/v|$, unlike the case of negligible wave damping (see (103)) discussed by Schlickeiser & Miller (1998). Therefore, in the following we will only take into account the TTD-contribution to particle scattering and assume $n = 0$ both in the resonance function (181) and in the calculation of the Fokker-Planck coefficients. This justified approximation greatly simplifies the evaluation of the Fokker-Planck coefficients. Since we consider only TTD-contribution, only fast and slow magnetosonic waves are subjects of it. It has been already emphasized that in the case on negligible damping, there is no TTD for shear Alfvén waves (Teufel, Lerche and Schlickeiser, 2003) and the

gyroresonant interactions provided by shear Alfvén waves is small compared to the same contribution provided by fast magnetosonic waves (see Sec. 5). As a consequence, we consider only fast and slow magnetosonic waves in this section.

With $n = 0$ the resonance function for fast mode (181) becomes

$$\begin{aligned}\mathcal{R}_F^j(0) &= \frac{2.9 \cdot 10^5 \beta V_A^2 k^2 \sin^2 \theta}{(2.9 \cdot 10^5 \beta V_A^2 k^2 \sin^2 \theta)^2 + [kv\mu \cos \theta + jV_A k]^2} \\ &= \frac{2.9 \cdot 10^5 \beta V_A^2 \sin^2 \theta}{(2.9 \cdot 10^5 \beta V_A^2 k \sin^2 \theta)^2 + [v\mu \cos \theta + jV_A]^2}\end{aligned}\quad (182)$$

and the Fokker-Planck coefficient (119) reads

$$\begin{aligned}D_{\mu\mu} &= \frac{\Omega^2}{B_0^2} (1 - \mu^2) \sum_{j=\pm 1} \int_{-\infty}^{\infty} d^3k \mathcal{R}_F^j(0) J_1^2(W) [1 + \cos 2\psi] \\ &\quad \left[\left(1 - \frac{j\mu V_A}{v} \cos \theta\right)^2 P_{RR}^j(\mathbf{k}) + \frac{\mu^2 V_A^2}{2v^2} \sin^2 \theta P_{\parallel\parallel} - \frac{V_A \mu}{\sqrt{2}v} \sin \theta \left(j + \frac{\mu V_A}{v} \cos \theta\right) [P_{R\parallel}^j + P_{\parallel R}^j] \right]\end{aligned}\quad (183)$$

Adopting the correlation tensor (104) with no magnetic helicity we obtain

$$P_{RR}^j(\mathbf{k}) = \frac{1 + \cos^2 \theta}{16\pi k^2} g^j(\mathbf{k}), \quad P_{\parallel\parallel}^j(\mathbf{k}) = \frac{\sin^2 \theta}{8\pi k^2} g^j(\mathbf{k}), \quad P_{\parallel R}^j(\mathbf{k}) = P_{R\parallel}^j(\mathbf{k}) = -\frac{\sin \theta \cos \theta}{8\sqrt{2}\pi k^2} g^j(\mathbf{k})\quad (184)$$

and we obtain

$$\begin{aligned}D_{\mu\mu} &= \frac{\Omega^2}{16\pi B_0^2} (1 - \mu^2) \sum_{j=\pm 1} \int_{-\infty}^{\infty} dk \int_0^{2\pi} d\psi \int_0^\pi d\theta \sin \theta \mathcal{R}_F^j(0) g^j(\mathbf{k}) J_1^2(W) [1 + \cos 2\psi] \\ &\quad \left[\left(1 - \frac{j\mu V_A}{v} \cos \theta\right)^2 (1 + \cos^2 \theta) + \frac{\mu^2 V_A^2}{2v^2} \sin^4 \theta + \frac{2V_A \mu}{v} \sin^2 \theta \cos \theta \left(j + \frac{\mu V_A}{v} \cos \theta\right) \right]\end{aligned}\quad (185)$$

Throughout this chapter we consider isotropic turbulence $g^j(\mathbf{k}) = g^j(k)$. Modifications due to different turbulence geometries are easily incorporated into the analysis.

For energetic cosmic ray particles with $v \gg V_A$ the Fokker-Planck coefficient (185) then simplifies to

$$D_{\mu\mu} \simeq \frac{\Omega^2}{4B_0^2} (1 - \mu^2) \sum_{j=\pm 1} \int_{-\infty}^{\infty} dk \int_{-1}^1 d\eta \mathcal{R}_F^j(0) g^j(k) J_1^2(W) (1 + \eta^2)\quad (186)$$

where

$$\mathcal{R}_F^j(0) = \frac{2.9 \cdot 10^5 \beta V_A^2 (1 - \eta^2)}{(2.9 \cdot 10^5 \beta V_A^2 k (1 - \eta^2))^2 + [v\mu\eta + jV_A]^2}\quad (187)$$

$$D_{pp} \simeq \frac{\Omega^2 p^2 V_A^2}{4B_0^2 v^2} (1 - \mu^2) \sum_{j=\pm 1} \int_{-\infty}^{\infty} dk \int_{-1}^1 d\eta \mathcal{R}_F^j(0) g^j(k) J_1^2(W) (1 + \eta^2) \quad (188)$$

$$D_{pp} \simeq \frac{p^2 V_A^2}{v^2} D_{\mu\mu} \quad (189)$$

$$D_{\mu p} = D_{p\mu} \simeq \frac{\Omega^2 p \mu V_A^2}{2\sqrt{2} B_0^2 v^2} (1 - \mu^2) \sum_{j=\pm 1} \int_{-\infty}^{\infty} dk \int_{-1}^1 d\eta \mathcal{R}_F^j(0) g^j(k) J_1^2(W) (1 + \eta^2) \quad (190)$$

We can further simplify (186) assuming equal intensity of forward and backward waves,

$$g^+(k) = g^-(k) = \frac{1}{2} g_{tot}(k) \quad (191)$$

which reads,

$$D_{\mu\mu} \simeq \frac{\Omega^2}{8B_0^2} (1 - \mu^2) \sum_{j=\pm 1} \int_{-\infty}^{\infty} dk \int_{-1}^1 d\eta \mathcal{R}_F^j(0) g_{tot}^j(k) J_1^2(W) (1 + \eta^2). \quad (192)$$

To illustrate our results, we adopt a Kolmogorov-type power law dependence of $g^j(k)$ above and below some minimum and maximum wavenumber k_{min} and k_{max} , respectively,

$$g_{tot}(k) = g_{tot} k^{-q} \quad (193)$$

for $k_{min} < k < k_{max}$.

The magnetic energy density in wave component j is given by

$$(\delta B_j)^2 = \int_0^{\infty} dk g^j(k) \quad (194)$$

which implies

$$g_{tot} = (q - 1)(\delta B)^2 / (k_{min}^{1-q} - k_{max}^{1-q}) = (q - 1)(\delta B)^2 k_{min}^{q-1} \quad (195)$$

for $k_{max} \gg k_{min}$.

6.1.2 Rate of Adiabatic Deceleration

From (190) we obtain for the symmetric wave case $I_0^+ = I_0^-$ that $D_{\mu p}(-\mu) = -D_{\mu p}(\mu)$ is antisymmetric in μ , so that the rate of adiabatic acceleration D

$$D = \frac{3v}{4p} \int_{-1}^1 d\mu (1 - \mu^2) \frac{D_{\mu p}(\mu)}{D_{\mu\mu}(\mu)} = 0 \quad (196)$$

is identically zero.

6.1.3 Pitch-angle Fokker-Planck Coefficient

With (193), (194) and (195), Fokker-Planck coefficient $D_{\mu\mu}$ reads as

$$D_{\mu\mu} \simeq \frac{\Omega^2}{4B_0^2} (q-1) (\delta B)^2 k_{min}^{q-1} (1 - \mu^2) \int_{k_{min}}^{k_{max}} dk k^{-q} \int_{-1}^1 d\eta \mathcal{R}_F(0) J_1^2(W) (1 + \eta^2). \quad (197)$$

Now, we must approximate the resonance function. For doing this we consider two cases:

- a) $\eta < \eta_c$
- b) $\eta > \eta_c$,

where $\eta_c = \epsilon/\mu$. Than, using $D_{\mu\mu}(-\mu) = D_{\mu\mu}(\mu)$ and substitution $s = R_L k \sqrt{1 - \mu^2}$, we derive

$$\begin{aligned} D_{\mu\mu} \simeq \alpha (q-1) (k_{min} R_L)^{q-1} \left(\frac{\delta B}{B_0}\right)^2 (1 - \mu^2)^{\frac{q+1}{2}} \int_{k_{min} R_L \sqrt{1 - \mu^2}}^{\infty} ds s^{-q} \left(\int_0^{\min(1, \epsilon/\mu)} d\eta (1 - \eta^4) \right. \\ \left. J_1^2(s\sqrt{1 - \eta^2}) \frac{1}{\frac{\alpha^2 (1 - \eta^2)^2 s^2}{R_L^2 (1 - \mu^2)} + V_A^2} + \int_{\min(1, \epsilon/\mu)}^1 d\eta (1 - \eta^4) \right. \\ \left. J_1^2(s\sqrt{1 - \eta^2}) \frac{1}{\frac{\alpha^2 (1 - \eta^2)^2 s^2}{R_L^2 (1 - \mu^2)} + (v\mu\eta)^2} \right), \end{aligned} \quad (198)$$

where $\epsilon = V_A/v$ and $\alpha = 2.9 \cdot 10^5 \beta V_A^2$.

Large values $\mu > \epsilon$:

For large pitch-angles $\mu > \epsilon$ we obtain

$$\begin{aligned} D_{\mu\mu}(\mu > \epsilon) \simeq \frac{(q-1)}{\alpha} (k_{min} R_L)^{q-1} \left(\frac{\delta B}{B_0}\right)^2 (1 - \mu^2)^{\frac{q+3}{2}} \int_{k_{min} R_L \sqrt{1 - \mu^2}}^{\infty} ds s^{-q} \\ \left(\int_0^{\epsilon/\mu} d\eta (1 - \eta^4) J_1^2(s\sqrt{1 - \eta^2}) \frac{1}{(1 - \eta^2)^2 s^2 + \frac{R_L^2 (1 - \mu^2) V_A^2}{\alpha^2}} + \right. \end{aligned}$$

$$\int_{\epsilon/\mu}^1 d\eta (1 - \eta^4) J_1^2(s\sqrt{1 - \eta^2}) \frac{1}{(1 - \eta^2)^2 s^2 + \frac{R_L^2(1 - \mu^2)(v\mu\eta)^2}{\alpha^2}}. \quad (199)$$

Small values $\mu < \epsilon$:

This case is important when treated damped waves. For the small pitch-angles $\mu < \epsilon$ we obtain

$$D_{\mu\mu}^F(\mu < \epsilon) \simeq \alpha(q - 1)(k_{min}R_L)^{q-1} \left(\frac{\delta B}{B_0}\right)^2 (1 - \mu^2)^{\frac{q+1}{2}} \int_{k_{min}R_L}^{\infty} \sqrt{1 - \mu^2} ds s^{-q} \left(\int_0^1 d\eta (1 - \eta^4) J_1^2(s\sqrt{1 - \eta^2}) \frac{1}{\frac{\alpha^2(1 - \eta^2)^2 s^2}{R_L^2(1 - \mu^2)} + V_A^2}\right). \quad (200)$$

We have already discussed in Sec. 6.1.1 that inclusion of resonance broadening due to wave damping in the resonance function guarantees dominance of transit-time damping. The main contribution of waves damping comes exactly in the region $|\mu| < \epsilon$ that is relevant in deriving the spatial diffusion coefficient and related mean free path which are given by the average over μ of the inverse of $D_{\mu\mu}$. Therefore we can further consider only the case $D_{\mu\mu}(\mu = 0)$, which simplifies the analysis enormously, and reads:

$$D_{\mu\mu}^F(\mu = 0) \simeq \frac{(q - 1)}{\alpha} (k_{min}R_L)^{q-1} \left(\frac{\delta B}{B_0}\right)^2 \int_{k_{min}R_L}^{\infty} ds s^{-q} \int_0^1 d\eta (1 - \eta^4) J_1^2(s\sqrt{1 - \eta^2}) \frac{1}{(1 - \eta^2)^2 s^2 + \frac{V_A^2 R_L^2}{\alpha^2}}. \quad (201)$$

In the last equation $s = kR_L$.

6.1.4 Cosmic Ray Mean Free Path for FMS Waves

In this section we calculate the mean free path which is connected with the spatial diffusion coefficient through

$$\lambda = \frac{3\kappa}{v} = \frac{3v}{4} \int_0^1 d\mu \frac{(1 - \mu^2)^2}{D_{\mu\mu}}. \quad (202)$$

For the case we are interested in, it can be written as

$$\lambda^{0F} = \frac{3\kappa}{v} = \frac{3v}{4} \frac{1}{D_{\mu\mu}(\mu = 0)} \int_0^\epsilon d\mu = \frac{3}{4} \frac{v_A}{D_{\mu\mu}^F(\mu = 0)} = \frac{3v_A}{4} \frac{\alpha}{(q - 1)} (k_{min}R_L)^{1-q} \left(\frac{B_0}{\delta B}\right)^2 \frac{1}{G}, \quad (203)$$

where

$$G = \int_{k_{min}R_L}^{\infty} ds s^{-q} \int_0^1 d\eta (1 - \eta^4) J_1^2(s\sqrt{1 - \eta^2}) \frac{1}{(1 - \eta^2)^2 s^2 + \frac{V_A^2 R_L^2}{\alpha^2}}. \quad (204)$$

Now, we consider two limits: $k_{min}R_L \ll 1$, and $k_{min}R_L \gg 1$, where $k_{min}R_L = T = E$ and is normalized with respect to E_c (where E_c is defined as for undamped case (174)).

$k_{min}R_L \gg 1$:

This case is treated in detail in Appendix B, where we derive

$$G(T \gg 1) = \frac{2}{5} \frac{10^{-14}}{q} T^{-(q+2)}, \quad (205)$$

$$\lambda^{0F}(T \gg 1) = \frac{15V_A\alpha}{8} \frac{q}{q-1} \left(\frac{B_0}{\delta B}\right)^2 10^{14} T^3, \quad (206)$$

where $T = k_{min}R_L$. At relativistic rigidities we find that $\lambda^0 \sim T^3$.

$k_{min}R_L \ll 1$:

This case is treated in detail in Appendix B, where we derive

$$G(T \ll 1) = \frac{1}{3} \frac{1}{q-1} T^{1-q}, \quad (207)$$

$$\lambda^{F0}(T \ll 1) = 36V_A\alpha \left(\frac{B_0}{\delta B}\right)^2. \quad (208)$$

In this energy limit the mean free path is constant with respect to T .

6.1.5 Cosmic Ray Momentum Diffusion from FMS Waves

In order to discuss the stochastic acceleration of the cosmic rays we calculate momentum diffusion coefficient. Instead of using (67), we use the time scale estimates that provides the product

$$\tau_D \tau_F = \left(\frac{3L}{V_A}\right)^2, \quad (209)$$

to be constant, given by macroscopic properties of the considered physical system (Schlickeiser 1986). τ_D is the time scale for particle to diffuse a length L by pitch-angle scattering along the ordered magnetic field (calculated from the diffusion coefficient κ or equivalent mean free path λ), τ_F is the stochastic acceleration time scale for a particle to increase its momentum by factor e due to resonant wave scattering (calculated

from the momentum diffusion coefficient A_2) and L is the typical scale length. Diffusion along magnetic field lines and stochastic acceleration due to resonant diffusion are twin processes: once we know the time scale for one of them, the time scale for the other process and this its relevance can be estimated from (209).

Thus, we derive momentum diffusion coefficient as:

$$A_2^{F0} = \frac{V_A^2}{3c\lambda^{F0}} p^2. \quad (210)$$

Using (206) and (208) we obtain for the momentum diffusion coefficient in the two limits:

$$A_2^{F0}(T \gg 1) = 6 \frac{q-1}{q} \frac{p^2}{cV_A\beta} \left(\frac{\delta B}{B_0}\right)^2 \frac{10^{-17}}{T^3}, \quad (211)$$

and

$$A_2^{F0}(T \ll 1) = 5 \frac{p^2}{cV_A\beta} \left(\frac{\delta B}{B_0}\right)^2 10^{-7}. \quad (212)$$

6.2 Slow Magnetosonic Waves

In order to find transport coefficients for slow magnetosonic waves we use derivations of Fokker-Planck coefficient $D_{\mu\mu}$ in Sec. 4.4.

With (120) and (179) the resonance function (100) for slow mode waves becomes

$$\mathcal{R}_S^j(n) = \frac{2.9 \cdot 10^5 \beta V_A^2 k^2 \sin^2 \theta}{(2.9 \cdot 10^5 \beta V_A^2 k^2 \sin^2 \theta)^2 + [kv\mu \cos \theta + jV_A k \sqrt{\frac{\eta\beta}{1+\beta}} + n\Omega]^2}, \quad (213)$$

and according to what have been concluded in Sec. 6.1.1 for fast magnetosonic waves, which holds for slow mode too, we consider $n = 0$ and resonance function (213) becomes

$$\begin{aligned} \mathcal{R}_S^j(0) &= \frac{2.9 \cdot 10^5 \beta V_A^2 k^2 \sin^2 \theta}{(2.9 \cdot 10^5 \beta V_A^2 k^2 \sin^2 \theta)^2 + [kv\mu \cos \theta + jV_A k \sqrt{\frac{\eta\beta}{1+\beta}}]^2} \\ &= \frac{2.9 \cdot 10^5 \beta V_A^2 \sin^2 \theta}{(2.9 \cdot 10^5 \beta V_A^2 k \sin^2 \theta)^2 + [v\mu \cos \theta + jV_A \sqrt{\frac{\eta\beta}{1+\beta}}]^2}. \end{aligned} \quad (214)$$

Following the same procedure as for fast mode waves in Sec. 6.1.1, we make same assumptions (191), (193) and (194), together with implication (195), we derive

$$D_{\mu\mu} \simeq \frac{\Omega^2}{4B_0^2}(1-\mu^2) \sum_{j=\pm 1} \int_{-\infty}^{\infty} dk \int_{-1}^1 d\eta \mathcal{R}_F^j(0) g^j(k) J_1^2(W) ((1+\eta^2)(1+\mu^2 \epsilon^2 \frac{\eta\beta}{1+\beta}) - 4\mu j \epsilon \sqrt{\frac{\eta\beta}{1+\beta}} \eta), \quad (215)$$

which can be simplified since we consider energetic cosmic ray particles $v \gg V_A$ to the same expression as in case for fast mode waves

$$D_{\mu\mu} \simeq \frac{\Omega^2}{4B_0^2}(1-\mu^2) \sum_{j=\pm 1} \int_{-\infty}^{\infty} dk \int_{-1}^1 d\eta \mathcal{R}_F^j(0) g^j(k) J_1^2(W) (1+\eta^2), \quad (216)$$

and finally,

$$D_{\mu\mu}^S \simeq \frac{\Omega^2}{4B_0^2} (q-1) (\delta B)^2 k_{min}^{q-1} (1-\mu^2) \int_{k_{min}}^{k_{max}} dk k^{-q} \int_{-1}^1 d\eta \mathcal{R}_F(0) J_1^2(W) (1+\eta^2), \quad (217)$$

The other two FP coefficients give

$$D_{pp} \simeq \frac{\Omega^2 p^2 V_A^2}{4B_0^2 v^2} (1-\mu^2) \frac{\beta}{1+\beta} \sum_{j=\pm 1} \int_{-\infty}^{\infty} dk \int_{-1}^1 d\eta \mathcal{R}_F^j(0) g^j(k) J_1^2(W) \eta (1+\eta^2), \quad (218)$$

$$D_{\mu p} = D_{p\mu} \simeq \frac{\Omega^2 p \mu V_A^2}{2\sqrt{2} B_0^2 v^2} \frac{\beta}{1+\beta} (1-\mu^2) \sum_{j=\pm 1} \int_{-\infty}^{\infty} dk \int_{-1}^1 d\eta \mathcal{R}_F^j(0) g^j(k) J_1^2(W) \eta (1+\eta^2), \quad (219)$$

and

$$D = \frac{3v}{4p} \int_{-1}^1 d\mu (1-\mu^2) \frac{D_{\mu p}(\mu)}{D_{\mu\mu}(\mu)} = 0 \quad (220)$$

is identically zero.

Next, we have to approximate the resonance function for slow mode waves. As in fast mode case, there are two cases:

- a) $\eta < \eta_c$
- b) $\eta > \eta_c$,

where

$$\eta_c^S = \frac{\epsilon^2}{\mu^2} \frac{\beta}{1+\beta}. \quad (221)$$

Note that $\eta_c^S \ll \eta_c^F$. Using $D_{\mu\mu}(-\mu) = D_{\mu\mu}(\mu)$ and substitution $s = R_L k \sqrt{1 - \mu^2}$, we derive

$$\begin{aligned}
D_{\mu\mu} \simeq & \alpha(q-1)(k_{min}R_L)^{q-1} \left(\frac{\delta B}{B_0}\right)^2 (1-\mu^2)^{\frac{q+1}{2}} \int_{k_{min}R_L}^{\infty} \sqrt{1-\mu^2} ds s^{-q} \left(\int_0^{\min(1, \frac{\epsilon^2}{\mu^2} \frac{\beta}{1+\beta})} d\eta (1-\eta^4) \right. \\
& J_1^2(s\sqrt{1-\eta^2}) \frac{1}{\frac{\alpha^2(1-\eta^2)^2 s^2}{R_L^2(1-\mu^2)} + V_A^2 \eta \frac{\beta}{1+\beta}} + \int_{\min(1, \frac{\epsilon^2}{\mu^2} \frac{\beta}{1+\beta})}^1 d\eta (1-\eta^4) \\
& \left. J_1^2(s\sqrt{1-\eta^2}) \frac{1}{\frac{\alpha^2(1-\eta^2)^2 s^2}{R_L^2(1-\mu^2)} + (v\mu\eta)^2} \right), \tag{222}
\end{aligned}$$

where $\epsilon = V_A/v$ and $\alpha = 2.9 \cdot 10^5 \beta V_A^2$.

Large values $\mu > \epsilon$:

For large pitch-angles $\mu > \epsilon$ we obtain

$$\begin{aligned}
D_{\mu\mu}(\mu > \epsilon) \simeq & \frac{(q-1)}{\alpha} (k_{min}R_L)^{q-1} \left(\frac{\delta B}{B_0}\right)^2 (1-\mu^2)^{\frac{q+3}{2}} \int_{k_{min}R_L}^{\infty} \sqrt{1-\mu^2} ds s^{-q} \\
& \left(\int_0^{\frac{\epsilon^2 \beta}{\mu^2(1+\beta)}} d\eta (1-\eta^4) J_1^2(s\sqrt{1-\eta^2}) \frac{1}{(1-\eta^2)^2 s^2 + \frac{R_L^2(1-\mu^2)V_A^2 \frac{\eta\beta}{1+\beta}}{\alpha^2}} + \right. \\
& \left. \int_{\frac{\epsilon^2 \beta}{\mu^2(1+\beta)}}^1 d\eta (1-\eta^4) J_1^2(s\sqrt{1-\eta^2}) \frac{1}{(1-\eta^2)^2 s^2 + \frac{R_L^2(1-\mu^2)(v\mu\eta)^2}{\alpha^2}} \right). \tag{223}
\end{aligned}$$

Small values $\mu < \epsilon$:

This case is important when treated damped waves for the same reason we have discussed for fast mode waves (Sec. 6.1.3). For the small pitch-angles $\mu < \epsilon$ we obtain

$$\begin{aligned}
D_{\mu\mu}^S(\mu < \epsilon) \simeq & \alpha(q-1)(k_{min}R_L)^{q-1} \left(\frac{\delta B}{B_0}\right)^2 (1-\mu^2)^{\frac{q+1}{2}} \int_{k_{min}R_L}^{\infty} \sqrt{1-\mu^2} ds s^{-q} \left(\int_0^1 d\eta (1-\eta^4) \right. \\
& \left. J_1^2(s\sqrt{1-\eta^2}) \frac{1}{\frac{\alpha^2(1-\eta^2)^2 s^2}{R_L^2(1-\mu^2)} + V_A^2 \frac{\eta\beta}{1+\beta}} \right). \tag{224}
\end{aligned}$$

$$\begin{aligned}
D_{\mu\mu}^S(\mu = 0) \simeq & \frac{(q-1)}{\alpha} (k_{min}R_L)^{q-1} \left(\frac{\delta B}{B_0}\right)^2 \int_{k_{min}R_L}^{\infty} ds s^{-q} \\
& \int_0^1 d\eta (1-\eta^4) J_1^2(s\sqrt{1-\eta^2}) \frac{1}{(1-\eta^2)^2 s^2 + \frac{V_A^2 \frac{\eta\beta}{1+\beta} R_L^2}{\alpha^2}}. \tag{225}
\end{aligned}$$

In the last equation $s = kR_L$.

6.2.1 Cosmic Ray Mean Free Path for SMS Waves

In this section we calculate the mean free path which is connected with the spatial diffusion coefficient through

$$\lambda^S = \frac{3\kappa^S}{v} = \frac{3v}{4} \int_0^1 d\mu \frac{(1-\mu^2)^2}{D_{\mu\mu}^S}. \quad (226)$$

For the case we are interested in, it can be written as

$$\begin{aligned} \lambda^{S0} &= \frac{3\kappa^S}{v} = \frac{3v}{4} \frac{1}{D_{\mu\mu}^S(\mu=0)} \int_0^\epsilon d\mu = \frac{3}{4} \frac{V_A}{D_{\mu\mu}(\mu=0)} = \\ &= \frac{3V_A}{4} \frac{\alpha}{(q-1)} (k_{min}R_L)^{1-q} \left(\frac{B_0}{\delta B}\right)^2 \frac{1}{G}, \end{aligned} \quad (227)$$

where

$$G = \int_{k_{min}R_L}^\infty ds s^{-q} \int_0^1 d\eta (1-\eta^4) J_1^2(s\sqrt{1-\eta^2}) \frac{1}{(1-\eta^2)^2 s^2 + \frac{V_A^2 \frac{\eta\beta}{1+\beta} R_L^2}{\alpha^2}}. \quad (228)$$

Now, we consider two limits: $k_{min}R_L \ll 1$, and $k_{min}R_L \gg 1$.

$k_{min}R_L \gg 1$:

This case is treated in detail in Appendix C, where we derive

$$G(T \gg 1) = \frac{2\sqrt{2}h}{\pi} \frac{10^{-13}}{q} T^{-(q+2)}, \quad (229)$$

$$\lambda^{0S}(T \gg 1) = \frac{3V_A\alpha}{8\sqrt{2}} \frac{q}{q-1} \left(\frac{B_0}{\delta B}\right)^2 \frac{\pi}{h} 10^{13} T^3, \quad (230)$$

where $T = k_{min}R_L$, $h = 2\text{arctanh}\sqrt{1-\delta} - 2\sqrt{1-\delta}$, with $\delta \ll 1$.

At relativistic rigidities we find that $\lambda^0 \sim T^3$.

$k_{min}R_L \ll 1$:

This case is treated in detail in Appendix C, where we derive

$$G(T \ll 1) = \frac{1}{3} \frac{1}{q-1} T^{1-q}, \quad (231)$$

$$\lambda^{0S}(T \ll 1) = 36V_A\alpha \left(\frac{B_0}{\delta B}\right)^2. \quad (232)$$

In this energy limit the mean free path is constant with respect to T .

6.2.2 Cosmic Ray Momentum Diffusion from SMS Waves

In order to discuss the stochastic acceleration of the slow mode waves, we use the same time scale estimates that was used for fast mode where we derived momentum diffusion coefficient as:

$$A_2^{0S} = \frac{V_A^2}{3c\lambda^{0S}} p^2. \quad (233)$$

Using (230) and (232) we obtain for the momentum diffusion coefficient in the two limits:

$$A_2^{0S}(T \gg 1) = 4 \frac{p^2}{cV_A\beta} \frac{q-1}{q} \frac{h}{\pi} \left(\frac{\delta B}{B_0}\right)^2 \frac{10^{-17}}{T^3}, \quad (234)$$

and

$$A_2^{0S}(T \ll 1) = 5 \frac{p^2}{cV_A\beta} \left(\frac{\delta B}{B_0}\right)^2 10^{-7}, \quad (235)$$

which is similar to ones obtained for fast mode waves.

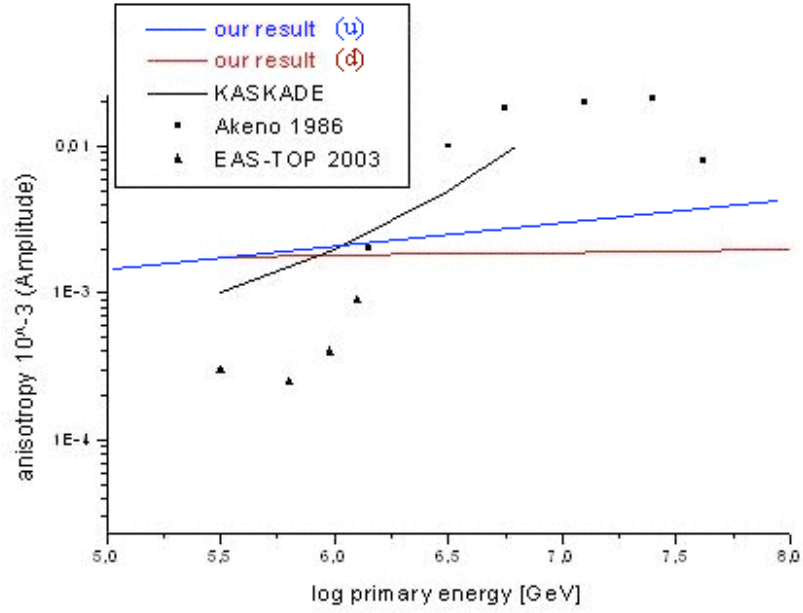


Figure 7: Anisotropy dependence on energy for particle energies below E_c . Result obtained from (176) for $E < E_c$ in case of undamped waves, and result obtained from (208) for $E < E_c$ in case of damped fast magnetosonic waves, compared to reported results from the literature (Antoni et al. 2004; Aglietta et al. 2003; Kifune et al.1986).

7 Summary

We have investigated the implications of isotropically distributed interstellar magnetohydrodynamic plasma waves on the scattering mean free path and the spatial anisotropy of high-energy cosmic rays. We demonstrate a drastic modification of the energy dependence of both cosmic ray transport parameters compared to previous calculations that have assumed that the plasma waves propagate only parallel or antiparallel to the ordered magnetic field (slab turbulence). In case of slab turbulence cosmic rays with Larmor radius R_L resonantly interact with plasma waves with wave vectors at $k_{res} = R_L^{-1}$. If the slab wave turbulence power spectrum vanishes for wavenumbers less than k_{min} , as a consequence then cosmic rays with Larmor radii larger than k_{min}^{-1} cannot be scattered in pitch-angle, causing the so-called Hillas limit for the maximum energy $E_{15}^H = 4Z \cdot (B_0/4\mu\text{G})(L_{\parallel,max}/\text{parsec})$ of cosmic rays being confined in the Galaxy. At about these energies this would imply a drastic increase in the spatial anisotropy of cosmic rays that has not been detected by KASCADE and other air shower experiments.

In case of isotropically distributed interstellar magnetohydrodynamic waves we demonstrated that the Hillas energy E^H is modified to a limiting total energy that is about 4 orders of magnitude larger $E_c = 2.03 \cdot 10^4 A n_e^{1/2} (L_{max}/1 \text{ pc}) \text{ PeV}$, where A denotes the mass number and L_{max} the maximum wavenumber of isotropic plasma waves. Below this energy the cosmic ray mean free path and the anisotropy exhibit the well known E^{2-q} energy dependence, where $q = 5/3$ denotes the spectral index of the Kolmogorov spectrum. At energies higher than E_c both transport parameters steepen to a E^3 -dependence. This implies that cosmic rays even with ultrahigh energies of several tens of EeV can be rapidly pitch-angle scattered by interstellar plasma turbulence, and are thus confined to the Galaxy.

The physical reason for the dramatically higher value of the limiting energy is the occurrence of dominating transit-time damping interactions of cosmic rays with magnetosonic plasma waves due to their compressive magnetic field component along the ordered magnetic field. This $n = 0$ resonance is not a gyroresonance implying that cosmic rays interact with plasma waves at all wavenumbers provided that the cosmic ray parallel speed (transit speed) equals the parallel phase speed of magnetosonic waves. Only at small values of the cosmic ray pitch-angle cosine $|\mu| \leq \epsilon = V_A/v$, where the cosmic ray particles

spirals at nearly ninety degrees with very small parallel speeds less than the minimum magnetosonic phase speed V_A , gyroresonant interactions are necessary to scatter cosmic rays. However, the gyroresonance condition of cosmic rays at $\mu = 0$ reads $k_{res} = (R_L \epsilon)^{-1}$ instead of the slab condition $k_{res} = (R_L)^{-1}$ causing the limiting energy enhancement from E^H to E_c by the large factor $\epsilon^{-1} = c/V_A \simeq \mathcal{O}(10^4)$.

Considering damped fast and slow mode waves caused by dominate viscous damping, we have calculated the Fokker-Planck coefficients, the spatial diffusion coefficient, the mean free path and the momentum diffusion coefficient of cosmic ray particles. We show that inclusion of resonance broadening due to wave damping in the resonance function guarantees that dominance of transit-time damping also holds for cosmic ray particles at small pitch angle cosines $\mu \leq |V_a/v|$, unlike the case of negligible wave damping. We determined energy dependence of the mean free path of the cosmic rays. We have found that for small energies it is approximately constant and for high energies is proportional to the third power of energy of the particle. For the acceleration of the cosmic rays we have used the time scale estimates to derive the momentum diffusion coefficient.

We have found that damping, at least for fast mode waves, has no dramatic influence comparing to undamped case. The key issue in order to change Hillas limit has oblique propagation of the waves in damped and undamped case.

The analysis for the influence of different types of damping, as well as the influence of different geometries of turbulence, will be the subject of further research.

8 Appendix A: Asymptotic calculation of the integral (164)

The task is to calculate the integral (164)

$$I_2 = \int_{U_A}^{\infty} dt t \left(t^2 + \frac{2n^2}{\epsilon^2}\right) \left[t^2 + \frac{n^2}{\epsilon^2}\right]^{-(q+4)/2} l(J_{n-1}(t) + J_{n+1}(t))^2, \quad (236)$$

for small and large values of $k_{min}R_L$ using the approximations of Bessel functions for small and large arguments (Abramowitz and Stegun 1972), yielding

$$J_n^2(t \ll 1) \simeq \frac{t^{2n}}{2^{2n}\Gamma^2[n+1]}, \quad (237)$$

and

$$J_n^2(t \gg 1) \simeq \frac{1}{\pi t} [1 + (-1)^n \sin(2t)]. \quad (238)$$

According to (158)

$$U_A = \max(0, [R_L^2 k_{min}^2 - \frac{n^2}{\epsilon^2}]^{1/2}),$$

the lower integration boundary $U_A = 0$ in the case $k_{min}R_L\epsilon \leq 1$ which includes in particular the limit $k_{min}R_L \ll 1$ because $\epsilon \ll 1$.

8.1 Case $k_{min}R_L\epsilon \leq 1$

With the identity

$$J_{n-1}(t) + J_{n+1}(t) = \frac{2nJ_n(t)}{t} \quad (239)$$

we obtain

$$I_2(k_{min}R_L\epsilon \leq 1) = 4n^2 \left[W\left[\frac{q+2}{2}\right] + \frac{n^2}{\epsilon^2} W\left[\frac{q+4}{2}\right] \right] \quad (240)$$

where

$$W[\alpha] \equiv \int_0^{\infty} dt t^{-1} \frac{J_n^2(t)}{[t^2 + \frac{n^2}{\epsilon^2}]^\alpha}. \quad (241)$$

With the asymptotics (237) and (238) we obtain

$$\begin{aligned}
W[\alpha] &\simeq \left(\frac{\epsilon}{n}\right)^{2\alpha} \left[\frac{1}{2^{2n}\Gamma^2[n+1]} \int_0^1 dt t^{2n-1} + \frac{1}{\pi} \int_1^{n/\epsilon} dt t^{-2} [1 + (-1)^n \sin(2t)] \right] \\
&+ \frac{1}{\pi} \int_{n/\epsilon}^{\infty} dt t^{-2(1+\alpha)} [1 + (-1)^n \sin(2t)] \simeq \left(\frac{\epsilon}{n}\right)^{2\alpha} \left[\frac{1}{\pi} [1 + (-1)^n 1.00813 - \frac{\epsilon}{n} \right. \\
&\left. - \frac{(-1)^n}{2} \left(\frac{\epsilon}{n}\right)^2 \cos\left(\frac{2n}{\epsilon}\right) \right] + \frac{1}{n 2^{2n+1} \Gamma^2[n+1]} \left. \right] + \frac{1}{\pi(1+2\alpha)} \left(\frac{\epsilon}{n}\right)^{1+2\alpha} + \frac{(-1)^n}{\pi} j_1, \quad (242)
\end{aligned}$$

where we use

$$2 \int_1^{\infty} dx x^{-2} \sin x = 2(\sin(1) - Ci(1)) = 1.00813$$

and where

$$\begin{aligned}
j_1 &= \int_{n/\epsilon}^{\infty} dt t^{-2-2\alpha} \sin 2t = 2^{2\alpha} \left[i^{-2-2\alpha} \Gamma[-(1+2\alpha), -2i \frac{n}{\epsilon}] + \right. \\
&\left. (-i)^{-2-2\alpha} \Gamma[-(1+2\alpha), 2i \frac{n}{\epsilon}] \right] \quad (243)
\end{aligned}$$

in terms of the incomplete gamma function. For large arguments $(n/\epsilon) \gg 1$ we obtain asymptotically

$$j_1 \simeq \frac{1}{2} \left(\frac{\epsilon}{n}\right)^{2+2\alpha} \cos\left(\frac{2n}{\epsilon}\right) \quad (244)$$

Collecting terms we find to lowest order in $\ll 1$

$$W[\alpha] \simeq \frac{1}{\pi} \left(\frac{\epsilon}{n}\right)^{2\alpha} \left[1 + (-1)^n 1.00813 + \frac{\pi}{n 2^{2n+1} \Gamma^2[n+1]} \right] \quad (245)$$

so that

$$I_2(k_{min} R_L \epsilon \leq 1) \simeq \frac{8}{\pi} \epsilon^{q+2} n^{-q} \left[1 + (-1)^n 1.00813 + \frac{\pi}{n 2^{2n+1} \Gamma^2[n+1]} \right] \quad (246)$$

8.2 Case $k_{min} R_L \epsilon > 1$

In this case $U_A = 0$ for $n \geq N + 1$, and $U_A = \sqrt{(R_L k_{min})^2 - (n/\epsilon)^2}$ for $n \leq N$, where

$$N = \inf[\epsilon R_L k_{min}] \quad (247)$$

denotes the largest integer smaller than $\epsilon R_L k_{min}$. Hence we obtain again (246) for $n \geq N + 1$

$$I_2(k_{min}R_L\epsilon > 1, n \geq N + 1) \simeq \frac{8}{\pi}\epsilon^{q+2}n^{-q}[1 + (-1)^n 1.00813 + \frac{\pi}{n2^{2n+1}\Gamma^2[n+1]}] \quad (248)$$

For values of $n \leq N$ we find that

$$I_2(k_{min}R_L\epsilon > 1, n \leq N) = 4n^2[V[\frac{q+2}{2}] + \frac{n^2}{\epsilon^2}V[\frac{q+4}{2}]] \quad (249)$$

where

$$V[\alpha] \equiv \int_{U_A}^{\infty} dt t^{-1} \frac{J_n^2(t)}{[t^2 + \frac{n^2}{\epsilon^2}]^\alpha} = (\frac{\epsilon}{n})^{2\alpha} \int_{\epsilon U_A/n}^{\infty} dt t^{-1} \frac{J_n^2(nt/\epsilon)}{[1+t^2]^\alpha} \quad (250)$$

We may express

$$k_{min}R_L\epsilon = N(1 + \phi) \quad (251)$$

with $\phi < 1/N$, so that the lower integration boundary in (250) is

$$U_A = [(\frac{k_{min}R_L\epsilon}{n} - 1)(\frac{k_{min}R_L\epsilon}{n} + 1)]^{1/2} = \frac{N}{n}[(1 + \phi - \frac{n}{N})(1 + \phi + \frac{n}{N})]^{1/2} \quad (252)$$

In cases where $N \geq 2$, (252) yields that for all values of n such that $1 \leq n \leq N - 1$ the lower integration boundary U_A is greater unity. Using the expansion (238) in this case we find that

$$V[\alpha, n \leq N - 1] \simeq \frac{1}{\pi}(\frac{\epsilon}{n})^{2\alpha+1} \int_{\epsilon U_A/n}^{\infty} dt t^{-2-2\alpha} [1 + (-1)^n \sin(\frac{2nt}{\epsilon})] \simeq \frac{1}{\pi(1+2\alpha)}(U_A^{-(2\alpha+1)}[1 + (-1)^n \frac{1+2\alpha}{2U_A} \cos(2U_A)]) \simeq \frac{U_A^{-(2\alpha+1)}}{\pi(1+2\alpha)} \quad (253)$$

In the remaining case $n = N$ the lower integration boundary (252)

$$\frac{\epsilon}{N}U_A = \sqrt{\phi(2+\phi)} \leq \sqrt{2.5\phi} < 1 \quad (254)$$

is smaller unity, so that we approximate (250) in this case by

$$V[\alpha, n = N] \simeq (\frac{\epsilon}{N})^{2\alpha}[\int_{\epsilon U_A/N}^1 dt t^{-1} J_N^2(\frac{Nt}{\epsilon}) + \int_1^{\infty} dt t^{-1-2\alpha} J_N^2(\frac{Nt}{\epsilon})] \simeq (\frac{\epsilon}{N})^{2\alpha}[j_2 + \frac{\epsilon}{\pi N(1+2\alpha)}(1 + (-1)^n(1+2\alpha)\frac{\epsilon}{2N} \cos(\frac{2N}{\epsilon}))] \quad (255)$$

where we approximate

$$j_2 = \int_{\epsilon U_A/N}^1 dt t^{-1} J_N^2\left(\frac{Nt}{\epsilon}\right) < \int_0^\infty dt t^{-1} J_N^2\left(\frac{Nt}{\epsilon}\right) = \frac{1}{2N} \quad (256)$$

by its upper limit to obtain

$$V[\alpha, n = N] \simeq \frac{\left(\frac{\epsilon}{N}\right)^{2\alpha}}{2N}. \quad (257)$$

Collecting terms in (249) we derive

$$I_2(k_{min} R_L \epsilon > 1, n = N) \simeq 4\epsilon^{q+2} N^{-(q+1)} \quad (258)$$

and

$$I_2(k_{min} R_L \epsilon > 1, n \leq N - 1) \simeq \frac{4n^2}{\pi(q+3)} U_A^{-(q+3)} \quad (259)$$

9 Appendix B: Evaluation of the function G

The task is to calculate the function G (204)

$$G = \int_{k_{min}R_L}^{\infty} ds s^{-q} \int_0^1 d\eta (1 - \eta^4) J_1^2(s\sqrt{1 - \eta^2}) \frac{1}{(1 - \eta^2)^2 s^2 + \frac{V_A^2 R_L^2}{\alpha^2}}, \quad (260)$$

and evaluate it in two energy limits.

9.1 Case $G(k_{min}R_L \gg 1)$

For energies $T \gg 1$ we substitute $s = xT$. Then, (204) reads as

$$\begin{aligned} G &= \int_1^{\infty} dx x^{-q} T^{-(1+q)} \int_0^1 d\eta (1 - \eta^4) J_1^2(xT\sqrt{1 - \eta^2}) \frac{1}{(1 - \eta^2)^2 x^2 + 10^{14}} = \\ &T^{-(1+q)} \int_1^{\infty} dx x^{-q} \left(\int_0^{1 - \frac{1}{2xT}} d\eta (1 - \eta^4) \frac{1}{\pi x T \sqrt{1 - \eta^2}} \frac{1}{(1 - \eta^2)^2 x^2 + 10^{14}} + \right. \\ &\quad \left. \int_{1 - \frac{1}{2xT}}^1 d\eta (1 - \eta^4) \frac{1}{4} x^2 T^2 (1 - \eta^2) \frac{1}{(1 - \eta^2)^2 x^2 + 10^{14}} \right), \end{aligned} \quad (261)$$

where we have used

$$J_{\nu}(z \gg 1) \approx \sqrt{\frac{2}{\pi \nu z}} \cos\left(\nu z - \frac{(2\nu + 1)\pi}{4}\right) \quad (262)$$

implying

$$J_1^2(z \gg 1) = \frac{1}{\pi x T \sqrt{1 - \eta^2}} (1 - \sin(2xT\sqrt{1 - \eta^2})) \simeq \frac{1}{\pi x T \sqrt{1 - \eta^2}} \quad (263)$$

($1/\xi \gg \sin \xi/\xi$) for the argument $z = xT \ll 1$, and

$$J_{\nu}(z \ll 1) \approx \frac{(z/2)^{\nu}}{\Gamma(\nu + 1)} \quad (264)$$

implying

$$J_1^2(z \ll 1) = \frac{1}{4} x^2 T^2 (1 - \eta^2), \quad (265)$$

for the argument $z = xT \gg 1$. We then obtain

$$\begin{aligned} T^{(1+q)} G(T \gg 1) &= \frac{T^2}{4} \int_1^{\infty} dx x^{-q+2} \int_{1 - \frac{1}{2xT}}^1 d\eta (1 - \eta^4) \frac{(1 - \eta^2)}{(1 - \eta^2)^2 x^2 + 10^{14}} + \\ &\frac{1}{\pi T} \int_1^{\infty} dx x^{-(q+1)} \int_0^1 d\eta \frac{(1 - \eta^4)}{\sqrt{1 - \eta^2}} \frac{1}{(1 - \eta^2)^2 x^2 + 10^{14}} \end{aligned}$$

$$\frac{1}{\pi T} \int_1^\infty dx x^{-(q+1)} \int_{1-\frac{1}{2xT}}^1 d\eta \frac{(1-\eta^4)}{\sqrt{1-\eta^2}} \frac{1}{(1-\eta^2)^2 x^2 + 10^{14}} = I_3 + I_1 - I_2. \quad (266)$$

Next, we evaluate each integral in turn.

$$I_2 = \frac{1}{\pi T} \int_1^\infty dx x^{-(q+1)} \int_0^{\frac{1}{2xT}} dm \frac{4m}{\sqrt{2m}} \frac{1}{4m^2 x^2 + 10^{14}} = \frac{2}{3} \frac{10^{-14}}{\pi(q+3/2)} T^{-\frac{5}{2}}, \quad (267)$$

where we have substitute $m = 1 - \eta$.

$$I_3 = \frac{T^2}{4} \int_1^\infty dx x^{-q+2} \int_0^{\frac{1}{2xT}} dm 4m \frac{2m}{10^{14}} = \frac{1}{12} \frac{10^{-14}}{q} T^{-1}, \quad (268)$$

where we have used the same substitution as in previous case and $10^{14} \gg 4m^2 x^2$. Note, that $I_2 \ll I_3$.

$$I_1 = \frac{1}{\pi T} \int_1^\infty dx x^{-(q+1)} \int_0^1 d\eta \frac{(1-\eta^4)}{\sqrt{1-\eta^2}} \frac{1}{10^{14}} = \frac{5}{16} \frac{10^{-14}}{q} \frac{1}{T}. \quad (269)$$

Combining all these three integrals we obtain

$$G(T \gg 1) = \frac{2}{5} \frac{10^{-14}}{q} T^{-(q+2)}. \quad (270)$$

9.2 Case $G(k_{min} R_L \ll 1)$

For energies $T \ll 1$ we use approximation for Bessel function (265). Then, (204) reads as

$$G(T \ll 1) = \frac{1}{4} \int_{k_{min} R_L}^1 ds s^{-q} \int_0^1 d\eta (1-\eta^4) \frac{(1-\eta^2)s^2}{(1-\eta^2)^2 s^2 + \frac{V_A^2 R_L^2}{\alpha^2}} = \frac{1}{4} \int_T^1 ds s^{-q} \int_0^1 d\eta (1+\eta^2) - \frac{M^2}{4} \int_T^1 ds s^{-q} \int_0^1 d\eta (1+\eta^2) \frac{1}{(1-\eta^2)^2 s^2 + M^2} = I_5 - I_4, \quad (271)$$

where $M^2 = \frac{V_A^2 R_L^2}{\alpha^2}$. We evaluate each integral in turn.

$$I_5 = \frac{1}{4} \int_T^1 ds s^{-q} \int_0^1 d\eta (1+\eta^2) = \frac{1}{3(q-1)} (T^{1-q} - 1) \simeq \frac{1}{3(q-1)} T^{1-q}, \quad (272)$$

since $T \ll 1$, and $1 < q < 2$.

$$I_4 = \frac{M^2}{4} \int_T^1 ds s^{-q} \int_0^1 d\eta (1 + \eta^2) \frac{1}{(1 - \eta^2)^2 s^2 + M^2} = \frac{1}{4} \int_T^1 ds s^{-q} I_6, \quad (273)$$

where

$$I_6 = \int_0^1 d\eta (1 + \eta^2) \frac{1}{((1 - \eta^2)^2 s^2 / M^2) + 1}. \quad (274)$$

Exact solution of integral I_6 reads

$$\frac{(-1)^{1/4} \left(\frac{(-2i+n) \arctan\left(\frac{(-1)^{1/4}}{\sqrt{-i+n}}\right)}{\sqrt{-i+n}} + \frac{i(2i+n) \arctan\left(\frac{(-1)^{3/4}}{\sqrt{-i+n}}\right)}{\sqrt{-i+n}} \right)}{2n\sqrt{1+n^2}} \quad (275)$$

where $n = M^2/s^2$. We can evaluate I_6 by

$$I_6 \approx \frac{1}{2n^3}, \quad (276)$$

which for I_4 gives

$$I_4 \approx \frac{1}{8M} \frac{1}{2-q} (1 - T^{(2-q)}). \quad (277)$$

In order to compare I_4 and I_5 and calculate $G(T \ll 1)$ we have to consider two cases, flat ($1 < q < 2$) and steep ($2 < q < 6$) turbulence spectrum.

9.2.1 Flat turbulence spectrum $1 < q < 2$

We investigate $G(T \ll 1) = I_5 - I_4$, where I_4 is evaluated for $1 < q < 2$ and reads

$$I_4 \approx \frac{1}{8(2-q)} \frac{1}{10^7 T} = \frac{1}{8(2-q)} \frac{10^{-7}}{T}, \quad (278)$$

so that,

$$G(T \ll 1) = \frac{1}{3} \frac{1}{q-1} T^{1-q} \left(1 - \frac{3(q-1)}{8(2-q)} 10^{-7} T^{(q-2)} \right). \quad (279)$$

Here, we have to analyze function $g(q, T) = 1 - \frac{3(q-1)}{8(2-q)} 10^{-7} T^{(q-2)}$. Function g attains minimum at $q_k = (3 \ln T \pm \sqrt{\ln^2 T + 4 \ln T}) / 2 \ln T$, and has vertical asymptote in $q = 2$ which is in agreement with assumption for flat turbulence spectrum. Since $q_k(T)$ is a function of T , as T becomes smaller the minimum peak becomes sharper, which gives that in very narrow region around q_k function $g \ll 1$, even become < 0 for $T < 10^{-7}$. As long as $T > 10^{-7}$ function $g \approx 1$. In Fig. 9 we show how function g depend on q for

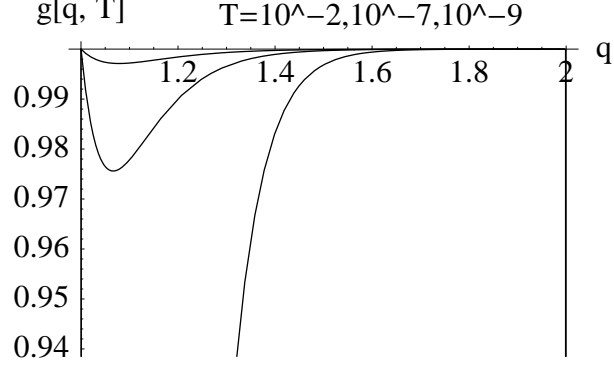


Figure 8: q dependance on the function g for 3 different fixed values of T

3 different fixed value of T . However, we can approximate $g \approx 1$ for $1 \gg T > 10^{-7}$ and $1 < q < 2$, and for $T < 10^{-7}$ but we have restriction $q_k + \sigma < q < 2$ where σ depends on smallness of T . In that case

$$G(T \ll 1, 1 < q < 2) = \frac{1}{3} \frac{1}{q-1} T^{1-q}. \quad (280)$$

9.2.2 Steep turbulence spectrum $2 < q < 6$

We investigate $G(T \ll 1) = I_5 - I_4$, where I_4 is evaluated for $2 < q < 6$ and reads

$$I_4 \approx \frac{1}{8(2-q)} \frac{1}{10^7 T} (1 - T^{2-q}) = \frac{-1}{8(2-q)} 10^{-7} T^{1-q}, \quad (281)$$

since $T \ll 1$, so that,

$$G(T \ll 1, 2 < q < 6) = T^{1-q} \left(\frac{1}{3(q-1)} + \frac{10^{-7}}{8(2-q)} \right) \approx \frac{1}{3} \frac{1}{q-1} T^{1-q}. \quad (282)$$

10 Appendix C: Evaluation of the function G

The task is to calculate the function G (228)

$$G = \int_{k_{min}R_L}^{\infty} ds s^{-q} \int_0^1 d\eta (1 - \eta^4) J_1^2(s\sqrt{1 - \eta^2}) \frac{1}{(1 - \eta^2)^2 s^2 + \frac{V_A^2 \frac{\eta\beta}{1+\beta} R_L^2}{\alpha^2}}. \quad (283)$$

and evaluate it in two energy limits.

10.1 Case $G(k_{min}R_L \gg 1)$

For energies $T \gg 1$ we substitute $s = xT$. Then, (228) reads as

$$\begin{aligned} G &= \int_1^{\infty} dx x^{-q} T^{-(1+q)} \int_0^1 d\eta (1 - \eta^4) J_1^2(xT\sqrt{1 - \eta^2}) \frac{1}{(1 - \eta^2)^2 x^2 + p^2 \eta} = \\ &T^{-(1+q)} \int_1^{\infty} dx x^{-q} \left(\int_0^{1 - \frac{1}{2xT}} d\eta (1 - \eta^4) \frac{1}{\pi x T \sqrt{1 - \eta^2}} \frac{1}{(1 - \eta^2)^2 x^2 + p^2 \eta} + \right. \\ &\quad \left. \int_{1 - \frac{1}{2xT}}^1 d\eta (1 - \eta^4) \frac{1}{4} x^2 T^2 (1 - \eta^2) \frac{1}{(1 - \eta^2)^2 x^2 + p^2 \eta} \right), \end{aligned} \quad (284)$$

where $p^2 = (v_A^2 R_L^2 \beta) / (\alpha^2 (1 + \beta))$, and we have used

$$J_\nu(z \gg 1) \approx \sqrt{\frac{2}{\pi \nu z}} \cos\left(\nu z - \frac{(2\nu + 1)\pi}{4}\right) \quad (285)$$

implying

$$J_1^2(z \gg 1) = \frac{1}{\pi x T \sqrt{1 - \eta^2}} (1 - \sin(2xT\sqrt{1 - \eta^2})) \simeq \frac{1}{\pi x T \sqrt{1 - \eta^2}} \quad (286)$$

$(1/\xi \gg \sin \xi/\xi)$ for the argument $z = xT \ll 1$, and

$$J_\nu(z \ll 1) \approx \frac{(z/2)^\nu}{\Gamma(\nu + 1)} \quad (287)$$

implying

$$J_1^2(z \ll 1) = \frac{1}{4} x^2 T^2 (1 - \eta^2), \quad (288)$$

for the argument $z = xT \gg 1$. We then obtain

$$\begin{aligned} T^{(1+q)} G(T \gg 1) &= \frac{T^2}{4} \int_1^{\infty} dx x^{-q+2} \int_{1 - \frac{1}{2xT}}^1 d\eta (1 - \eta^4) \frac{(1 - \eta^2)}{(1 - \eta^2)^2 x^2 + p^2 \eta} + \\ &\frac{1}{\pi T} \int_1^{\infty} dx x^{-(q+1)} \int_0^1 d\eta \frac{(1 - \eta^4)}{\sqrt{1 - \eta^2}} \frac{1}{(1 - \eta^2)^2 x^2 + p^2 \eta} \end{aligned}$$

$$\frac{1}{\pi T} \int_1^\infty dx x^{-(q+1)} \int_{1-\frac{1}{2xT}}^1 d\eta \frac{(1-\eta^4)}{\sqrt{1-\eta^2}} \frac{1}{(1-\eta^2)^2 x^2 + p^2 \eta} = I_3 + I_1 - I_2. \quad (289)$$

Next, we evaluate each integral in turn.

$$I_2 = \frac{1}{\pi T} \int_1^\infty dx x^{-(q+1)} \int_0^{\frac{1}{2xT}} dm \frac{4m}{\sqrt{2m}} \frac{1}{4m^2 x^2 + p^2(1-m)} = \frac{1}{\pi T} \int_1^\infty dx x^{-(q+1)} I'_2(m, x), \quad (290)$$

where we have substitute $m = 1 - \eta$.

$$I_3 = \frac{T^2}{4} \int_1^\infty dx x^{-q+2} \int_0^{\frac{1}{2xT}} dm \frac{8m^2}{p^2(1-m) + 4m^2 x^2} = \frac{T^2}{4} \int_1^\infty dx x^{-q+2} I'_3(m, x), \quad (291)$$

where we have used the same substitution as in previous case.

$$I_1 = \frac{1}{\pi T} \int_1^\infty dx x^{-(q+1)} \int_0^1 dm \frac{4m}{\sqrt{2m}} \frac{1}{p^2(1-m) + 4m^2 x^2} = \frac{1}{\pi T} \int_1^\infty dx x^{-(q+1)} I'_1(m, x). \quad (292)$$

In order to compare functions under integration with respect to m , we write out following integrals

$$I'_2(m, x) = \int_0^{\frac{1}{2xT}} dm \frac{4m}{\sqrt{2m}} \frac{1}{4m^2 x^2 + p^2(1-m)} = \frac{2\sqrt{2}}{p^2} \int_0^{\frac{1}{2xT}} dm f_1 \quad (293)$$

$$I'_3(m, x) = \int_0^{\frac{1}{2xT}} dm \frac{8m^2}{p^2(1-m) + 4m^2 x^2} = \frac{8}{p^2} \int_0^{\frac{1}{2xT}} dm f_2, \quad (294)$$

$$I'_1(m, x) = \int_0^1 dm \frac{4m}{\sqrt{2m}} \frac{1}{p^2(1-m) + 4m^2 x^2} = \frac{2\sqrt{2}}{p^2} \int_0^1 dm f_1, \quad (295)$$

where $f_1 = \frac{\sqrt{m}}{1-m}$ and $f_2 = \frac{m^2}{1-m}$, where we have approximated denominator as $1 - m$, as long as holds $\frac{4x^2}{p^2} \ll 1$. Analyzing f_1 and f_2 in given intervals of integration we deduce that $I_2 \ll I_3 \ll I_1$, since $f_1 \gg f_2$ and f_1 is dominant in interval $[0, 1)$.

Integral I'_1 diverge for $m = 1$, so we integrate up to $b = 1 - \delta$ where $\delta \ll 1$. Combining all, we obtain

$$G(T \gg 1) = \frac{2\sqrt{2}}{\pi} \frac{h}{qp^2} T^{-(q+2)}, \quad (296)$$

where $h = 2 \operatorname{arctgh} \sqrt{b} - 2\sqrt{b}$.

10.2 Case $G(k_{min}R_L \ll 1)$

For energies $T \ll 1$ we use approximation for Bessel function (288). Then, (283) reads as

$$\begin{aligned} G(T \ll 1) &= \frac{1}{4} \int_{k_{min}R_L}^1 ds s^{-q} \int_0^1 d\eta (1 - \eta^4) \frac{(1 - \eta^2)s^2}{(1 - \eta^2)^2 s^2 + \frac{V_A^2 R_L^2 \eta \beta}{\alpha^2(1+\beta)}} = \\ &= \frac{1}{4} \int_T^1 ds s^{-q} \int_0^1 d\eta (1 + \eta^2) - \frac{p^2}{4} \int_T^1 ds s^{-q} \int_0^1 d\eta (1 + \eta^2) \frac{\eta}{(1 - \eta^2)^2 s^2 + p^2 \eta} = I_5 - I_4, \end{aligned} \quad (297)$$

where $p^2 = \frac{V_A^2 R_L^2 \beta}{\alpha^2(1+\beta)}$. We evaluate each integral in turn.

$$I_5 = \frac{1}{4} \int_T^1 ds s^{-q} \int_0^1 d\eta (1 + \eta^2) = \frac{1}{3(q-1)} (T^{1-q} - 1) \simeq \frac{1}{3(q-1)} T^{1-q}, \quad (298)$$

since $T \ll 1$, and $1 < q < 2$.

In order to estimate I_4 we write

$$I_4 = \frac{p^2}{4} \int_T^1 ds s^{-q} \int_0^1 d\eta (1 + \eta^2) \frac{\eta}{(1 - \eta^2)^2 s^2 + p^2 \eta} = \frac{1}{4} \int_T^1 ds s^{-q} I_6, \quad (299)$$

where

$$I_6 = \int_0^1 d\eta (1 + \eta^2) \frac{\eta}{((1 - \eta^2)^2 w^2) + \eta}, \quad (300)$$

and $w^2 = s^2/p^2$. Here, we compare functions in integrals I_5 with respect to η named $f_1 = (1 + \eta^2)$ and in I_6 named $f_2 = (1 + \eta^2) \frac{\eta}{((1 - \eta^2)^2 w^2) + \eta}$.

We find that for $w^2 \gg 1$ one has $f_1 > f_2$ all over interval $[0, 1)$. Close to $\eta = 1$ these two functions tend to infinity, so we restrict our calculation up to $\eta = 1 - \delta$, where $\delta \ll 1$.

Combining these two integrals we obtain,

$$G(T \ll 1, 1 < q < 2) = \frac{1}{3} \frac{1}{q-1} T^{1-q}. \quad (301)$$

In the case $w^2 \ll 1$, $f_1 = f_2$ and integral vanishes.

References

- Abramowitz, M. & Stegun, I. A. 1972, Handbook of Mathematical functions
- Allen, G. E., Keohane, J. W., Gotthelf, E. V. et al., 1997, ApJ 487, L97
- Amelio-Camella, G., Ellis, J., Mavromatos, N. E., Nanopoulos, D. V. & Srakar, S., 1997, Nature 393, 763
- Antoni, T., Apel, W. D., Badea, A. F. et al., 2004, ApJ 604, 687
- Armstrong, J. W., Rickett, B. J. & Spangler, S. R., 1995, ApJ 443, 209
- Begelman, M. C., Rudak, B., Sikora, M., 1990, Astrophys. J. 362, 38
- Blandford, R. D., Eichler, D., 1987, Phys. Rep. 154, 1
- Borkowski, K. J., Rho, J., Reynolds, S. P. & Dyer, K. K., 2001, ApJ 550, 334
- Braginskii, S. I., 1949, Sov. Phys. Dokl. 2, 345
- Böttcher, M., Schlickeiser, R. & Marra, A., 2001, ApJ 563, 71
- Büsching, I., Pohl, M. & Schlickeiser, R., 2001, A& A 377, 1056
- Cho, Y., Lazarian, A., Vishniac, E., 2002, ApJ, 566, 49
- Coleman, S. & Glashow, S. L., 1997, Phys. Lett. B405, 249
- Compton, A. H., Getting, I. A., 1935, Phys. Rev. 47,817
- Dogan, A., Spanier, F., Vainio, R., Schlickeiser, R., 2006, J. Plasma Physics 72, 419
- Enomoto, R., Tanimori, T., Naito, T. et al., 2002, Nature 416, 823
- Fisk, L. A., Kozlovsky, B & Ramaty, R., 1974, ApJ 180, L35
- Gary, S.P., 1986, J. Plasma Phys. 35, 431
- Goldreich, P., Sridhar, S., 1995, ApJ 438, 763
- Gradshteyn, I. S., Ryzhik, I. M., 1965, Table of Integrals, Series, and Products, Academic Press, New York
- Green, M. S., 1951, J. Chem. Phys. 19, 1036
- Greisen, K., 1966, Phys. Rev. Lett. 16, 748
- Hall, D. E., Sturrock, P. A., 1967, Phys. Fluids 10, 2620

Hasselmann, K., Wibberenz, G., 1968, *Z. Geophys.* 34, 353

Hillas, A. M., 1984, *ARAA* 22, 425

Jokipii, J. R., 1966, *ApJ* 146, 480

Koyama, K., Petre, R., Gotthelf, E. V. et al., 1995, *Nature* 378, 255

Koyama, K., Kinugasa, K., Matsuzaki, K. et al., 1997, *PASJ* 49, L7 *Nature* 378, 255

Kubo, R., 1957. *J. Phys. Soc. Japan* 12, 570

Kulsrud, R. M., Pearce, W. P., 1969, *ApJ* 156, 445

Lerche, I. & Schlickeiser, R., 2001, *A& A* 378, 279

Lithwick, Y., Goldreich, P., 2001, *ApJ* 567, 479

Lotz, W., 1967a, *ApJS* 14, 207

Lotz, W., 1967b, *Z. Phys.* 206, 205

Lund, N., 1986, *Cosmic Rays in Contemporary Astrophysics*, ed. by M.M. Shapiro (Reidel, Dordrecht, The Netherlands)

Mannheim, K., Biermann, P. L., 1989, *A& A* 221, 211

Mannheim, K., Schlickeiser, R., 1994, *A& A* 286, 983

Minter, A. H. & Spangler, S. R., 1997, *ApJ* 485, 182

Möbius, E., Hovestadt, D., Klecker, B., Scholer, M., Gloeckler, G. & Ipavich, F.M., 1985, *Nat.* 318, 426

Peskin, M. E. & Schroeder, D. V., 1995, *An Introduction to Quantum Field Theory*, Addison-Wesley, Reading

Pohl, M., Lerche, I., & Schlickeiser, R., 2002, *A& A* 383, 309

Pohl, M., Schlickeiser, R., 2000, *A& A* 354, 395

Ragot, B. R. & Schlickeiser, R., 1998, *Astropart. Phys.* 9, 79

Reimer, O. & Pohl, M., 2002, *A& A*

Rickett, B. J., 1990, *AR A&A* 28, 561

Rucinski, D., Cummings, A. C., Gloeckler, G., Lazarus, A. J., Möbius, E. & Witte, M. R., 1996, *Space Sci. Rev.* 78, 73

Samorski, M., Stamm, W., *Astrophys. J.* 268, L17

Schlickeiser, R., 1986, *Cosmic Radiation in Contemporary Astrophysics*, M. M. Shapiro, 27

Schlickeiser, R., 1989, *ApJ* 336, 243

Schlickeiser, R., Achatz, U., 1993a, *J. Plasma Phys.* 49,63

Schlickeiser, R. & Miller, J. A., 1998, *ApJ* 492, 352

Schlickeiser, R., Dermer, C. D., 2000, *A& A* 360, 789

Schlickeiser, R., Vainio, R., Böttcher, M., Lerche, I., Pohl, M. & Schuster, C., 2002, *A& A* 393, 69

Schlickeiser, R., 2002, *Cosmic Ray Astrophysics*, Springer, Berlin

Schlickeiser, R., 2003, *Lecture Notes in Physics* 612. 230

Schlickeiser, R., 2003, *A& A*, submitted

Shalchi, A. & Schlickeiser, R., 2004, *A& A* 420, 821

Skilling, J., 1975, *Monthly Not. Royal Astron. Soc.* 172, 557

Slane, P., Gaensler, B. M., Dame, T. M. et al., 1999, *ApJ* 525, 357

Sofue, Y., Fujimoto, M., Wielebinski, R., 1986, *ARAA* 24, 459

Sokolsky, P., 1979, *Intro. to Ultrahigh Energy Cosmic Ray Physics*, Addison-Wesley, Redwood City, 503

Spangler, S. R., 1991, *ApJ* 376, 540

Stecker, F. W., 1968, *Phys. Rev. Lett.* 21, 1016

Sikora, M., Kirk, J. G., Begelman, M. C., Schneider, P., 1987, *ApJ* 320, L81

Stringer, T. E., 1963, *Plasma Phys., J. Nucl. Energy C* 5, 89

Sturrock, P. A., 1994, *Plasma Physics*, Cambridge University Press, Cambridge

Swansson, D. G., 1989, *Plasma Waves*, Pergamon Press, Oxford

Tanimori, T., Hayami, Y., Kamei, S. et al., 1998, *ApJ* 497, L25

Turner, M. S. et al., 2002, *Report to the National Academy of Science*

- Urch, I. H., 1977, *Astrophys. Space Sci.* 46, 389
- Vainio, R., Pohl, M. & Schlickeiser, R., 2003, *A&A*, submitted
- Watson, A. A., 1984, *Adv. Space. Res.* 4, 35
- Weaver, T. A., 1976, *Phys. Rev. A* 13, 1563
- Whittaker, E. T., Watson, G. N., 1978, *A Course of Modern Analysis*, Cambridge University Press, Cambridge
- Weekes, T. C., 1972, *High Energy Astrophysics*, Chapman and Hall, London
- Zatsepin, G. T., Kuzmin, V. A., 1966, *Soviet Phys. JETP Letters* 4, 78
- <http://www.cosmic-ray.org/>
- <http://www-zeuthen.desy.de/>

Acknowledgment

I would like, first, to express my gratitude to Prof. Reinhard Schlickeiser for offering me the opportunity to work in the Theoretical astrophysics group at the Ruhr-University in Bochum, for constant support and interest in my work. I am specially grateful that he, in spite of his overwhelming responsibilities as a chef of this group, always had time for very detailed discussions of this thesis. Also, I am grateful for his patience and encouragement, whenever it was difficult.

I am thankful to Prof. Ralf-Jürgen Dettmar from the Astronomy department who has been chosen me as a PhD student, for the first. I very much appreciate his trust and encouragement in changing field of work.

In memorial to Prof. Marko Leko, I would use this opportunity to acknowledge his influence to choose astrophysics in basic studies and for all advises and help he always offered.

I am very much thankful to my colleagues Dr Mara Šćepanović, Dr Ana Dubak and Prof. Žarko Kovačević from the Montenegro University, for their patience, friendship and useful discussions when I had some doubts. Also, I would like to thank to Igor Ivanović who was always available for technical support.

For help and friendship while spending time in Bochum, I need to thank Olivera Stepanović, Eva Kovačević and Christian Röken. Also, all my gratitude goes to Sandra, Tijana and Maja, who have been good friends everywhere.

For help dealing with all administrative issues I would like to give the thanks to secretary of our group Mrs Angelika Schmitz.

Last but not least, words of warmest gratitude belong to my parents and parents in law, for their endless support and understanding, most of all to my husband Vladimir and my daughter Ana whose the most beautiful smile in the world cheered my spirit in the difficulties of past month.

Curriculum Vitae

Name: Miroslava Vukčević

Date/Place of birth: 23. 06. 1971. Belgrade, Serbia

Education: Primary School 1978-1986, Belgrade

High School 1986-1990, Technical School, Belgrade

University diploma 1990-1996, Belgrade University, Faculty of Science

Master's degree 1999-2001, University of Tokyo, Faculty of Quantum Engineering and Systems Science, Japan

Work experience: 1996-2002 Institute of Nuclear Sciences VINCA, Belgrade

1998/1999, 2001/2002 Assistant, Belgrade University, Faculty of Electrical Engineering

2004- Assistant, University of Montenegro, Faculty of Science, Montenegro